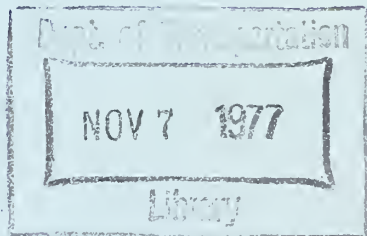


HE
18.5
.A39
no.
DOT-
TST-
77-74
C.2

-77-74

DEVELOPMENT OF DESIGN PROCEDURES STABILIZED SOIL SUPPORT SYSTEM FOR SOFT GROUND TUNNELING VOLUME II - PRELIMINARY RESULTS



**Final Report
August 1977**

UNDER CONTRACT: DOT-OS-50123

Document is available to the U.S. public through the
National Technical Information Service
Springfield, Virginia 22161

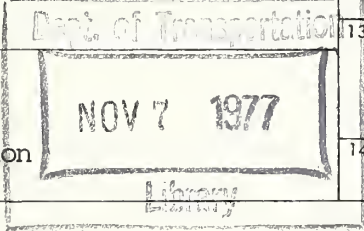
**Prepared For:
U.S. DEPARTMENT OF TRANSPORTATION
OFFICE OF THE SECRETARY
Office of University Research
Washington, D.C. 20590**

NOTICE

This document is disseminated under the sponsorship of the Department of Transportation in the interest of information exchange. The United States Government assumes no liability for its contents or use thereof.

HE
18-5
1939
DOT
TST
77-74
c.2

1. Report No. DOT-TST-77-74		2. Government Accession No.		3. Recipient's Catalog No.	
4. Title and Subtitle DEVELOPMENT OF DESIGN PROCEDURES FOR STABILIZED SOIL SUPPORT SYSTEMS FOR SOFT GROUND TUNNELING - VOLUME II PRELIMINARY RESULTS				5. Report Date August 1977	
				6. Performing Organization Code	
7. Author(s) Peter Koenzen G. Wayne Clough, David Y. Tan, William M. Kuck and				8. Performing Organization Report No.	
9. Performing Organization Name and Address Department of Civil Engineering Stanford University Stanford, California 94305				10. Work Unit No. (TRAIS)	
				11. Contract or Grant No. DOT-OS-50123	
12. Sponsoring Agency Name and Address Office of University Research Office of the Secretary U. S. Department of Transportation Washington, D. C. 20590				13. Type of Report and Period Covered Final Report - Volume II	
				14. Sponsoring Agency Code OST/TST-60	
15. Supplementary Notes OST Technical Monitor: Russell K. McFarland, TST-45					
16. Abstract This report describes the experimental and analytical work carried out at Stanford University during the first year of a research effort devoted to the development of a rational design methodology for grouted tunnels. The long range objective of this work is to provide a designer with a simple tool which can be used to select the size, strength and stiffness of a grouted soil zone around a tunnel which will economically and effectively limit surface deformations caused by tunneling. The first year effort has been devoted to: <ol style="list-style-type: none"> 1. Developing laboratory procedures to study load-deformation response of chemically stabilized soils. 2. Performing laboratory tests of typical stabilized soils and evaluating the observed behavior. 3. Performing load tests on soil samples grouted under field conditions. 4. Developing a finite element code which can reasonably model the effects of tunnel construction in grouted soil zones. 5. Documenting existing field case histories and applying the new finite element code to study some of the actual tunneling cases. 					
17. Key Words tunneling, transportation, grouted, soil, deformations, load, finite element code			18. Distribution Statement Document is available to the U. S. Public through the National Technical Information Service, Springfield, Virginia 22161		
19. Security Classif. (of this report) UNCLASSIFIED		20. Security Classif. (of this page) UNCLASSIFIED		21. No. of Pages	22. Price



PREFACE

This report was written under the auspices of Contract No. DOT-OS-50123 with the United States Department of Transportation, Office of University Research, Office of the Secretary. This is Volume II of a series of three reports covering the results of research on use of stabilized soil support for shallow ground tunnels; the first volume entitled "The Practice of Chemical Stabilization Around Soft Ground Tunnels in England, France and Germany" was completed in 1976 and described European and English field procedures for stabilizing soil and their application to actual projects.

The present volume, entitled "Development of Design Procedures for Stabilized Soil Support Systems for Soft Ground Tunneling Volume II - Preliminary Results," contains preliminary results of the first year of research. The third volume will report on subsequent efforts in the research, which will be primarily devoted towards development of a design procedure for stabilized soil support systems.

The contract monitor for all of the work has been Mr. Russell K. McFarland who has provided support and key contacts to facilitate the effort.

A number of individuals have made contributions to the work described herein by providing valuable discussion time and information for the researchers. These include Messers. E. D. Graf and W. H. Baker. Their assistance is appreciated. Students at Stanford in addition to those listed as authors on the report, who have contributed to the work are G. Kasali Phillipe Mayu and F. Mensah Dwumah.

Authors of the report include Dr. G. W. Clough, Associate Professor of Civil Engineering of Stanford University, Messers. D. Y. Tan and W. M. Kuck, graduate students at Stanford and Dr. P. Koenzen, visiting researcher from Karlsruhe University, West Germany.

TABLE OF CONTENTS

	<u>Page</u>
PREFACE	ii
TABLE OF CONTENTS	iii
TABLE OF FIGURES	v
LIST OF TABLES	vii
ABSTRACT	viii
CHAPTER I	1
CHAPTER II	5
BACKGROUND	5
GROUT TYPES	5
Cement and Clay Cement	5
Sodium Silicate Systems	8
Resins	9
TUNNEL GROUTING EXPERIENCE	10
Stabilized Soil Zones	10
Strengths of Stabilized Soil Zones	18
Performance of Grouted Tunnels	19
DESIGN OF STABILIZATION SOLUTIONS	20
BEHAVIOR OF SOILS STABILIZED BY SILICATE SYSTEMS	21
Unconfined Compression Strength	21
Effect of Confining Stress or Strength	28
Stress-Strain Behavior	30
Modeling Observed Stress-Strain Behavior	31
SUMMARY	31
CHAPTER III	34
LABORATORY TEST PROGRAM	34
LABORATORY PROCEDURES FOR GROUTING SOIL SAMPLES	34
Existing Techniques to Create Grouted Samples	35
Techniques Used in Present Investigation	35
TESTING METHODS	38
TEST MATERIALS AND SAMPLE DENSITIES AND PERMEABILITIES	41
TESTING PROGRAM	44
RESULTS OF TEST PROGRAM	45
General Stress-Strain Response	45
Effects of Confining Pressure, Chemical Concentration and Large Strains	45
Effect of Age	57
Effect of Constant Load	59
Strength of Grouted Samples	59
Initial Tangent Modulus Values - Grouted Samples	69
SUMMARY	73
CHAPTER IV	74
FINITE ELEMENT CODE DEVELOPMENT AND PARAMETRIC STUDIES	74
DEFINITION OF THE PROBLEM TO BE ANALYZED	75
DESCRIPTION OF FINITE ELEMENT CODE CAPABILITIES	78
Type of Element	79
Stress-Strain-Models	79
Simulation of Excavation Effects	80
Modeling Effects of Liner and Shield Pitch	83
TESTING OF THE PLANE STRAIN ANALYSIS CAPABILITY	86
Results - Initially Unstressed Medium With a Cylindrical Hole Subjected to Boundary Stresses	89

TABLE OF CONTENTS

	<u>Page</u>
Results - Initially Stressed Medium With Cylindrical Hole Excavated in Stages	89
TESTING OF THE AXISYMMETRIC ANALYSIS CAPABILITY	93
PRELIMINARY PLANE STRAIN PARAMETRIC STUDIES	94
Problems Studied	94
Finite Element Representation	99
Material Parameters	99
Loading and Tunneling Conditions	102
Results	102
SUMMARY	106
CHAPTER V	107
FIELD GROUTING SITES	107
GENERAL DESCRIPTION OF FIELD TRIALS AND RELATED LABORATORY WORK	108
RESULTS OF WORK AT TEST SITE I - ROOSEVELT HIGH SCHOOL	111
Soil Conditions	113
Test Injections	113
Load Test Results	117
RESULTS OF WORK AT TEST SITE II - ALAMEDA ISLAND	120
Soil Conditions	120
Test Injections	120
Load Test Results	125
SUMMARY	127
CHAPTER VI	128
DOCUMENTATION OF TUNNEL GROUTING CASE HISTORIES	128
SOIL AND TUNNELING CONDITIONS AT PROJECT SITES	128
GROUTING SCHEMES	133
PERFORMANCE DATA AND INSTRUMENTATION FOR PROJECT I	137
FINITE ELEMENT STUDIES OF PROJECT I	138
Soil Conditions	141
Grout Zone Locations and Properties	141
Parameters and Subsurface Profiles Used in Analyses	145
Finite Element Mesh and Boundary Conditions	148
Results of Finite Element Analyses	151
SUMMARY	155
CHAPTER VII	156
SUMMARY AND CONCLUSIONS	156
REFERENCES	159

LIST OF FIGURES

<u>Figure</u>	<u>Description</u>	<u>Page</u>
1.1	EXAMPLES OF APPLICATIONS FOR GROUTING IN URBAN TUNNELING	2
2.1	CATEGORIES OF GROUTING AGENTS COMMONLY USED IN TUNNELING	7
2.2	GROUTING ZONES IN EUROPEAN CITIES	12
2.3	TYPICAL SECTION DESIGN FOR GROUT TREATMENT, PARIS METRO (COURTESY SOLETANCHE, S.A., PARIS, FRANCE	14
2.4	INCREASE IN UNCONFINED COMPRESSIVE STRENGTH WITH SILICATE AND HARDNER CONTENT (AFTER RHONE-PROLENC, 1975)	24
2.5	VARIATION IN STRESS-STRAIN RESPONSE WITH RATE OF LOADING (AFTER KOENZEN, 1975)	26
2.6	RESPONSE OF GROUTED SOIL TO CONSTANT LOAD (AFTER KOENZEN, 1975)	27
2.7	CHANGE IN UNCONFINED STRENGTH OF GROUTED SOIL WITH CURING (AFTER WARNER, 1972)	29
2.8	MOHR ENVELOPES FOR GROUTED SOIL FROM TRIAXIAL TESTS (AFTER GARTUNG AND KANY, 1975)	29
2.9	SIMPLIFIED VISCOELASTIC MODEL FOR GROUTED SOIL (AFTER KOENZEN, 1975)	32
3.1	SCHEMATIC OF GROUTING APPARATUS	37
3.2	LOADING AND RECORDING APPARATUS WITH SAMPLE IN PLACE FOR TESTING	40
3.3	GRAIN SIZE CURVES	42
3.4	STRESS-STRAIN BEHAVIOR OF SAMPLES TESTED AT $\sigma_3 = 138\text{kN/m}^2$	52
3.5	STRESS-STRAIN BEHAVIOR OF SAMPLES TESTED AT $\sigma_3 = 69\text{kN/m}^2$	53
3.6	STRESS-STRAIN BEHAVIOR OF 30% SILICATE SAMPLES TESTED AT VARIOUS CONFINING PRESSURES	54
3.7	EXAMPLES OF FAILURE MODES OF GROUTED SAMPLES	56
3.8	EFFECT OF CURE TIME ON STRESS-STRAIN RESPONSE	58
3.9	RESPONSE OF SAMPLES TO CONSTANT LOAD	60
3.10	STRENGTH ENVELOPES FOR 30% SILICATE SAMPLES, MONTEREY #16 SAND	62
3.11	STRENGTH ENVELOPE FOR 30% SILICATE SAMPLES, MONTEREY #30 SAND	64
3.12	STRENGTH ENVELOPES FOR 30, 50 AND 70% SILICATE SAMPLES	65
3.13	VARIATION OF COHESION WITH % SILICATE	68
3.14	EFFECT OF CURING TIME ON UNCONFINED STRENGTH	68
3.15	DETERMINATION OF INITIAL TANGENT MODULUS FROM TRANSFORMED STRESS-STRAIN CURVE	70
3.16	VARIATION OF INITIAL TANGENT MODULUS VALUES WITH CONFINING PRESSURE	72
4.1	DEVELOPMENT OF GAP BEHIND A TUNNEL SHIELD	76
4.2	CONDITIONS FOR FINITE ELEMENT ANALYSES	77
4.3	COMPARISON OF THEORETICAL AND OBSERVED STRESS-STRAIN CURVES	81
4.4	RADIAL LINER SPRINGS USED TO LIMIT INWARD MOVEMENTS AROUND TUNNEL	85

LIST OF FIGURES

<u>Figure</u>	<u>Description</u>	<u>Page</u>
4.5	PROBLEM ANALYZED IN PLANE STRAIN VERIFICATION STUDIES	87
4.6	FINITE ELEMENT MESH FOR PLANE STRAIN VERIFICATION STUDIES	88
4.7	COMPARISON OF FINITE ELEMENT PREDICTIONS AND CLOSED FORM SOLUTION RESULTS	90
4.8	DETAILS OF PARAMETRIC STUDY PROBLEMS	98
4.9	FINITE ELEMENT MESH FOR PARAMETRIC STUDY PROBLEM	100
4.10	PREDICTED SETTLEMENTS FROM PARAMETRIC STUDIES	103
4.11	EFFECT OF GROUT ZONE SIZE AND STRENGTH ON MAXIMUM SURFACE SETTLEMENT	105
5.1	EXAMPLES OF SINGLE GROUT BULB INJECTIONS. ALAMEDA TEST SITE	109
5.2	EXAMPLES OF MULTIPLE GROUT BULB INJECTIONS - ALAMEDA TEST SITE	110
5.3	SITE LOCATIONS OF TEST INJECTIONS	112
5.4	SOIL PROFILE AND GRAIN SIZE ANALYSIS OF SOIL WHERE GROUT WAS INJECTED, ROOSEVELT HIGH SCHOOL SITE	114
5.5	LAYOUT OF TEST INJECTIONS, ROOSEVELT HIGH SCHOOL SITE	115
5.6	COMPARISON OF STRENGTHS OF FIELD SIROC SAMPLES TO LABORATORY SIROC SAMPLES WITH MONTEREY SAND	119
5.7	SOIL PROFILE AND GRAIN SIZE ANALYSES OF SOIL WHERE GROUT WAS INJECTED, ALAMEDA ISLAND SITE	121
5.8	LAYOUT OF TEST INJECTIONS, ALAMEDA ISLAND SITE	122
6.1	SOIL PROFILE AT PROJECT I	130
6.2	SOIL PROFILE AT PROJECT II	131
6.3	SOIL PROFILE AT PROJECT III	132
6.4	STABILIZED ZONES FOR PROJECT I	134
6.5	STABILIZED ZONES AT PROJECT II	135
6.6	STABILIZED ZONES AT PROJECT III	136
6.7	INSTRUMENTATION LAYOUT, PROJECT I	139
6.8	INSTRUMENTATION SCHEME, PROJECT I	140
6.9	BORINGS AT PROJECT I	143
6.10	COMPARISON OF BORING LOGS AND SOIL CONDITIONS IN IDEALIZED SECTIONS FOR PROJECT I	144
6.11	GROUTING PROFILES USED IN FINITE ELEMENT ANALYSES OF PROJECT I	146
6.12	FINITE ELEMENT MESH USED IN ANALYSES OF PROJECT I	150
6.13	PREDICTED SURFACE SETTLEMENTS FOR PROJECT I	153
6.14	PREDICTED LATERAL MOVEMENTS FOR PROJECT I	154

LIST OF TABLES

<u>Table</u>	<u>Description</u>	<u>Page</u>
2.1	SPECIALTY TOPICS CONCERNED WITH CHEMICAL STABILIZATION	6
2.2	CASE HISTORY DATA, GROUTED TUNNELS	15
2.3	EXPERIMENTAL PROGRAMS ON SILICATE STABILIZED SOIL	23
3.1	GROUT CONSTITUENTS USED IN LABORATORY TESTS	43
3.2	RESULTS OF LABORATORY TESTS, FIRST YEAR PROGRAM	46
3.3	EFFECTS OF TYPE OF SAMPLE TUBE	69
4.1	COMPARISON OF TANGENTIAL STRESSES BETWEEN THEORETICAL AND FINITE ELEMENT RESULTS--ONE-STEP EXCAVATION (kN/m ²)	91
4.2	COMPARISON OF RADIAL STRESSES BETWEEN THEORETICAL AND FINITE ELEMENT RESULTS--ONE-STEP EXCAVATION (kN/m ²)	91
4.3	COMPARISON OF TANGENTIAL STRESSES BETWEEN THEORETICAL AND FINITE ELEMENT RESULTS--THREE-STEP EXCAVATION (kN/m ²)	92
4.4	COMPARISON OF RADIAL STRESSES BETWEEN THEORETICAL AND FINITE ELEMENT RESULTS--THREE-STEP EXCAVATION (kN/m ²)	92
4.5	COMPARISON OF TANGENTIAL STRESSES BETWEEN THEORETICAL AND FINITE ELEMENT AXISYMMETRIC ANALYSIS RESULTS (kN/m ²)	95
4.6	COMPARISON OF RADIAL STRESSES BETWEEN THEORETICAL AND FINITE ELEMENT AXISYMMETRIC ANALYSIS RESULTS (kN/m ²)	96
4.7	COMPARISON OF RADIAL DISPLACEMENTS BETWEEN THEORETICAL AND FINITE ELEMENT AXISYMMETRIC ANALYSIS RESULTS (10 ⁻⁴ m)	97
4.8	PARAMETERS USED IN PRELIMINARY GROUTED TUNNEL ANALYSES	101
5.1	CHEMICAL GROUTS USED AT TEST INJECTIONS, ROOSEVELT HIGH SCHOOL	116
5.2	RESULTS OF LOAD TESTS AT FIELD SITE I - ROOSEVELT HIGH SCHOOL	118
5.3	CHEMICAL GROUTS USED AT TEST INJECTIONS, ALAMEDA ISLAND	124
5.4	RESULTS OF LOAD TESTS AT FIELD SITE II--ALAMEDA ISLAND	126
6.1	WMATA CASE HISTORIES	129
6.2	AVERAGE PHYSICAL PROPERTIES OF SUBSURFACE SOILS AT SITE OF PROJECT I	142
6.3	SOIL PARAMETERS USED IN FINITE ELEMENT STUDIES	149

ABSTRACT

This report describes the experimental and analytical work carried out at Stanford University during the first year of a research effort devoted to the development of a rational design methodology for grouted tunnels.

The long range objective of this work is to provide a designer with a simple tool which can be used to select the size, strength and stiffness of a grouted soil zone around a tunnel which will economically and effectively limit surface deformations caused by tunneling.

The first year effort has been devoted to:

1. Developing laboratory procedures to study load-deformation response of chemically stabilized soils.
2. Performing laboratory tests of typical stabilized soils and evaluating the observed behavior.
3. Performing load tests on soil samples grouted under field conditions.
4. Developing a finite element code which can reasonably model the effects of tunnel construction in grouted soil zones.
5. Documenting existing field case histories and applying the new finite element code to study some of the actual tunneling cases.

Progress towards all these objectives has been made. Over 100 load tests have been performed on stabilized soil samples, demonstrating the influence of a number of key variables on grouted soil performance. The data suggests that the behavior is complex and is a strong function of duration and rate of loading, confining pressure, and chemical concentrations in the grouts. It appears however that a reasonable analytical model for the behavior can be formulated and work in this area is proceeding.

A general purpose finite element code for grouted tunnel analysis has been developed and verified. The program can accommodate heterogeneous soil and groundwater conditions, gravity stress fields, complex soil behavior and effects of variations in tunneling construction sequences and procedures. Preliminary parametric studies using the code demonstrate that the size, shape, strength and stiffness of the stabilized soil zone influence the amount of surface settlement. There is clearly a point of diminishing returns in limiting movements by increasing size, strength or stiffness. Optimization of this point for various tunneling conditions is obviously desirable, since requiring more of any of these qualities than is necessary reduces the economics of a grouting solution.

Case history data show that, in general, grouting has been effective in limiting surface movements above tunnels. Preliminary finite element studies have been performed on one of the case histories and they show both the benefits and difficulties associated with quantification of grouted tunnel behavior. The results suggest that precise prediction of performance is difficult because material parameters for grouted soils are not well defined and because construction sequence has a major influence on behavior and this is not usually prescribed in advance of a project. However, in spite of these problems, the predicted results from the finite element program are consistent with trends of field results and are very useful in explaining observed performance. Better predictive capabilities will be available as more data are developed to describe grouted soil behavior. Problems introduced by construction sequence can be alleviated by integrating the analysis with early stages of construction so that actual sequences

can be accommodated into the analyses.

CHAPTER I

INTRODUCTION

Chemical injection stabilization can be used in pervious soils and weathered rocks to minimize problems usually associated with tunneling in these materials, such as ground water inflow, running soil, loss of ground and surface settlements. Also by using this technique, the need for compressed air can be eliminated and undesirable tunneling characteristics relative to machine boring can be reduced. Applications of the stabilization technology are relatively common in Europe and Japan and are on the increase in the United States. Its use is most common in urban areas where particularly critical groundwater or settlement problems exist.

Some examples are depicted in Figure 1.1, illustrating how grouting can be used to seal water out of a tunnel, create strengthened soil zones to support overlying structures, and form excavation walls of stabilized soil. Details of such applications have been described in a previous report to the Department of Transportation by the senior author of this report (Clough, 1976).

The use of the chemical stabilization technology in the United States has been limited, although there have been a number of recent significant jobs for the Washington Metro, including the following:

1. New Jersey Avenue Trunk Sewer Crossing, Contract Flb - chemical stabilization used in lieu of conventional underpinning to support trunk sewer above WMATA tunnels.
2. Seventh Street Bridge at I-95 - chemical stabilization used in lieu of conventional underpinning to support center pier of bridge; four WMATA tunnels pass beneath the bridge.
3. J. F. Kennedy Memorial Center - chemical stabilization used to solidify and impermeabilize water bearing soils to halt loss of ground incurred during WMATA tunneling.

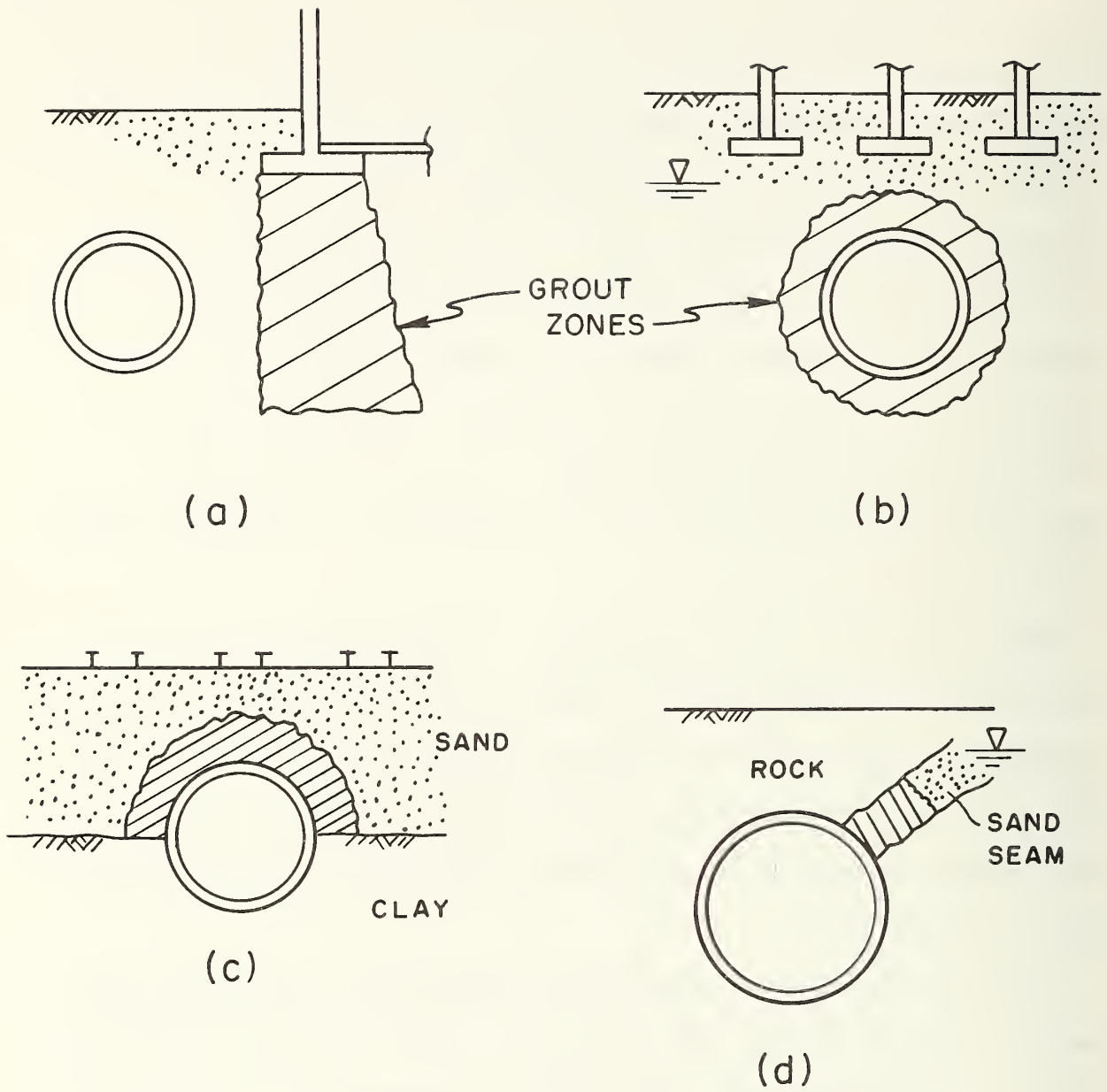


FIGURE 1.1. EXAMPLES OF APPLICATIONS FOR GROUTING IN URBAN TUNNELING

4. Wisconsin Avenue, WMATA Rockville Route - quick set cement grouting used to strengthen highly weathered rock and soil in order to allow advance of hard rock tunnel boring machine for WMATA tunnel.
5. Anacostia Freeway, Penn Central Railroad Crossing, WMATA Addison Route - chemical stabilization to be used to strengthen and impermeabilize soils to provide underpinning support and improve tunneling operations.

On three of these projects, ground surface settlements have been or are being measured. Details of the projects are given in Chapter VI.

It is interesting that in each instance of metro work where underpinning support was needed, chemical stabilization was found to be cheaper than existing conventional structural procedures. For the Anacostia Freeway project, independent cost estimates showed the chemical stabilization to be one-fourth the cost of conventional underpinning methods. In addition to this direct cost savings, the chemical stabilization also will reduce the need for dewatering and minimize any possibility of a ground run into the tunnel which might endanger workers' lives and adjacent property or utilities.

The cost and engineering advantages of chemical stabilization argue for its increased use in the United States. However, there is presently a distinct lack of objective engineering information on stabilized soil behavior, mode of grout penetration into the ground, quality control procedures for injection work and design procedures to choose sizes and properties of stabilized zones around tunnels. Where information of this type does exist, it is often proprietary. This report describes the results of a study designed to help remedy these problems. The information contained herein covers the experimental and analytical work of the first year of the contract. A previous report has detailed information

on existing European grout injection methods, design techniques, and quality control procedures (Clough, 1976).

The objectives of the first year of the research contract pertinent to this report were as follows:

1. Develop a method of preparing grouted soil samples for laboratory testing.
2. Perform laboratory tests to ascertain an understanding of deformation and strength response of grouted soils.
3. Define important material parameters to be studied in more detail in later laboratory work.
4. Carry out several small-scale field trials of grout injection where samples of different grouts are injected into the ground.
5. Sample the field grouted samples and test them in the laboratory; compare the results to behavior of laboratory grouted soils.
6. Develop plane strain and axisymmetric finite element codes which allow study of grouted tunneling problems.
7. Perform preliminary finite element analyses showing the influence of properties of the grouted zone around tunnels on tunnel performance.
8. Collect data on performance of full-scale grouted tunnel sections and provide finite element analyses for behavioral studies where possible.

CHAPTER II

BACKGROUND

The literature surrounding the subject of chemical stabilization of soils is vast; various specialty subject areas are summarized in Table 2.1 along with references which cover them. It is the intent in this chapter to deal with only a few of these topics which directly pertain to the purposes of this report. Included herein are an introduction to grout types, and a review of past experience with tunnel grouting, tunnel grouting design procedures and the engineering properties of grouted soil.

GROUT TYPES

There are a large variety of grouts which can be used in chemically stabilizing soils. However, the number of these grouts which are commonly employed and are economical in tunnel work is relatively small. Figure 2.1 lists these agents along with an indication of their purpose (strengthening or water tightening) and soil types where the agent can be injected. Penetrability and cost are generally the keys as to which grout is considered applicable for a given project. The following discussion summarizes the basic characteristics of the grouts listed in Fig. 2.1.

Cement and Clay Cement

Almost all grouts will penetrate coarse sands or gravels. However, because cement and clay cement are the cheapest grouts they are preferred for stabilizing coarse grained soils. Clay cement is more commonly used in tunnel work rather than cement because it is able to penetrate finer grained soils, is a more stable solution, and set time can be more closely controlled. Set time of clay cement grout can be established as low as a

TABLE 2.1 SPECIALTY TOPICS CONCERNED WITH
CHEMICAL STABILIZATION

ITEM	REFERENCES
Types of Grouts	(3), (4), (12), (16)
Methods of Injection	(3), (6), (12), (16)
Chemistry of Grouts	(3)
Theory of Grouting	(3), (14), (20)
Types of Applications	(6), (9), (11), (12), (13), (17)
Costs	(6), (11)
Behavior of Grouted Soils	(10), (14), (15), (19), (20), (22)
Uses of Grouting for Tunneling	(3), (4), (6), (9), (11), (12), (13), (16)
Quality Control	(2), (6)
Patents	(1)

FIGURE 2.1. CATEGORIES OF GROUTING AGENTS COMMONLY USED IN TUNNELING

Grouting Agent	Applicable Ground Conditions	Purpose of Treatment	Comment
Quick Set Clay Cement	Fissured rock or soil; coarse sands or gravels	Strengthening or Water tightening	
Silicates	Coarse to fine sands, silty sands only in very dilute solutions	Strengthening or Water tightening	Relatively low cost, environmentally safe, durable if not exposed to air
Acrylamide	Finely fissured rock or soil, fine sands, silty sands	Water tightening	Very low viscosity, toxic, must be handled with care, expensive relative to silicate
Phenolic Resins	Finely fissured rock or soil, fine to silty sand	Strengthening or Water tightening	Very low viscosity, expensive relative to silicate
Lignochrome	Coarse to fine sands	Strengthening or Water tightening	Relatively low cost, toxic, must be handled with care
Foams	Coarse to fine sands	Strengthening or Water tightening	High cost, toxic, can provide very high strength

few minutes. Fast set times guarantee that the grout will harden close in to the vicinity of the grout pipe and thus location of the grout is well established. Clay cement is often used as a preinjection in sands with a mixture of grain sizes to fill coarse voids prior to injections using more penetrable grouts.

Sodium Silicate Systems

Medium and fine-grained sands can be treated via silicate gels, lignochrome resins or asphaltic emulsions. Of these grouts, the silicate gels find the most common application. The silicate precipitate or gel can be formed by adding to a sodium-silicate solution any of the following: sodium bicarbonate, hydrochloric acid, sodium aluminate, copper sulfate, ethyl acetate, glyoxyl, formamide, or calcium chloride. The reaction with calcium chloride is almost instantaneous while the others create a slower and controllable reaction. When grouting with calcium chloride, the sodium silicate and calcium chloride are injected into the ground through separate pipes so that the flash reaction occurs in the ground when the two agents encounter each other. This is known as "two shot" or Joosten grouting. This type of treatment, when performed correctly, creates a strong and durable stabilized soil and is a reliable and well established procedure. However, the use of two separate injections to get the grout in the soil drives up the cost, and the technique is now used primarily in very shallow work where injection pipes can be driven quickly.

The controllable reaction time of the sodium silicate with agents such as formamide or ethyl acetate allows mixing before injection, a procedure called a "one-shot" process. The actual gel time of the

grout mixture is a function of the percentage of the reactive used. Often a third agent is added to speed the gelling; calcium chloride is commonly used for this purpose. The gel time can be controlled from hours to as low as several minutes. In practice, a gel time of one hour is common unless the ground water in the injection area is moving when a smaller gel time might be used.

The wide variety of gelling agents for the "one-shot" grouts offers flexibility in choice of reactives. However, it creates problems in that many of the combinations are proprietary; almost every grouting contractor offers a different specialty product of the silicate type grout. Also few, if any, of the grouts has been thoroughly tested, especially in regard to stress-strain behavior of the grouted soil and durability. In a subsequent section of this report the known information on silicate stabilized soil behavior will be reviewed.

Resins

For fine-grained soils in the silt category, only resin grouts have a low enough viscosity for penetration. For comparison, the viscosity of resin grouts can be as low as 1.5 centipoise while silicate grout viscosity is in the range of 30 centipoise. Two types of resin grouting agents are available on the commercial market, the phenolic and the acrylamides. The well known American Cyanamide product AM-9 is an acrylamide resin. Acrylamide resins are effective in water tightening of soil but provide little strength increase. Phenolic resins give both water tightening and strength increase effects, but are not as well known in the U.S. as the AM-9 type grout.

Both types of resins are expensive and typically find only spot use.

Costs per cubic yard of resin treated soil range from \$200 to \$300 as opposed to the \$50 to \$200 per cubic yard for silicate treatment.

TUNNEL GROUTING EXPERIENCE

Grouting is largely an art because (1) the subsurface materials to be stabilized are typically variable and (2) the chemical grouts used in the injections, and the injections themselves require exceptional care to insure a proper in-situ product. Thus, experience is an important component in the grouted tunnel technology. This section of the report summarizes available published information on grout zone size and properties and performance data. Details conveying methods of grouting for tunnels are given in another report produced for this research project (Clough, 1976).

Stabilized Soil Zones

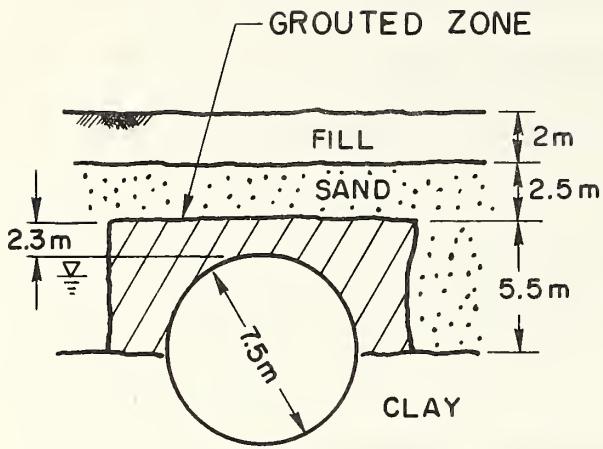
The required shape and size of a grouted zone for a tunnel is primarily a function of the following parameters:

1. Soil type(s) and distribution
2. Strength and stiffness of soil
3. Groundwater conditions
4. Depth and size of tunnel
5. Nature of overlying structures or loads
6. Relative location of tunnel and nearby structures or loads
7. Strength and stiffness of grouted soil
8. Purpose of grouting effort (strengthening or water tightening?)

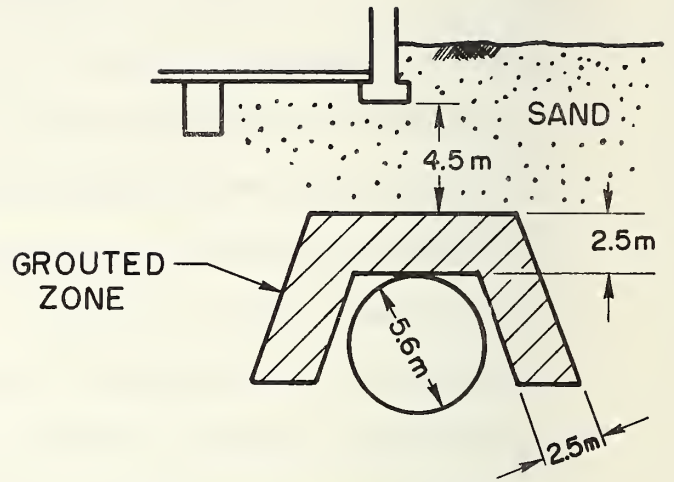
Some examples of grouting zones used in European and English projects are depicted in Fig. 2.2. The simplest geometry for a stabilized region is that used in the Frankfurt example. Here a rectangular zone, 3m thick and 10m long, was used which surrounded only the upper half of the tunnel. The zone did not surround the whole tunnel because the lower part of the tunnel was in impervious clay; only the sands were stabilized. The grouted soil strength in this case was reported to be very high; unconfined compressive strengths of 2900 kN/m^2 (420 psi) were supposedly obtained.

A variation on the Frankfurt type solution is shown in Fig. 2.2 (b) for Nuremberg. The soil conditions are homogeneous sands and ground water is not a problem. In this case the structural part of the grout zone consists of an arch made up of trapezoids, 2.5m thick, which surround the tunnel. The grouted soil in the arch is designed for an unconfined compressive strength of at least 1050 kN/m^2 (150 psi). Inside the arch the soil is partially grouted with a mix designed to give only a modest strength to the soil. This area is injected with grout prior to the hard grout regions so as to prevent penetration of hard grout into the area to be tunneled. Grouting is being performed in Nuremberg using tube a manchette procedures which allow for definitive control on grout placement and injection of different strength grouts as shown.

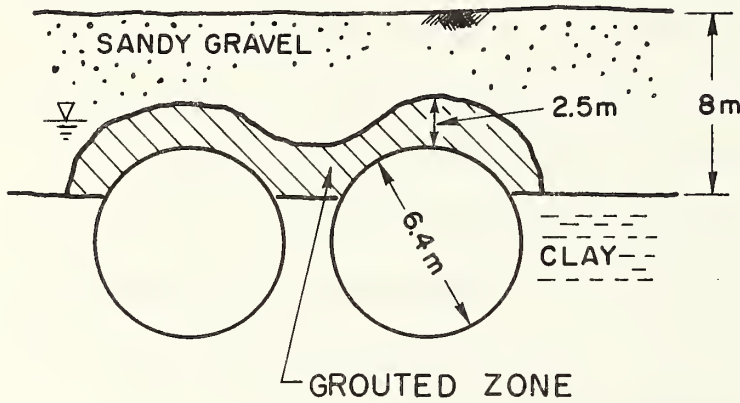
Where groundwater is a problem, the grout zone must completely seal off the pervious soils around the tunnel. In Fig. 2.2 (c), a tunnel in London is shown where the top half is in pervious soil but the bottom half is in impervious soil. The stabilized zone, 2.5m thick, forms a semi-circular arch over the tunnel designed to seal off the pervious



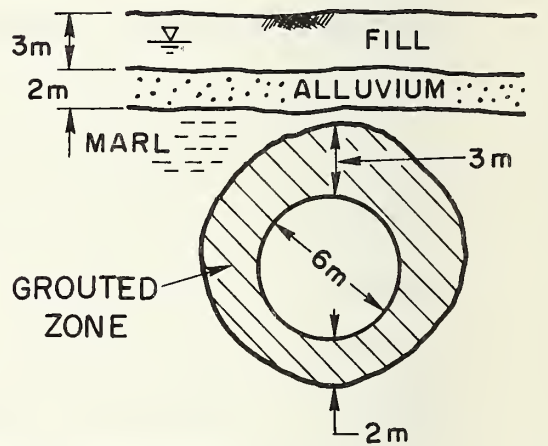
(a) FRANFORT EXPRESSWAY
(After Ref. 11)



(b) NUREMBURG SUBWAY
(After Ref. 6)



(c) LONDON SUBWAY
(After Ref. 6)



(d) PARIS SUBWAY
(After Ref. 6)

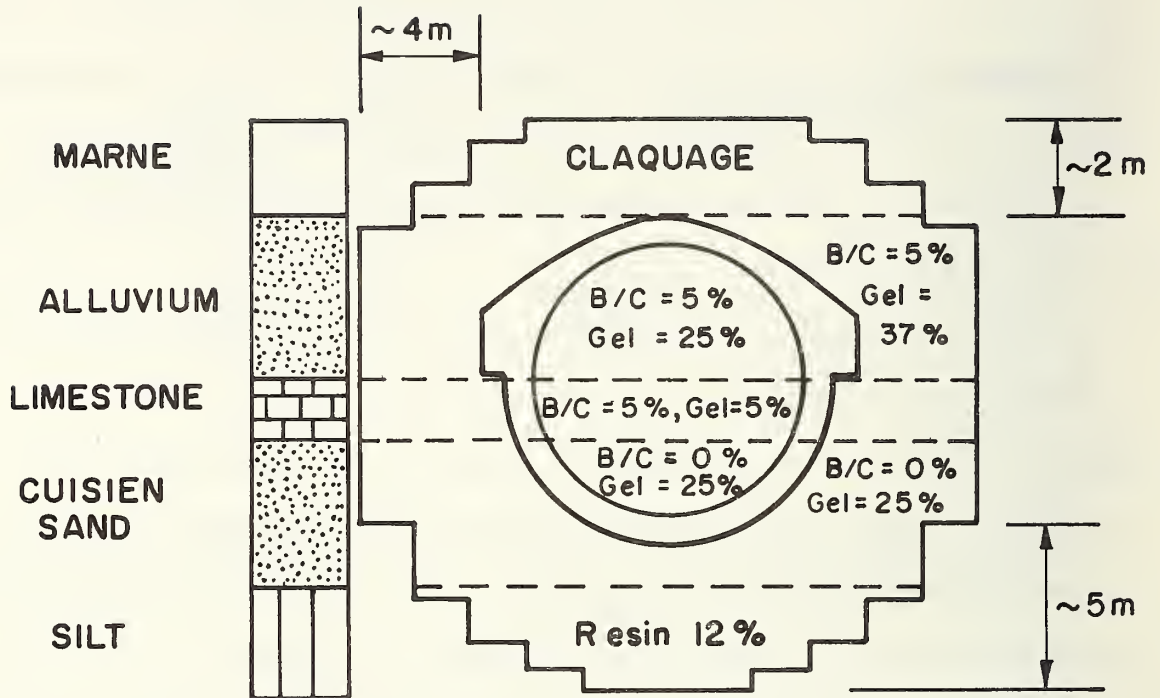
FIGURE 2.2. GROUTING ZONES IN EUROPEAN CITIES

soils and provide strength. The thickness was selected to insure water tightness as well as to minimize surface settlements above the tunnel. Strength values were not specified nor measured for this project.

For cases where pervious soils surround the tunnel, the grout zone needs to completely encircle the tunnel. As shown in Fig. 2.2 (d), these zones are often made thicker at the top than at the bottom since the top-most zones are carrying a greater structural load in the event of overlying structural loads.

In nonhomogeneous soil profiles, the grouting zones in Europe are often varied in section as well as along the profile. An example of a complex case in section is shown in Fig. 2.3, for a Paris Metro line. Five soil types appear in the section and grout zone sizes and types of grouts are varied to suit the different soils. Maximum thickness of the zone is 5m in the weakest soil. Placement of different grouts within a section as in Fig. 2.3 requires use of a sophisticated procedure such as the tube a manchette technique.

The examples in Figs. 2.2 and 2.3 illustrate typical kinds of grout zones used in tunneling. Further information is given in Table 2.2, which documents the sizes and shapes of grouted zones for 17 cases of European and U.S. practice. Sizes of the zones vary considerably because, in part, the requirements of the problems are different and also because no consistent design procedures are available. The minimum thickness of any of the stabilized zones after tunneling appears to be around 2 meters.



Note: B/C = Bentonite Cement
 Gel = Silicate Basalt Gel
 Percentages are by volume
 of soil treated.

FIGURE 2.3. TYPICAL SECTION DESIGN FOR GROUT TREATMENT, PARIS METRO
 (COURTESY SOLETANCHE, S.A., PARIS, FRANCE)

TABLE 2.2. CASE HISTORY DATA, GROUTED TUNNELS

Location	Size of Tunnel or Opening	Purpose of Treatment	Description of Grouted Area	Estimated Maximum Strength of Grouted Soil (Type of Treatment)
Paris 1970	10 m diam.	Make sands impervious Minimize movements Reduce pressure of compressed air	Surrounds tunnel-thickness, 4 m top bottom	966 kN/m ² (combined treatment, clay cement, silica gel and resin grout)
Paris 1970	27 m span	Same as 1	Surrounds opening-thickness, 8 m top 3 m bottom	(Not given)
Hamburg 1972	2 Tunnels 7 m diam. 5 m apart	Minimize movements	Rectangular zone around upper half of tunnels, 7 m thick 10 m long	1450 kN/m ² (silica gel grout)
Munich 1972	2 Tunnels 7 m diam. 5 m apart	Same as 1	Rectangular zone around upper half of tunnels, 2 m thick	1970 kN/m ² (clay cement and silica gel grout)
Frankfort 1972	7 m diam.	Minimize movements of overlying rail-road tracks	Rectangular zone around upper half of tunnels, 3 m thick 10 m long	2890 kN/m ² (silica gel grout)
Vienna 1972	7 m diam.	Same as 1	Rectangular zone around upper half of tunnels, 7 m thick	1970 kN/m ² (silica gel grout)
Milan 1972	2 Tunnels, 7 m diam. 10 m apart	Minimize movements of overlying underground canal and expressway	Rectangular zone around upper portion of tunnels, 7 m thick 30 m long	(Not given)

TABLE 2.2 Continued

Location	Size of Tunnel or Opening	Purpose of Treatment	Description of Grouted Area	Estimated Maximum Strength of Grouted Soil (Type of Treatment)
London 1965	4 m diam.	Same as 1	Not described	(Not given)
London 1963	3 m diam.	Make sands impervious	Arched zone around sandy bottom of tunnel	480 kN/m ² (resin grout)
Seafield Colliery, England 1963	6 m wide 4 m high	Stabilize running sandstone	Arched zone around top of opening	(Not given) (AM-9 grout)
New York City 1972	3 to 5 m diam.	Same as 1	Arched zone around soil zones of mixed-face tunnels, about 3 m in thickness	(Not given) (AM-9 and terranier)
London 1975	6.4 m diam.	Same as 1	Arched zone around top half of tunnel, 2.5 m thick	(Not given) (Silica gel grout)
Paris 1975	7 m diam.	Same as 1	Circular zone surrounds tunnel, 2-5 m thick	(Not given) (Clay cement, silica gel grout)
Nuremburg 1975	5.6 m diam.	Minimize movements	Trapezoidal arches 2.5 to 5 m thick	1030 kN/m ² (Silica gel grout)

TABLE 2.2 Continued

Location	Size of Tunnel or Opening	Purpose of Treatment	Description of Grouted Area	Estimated Maximum Strength of Grouted Soil (Type of Treatment)
Washington, D.C. 1974	6.5 m	Minimize movements	Rectangular zones	(Not given) (Clay cement, silica gel grout)
Washington, D.C. 1975-1976	6.5 m	Minimize movements, restrain groundwater	Rectangular zones	(Not given) (Silica gel grout)
Washington, D.C. 1976	6.5 m	Minimize movements, restrain groundwater	Rectangular zones	520 kN/m ² (Silica gel grout)

Strengths of Stabilized Soil Zones

In a majority of cases in Table 2.2, the grouted soil strength is given; values range from 480 to 2900 kN/m² (70 to 420 psi). In none of the cases except Nuremberg is it known exactly how the strengths of the soils were measured. Since the strength of a grouted soil varies with sampling technique, curing environment, loading rate and confining pressure, it is important to define testing conditions. Based on European practice, it seems likely that the "strength" given in Table 2.2 are from unconfined compression tests conducted at a relatively high loading rate. As such, the strength values can only be taken as indices which are useful as classification parameters. The actual field strength of the grouted soils is a function of stress level around the tunnel, rate of tunnel advance, water conditions and other variables.

In accordance with past European practice, the strength of the grouted soils were most likely not a specified requirement for the jobs. On more recent projects, minimum strengths are being required and must be verified by testing. In the Nuremberg case in Table 2.2, a minimum strength and the test procedures to obtain the strength are specified. The grouted soils must be able to demonstrate an ability to achieve an unconfined strength of 1034 kN/m² (150 psi) and show resistance to increasing deformations under constant load. Sampling of the grouted soils is carried out by coring, a technique only reliable for higher strength grouted soils.

It is significant that many of the strengths shown in Table 2.2 are above 1380 kN/m² (200 psi). Such values can only be obtained where the soils are clearly groutable and relatively high chemical concentrations are used in the grouts. The silicate gels used in many of the cases

described in Table 2.2 are likely composed of 60 percent or higher of sodium silicate (by volume). This type of grout is relatively viscous and useable only for coarser grained sands.

Performance of Grouted Tunnels

The performance of a grouting system around a tunnel may be gauged in terms of the elimination of water inflow into the tunnel, the elimination of runs of soil into the tunnel or minimization of settlements above the tunnel. Published data on performance of grouted tunnels generally indicates very satisfactory behavior. Unfortunately, few problems are usually brought out in to open discussion in printed literature.

In private correspondence, however, some problem areas have been identified such as:

1. Settlements caused by careless drilling procedures for large numbers of grout holes.
2. Poor contact between grout and foundation elements where such contact is called for.
3. Lack of grout penetration into silty zones with a sandy soil.
4. Creep of grout zones under extended loading.

These problems generally lead to no more than minor difficulties; in only two instances known to the authors have serious failures resulted. In both cases, large settlements of walls underpinned by grouting occurred. The resulting effects were exaggerated because the grout zone was an exposed, unsupported underpinning wall subjected to long term foundation loads. By proper design and construction procedures these problems can be avoided.

DESIGN OF STABILIZED SOIL SUPPORT SYSTEMS

The design of a chemical stabilized soil support system for a tunneling problem has been in the past largely a function of experience. The wide variation in grout zone sizes and strengths employed for similar cases in Table 2.2 illustrates that the practice is not standardized. In certain locations experience alone may provide an effective means of design. For example, in London where soil conditions are very consistent, experience from one area can be directly extrapolated to another. This system breaks down, however, when new grouts are used or where different soil conditions are encountered.

Development of a new and consistent design tool for ground support is faced with a formidable array of problems. First, the tunnel problem itself is hardly amenable to closed form analysis because of inhomogeneous ground conditions, and nonlinear soil and grout material behavior. Second, the physical aspects such as actual in-situ grout zone size and influence of method of tunneling are important and these are hard to accurately define prior to actual construction. It would appear that a new design tool must ultimately combine the results of sophisticated analytical solutions which can simulate the complex ground condition and behavior, with results of past experience which contains valuable information as to tolerances and influence of different tunneling and grouting procedures.

The finite element method offers the greatest promise in providing an analytical tool with the capabilities to handle the grouted tunnel problem. It has great flexibility in modeling complex soil conditions and soil behavior and accounting for the interaction of the various

elements of the problem. In several instances it has already been applied to specific grouted tunnel problems in Europe, primarily to provide information which would confirm the effectiveness of a design developed on the basis of experience. Research in the present Stanford program is designed to adapt the finite element method as a general grout zone design tool. The results of the analyses will be integrated with those of past experience.

BEHAVIOR OF SOILS STABILIZED BY SILICATE SYSTEMS

Detailed study of grouted soil behavior is a relatively recent endeavor. The grouted soil presents a special problem for investigation since it is a combination of two materials, soil and grout, both of which have complex behaviors. Soil typically exhibits nonlinear and plastic stress-strain response. The grout adds a component whose behavior varies with small changes in chemical concentrations, temperature and curing environment. Additionally, grouts are usually subject to creep and loss of strength with constant load. Published information on the behavior of the combined soil-grout system, where silicate grouts have been used, are reviewed in the following paragraphs.

Unconfined Compression Strength

Much of the available information on grouted soil behavior deals with strength. The primary mode of testing has been the unconfined compression test. Because conditions in this test are not necessarily representative of stress conditions in the ground, the results should not be taken as yielding an in-situ strength. The unconfined compression test does provide information which allows comparison of sample behaviors and it is simple to conduct.

Recent unconfined strength test programs on silicate stabilized soils have been reported by Warner (1972), Koenzen (1975), Rhone Prolenc Industries (1975) and Gartung and Kany (1975). These investigations have shown the strength of a silicate stabilized sand to significantly depend upon the following parameters:

1. Percentage silicate
2. Percentage hardener
3. Rate of loading
4. Age
5. Curing environment

Factors which have been found to be of a lesser influence on strength are:

1. Sand density
2. Grain size of sand
3. Initial moisture content of sand

Table 2.3 presents a summary of the important facets of the various test programs. This information shows that each of the investigations is different from each other, often in two or more important characteristics, meaning that comparisons of the results of the investigation is difficult. Only Koenzen (1975) and Gartung and Kany (1975) used the same test procedures, with the grain size of the test sand the single difference between the two. Thus, most of the available results have to be viewed independently of one another.

The influence of silicate and hardener content on the strength of a grouted sand is illustrated in Fig. 2.4 via results provided by Rhone-Prolenc (1975). The hardener in this case is Durcisseurs 600a Rhone-Prolenc product. It is apparent from the data that as more silicate is

TABLE 2.3 EXPERIMENTAL PROGRAMS ON SILICATE STABILIZED SOIL

Reference	Grout Mix(es) (% by volume)	Type Sand(s)	Rates of Loading	Age of Samples at Test - days	Curing Environment
Warner (1972)	Variable Silicate % Hardeners=Formamide and unspecified others		20 psi/sec. -failure in 10-20 min.	Varies -- 0 to 730	Submerged, air dry, oven dry
Koenzen (1975)	70% Silicate	Fine to Medium Sand, 0% Pass- ing, 200 Sieve	Varied from constant to 0.2% /min.	3,7,28 & 100 days	Closed tube, soil initially saturated.
Rhone- Prolenc (1975)	Variable Silicate % Durcisseus 600 from 2-9%	Medium, 0% Passing, 200 Sieve	25% /min.	2 to 7 days	Closed tube
Gartung and Kany (1975)	70% Silicate 12.5% Formamide	Coarse, 0% Passing 200 Sieve	0.02% /min. to 2%/min.	7 days	Closed tube, soil initially saturated
French Underground Committee (1976)	Variable Silicate % Durcisseus 600, 2-9% or Ethyl Acetate, 3-10%	Medium, 0% Passing 200 Sieve	25% /min.	1	Closed tube

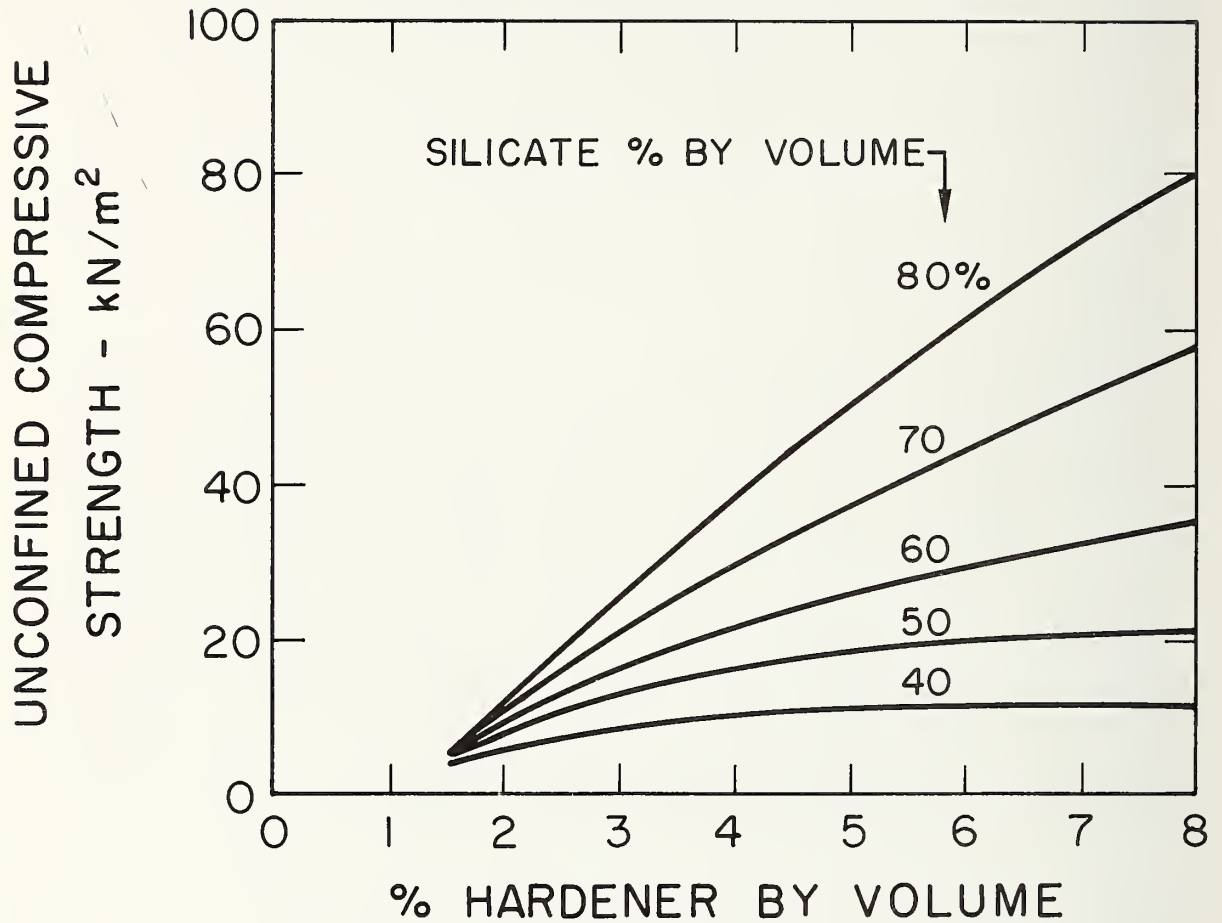


FIGURE 2.4. INCREASE IN UNCONFINED COMPRESSIVE STRENGTH WITH SILICATE AND HARDNER CONTENT (AFTER RHONE-PROLENC, 1975)

used, the strength increases, although this effect is greatest when using higher percentages of hardener. Increasing the hardener percentage also results in an increase in strength, this effect being larger for higher silicate contents. Higher percentages of hardener, in addition, shorten gel times, thus increasing the rate of strength gain. According to the results in Fig. 2.4, using the highest percentages of silicate and hardener, yields a sample unconfined compressive strength of 4800 kN/m^2 (700 psi). It should be kept in mind that these strengths were obtained on samples tested at the very high strain rate of 25%/min. Slower strain rates would undoubtedly result in lowered strength values.

Rate of loading effects are demonstrated by the results of Koenzen (1975) in Fig. 2.5. In five strain controlled tests the strain rate was varied from 0.2%/min, a typical laboratory rate, to 0.0004%/min, and the peak strength demonstrated a decrease as the load rate was slowed. The strength in the case of the fastest test is about twice that of the slowest test. Koenzen (1975) has further demonstrated rate effects by conducting constant load creep tests, typical results from which are shown in Fig. 2.6. Regardless of load level, all samples show creep strain developing with time, however, the effects are more dramatic as load level is increased. In Fig. 2.6 creep rupture occurs at 6.0 Kg/cm^2 . This failure load is only 40 percent of the peak failure load from the constant strain rate uniaxial test conducted at 0.2% strain per minute (see Fig. 2.5). Warner (1972) has also demonstrated this loss in strength under constant loads, noting a reduction in strength of 20% to 80% for each of six different types of grouts when creep test results are compared to short term load tests.

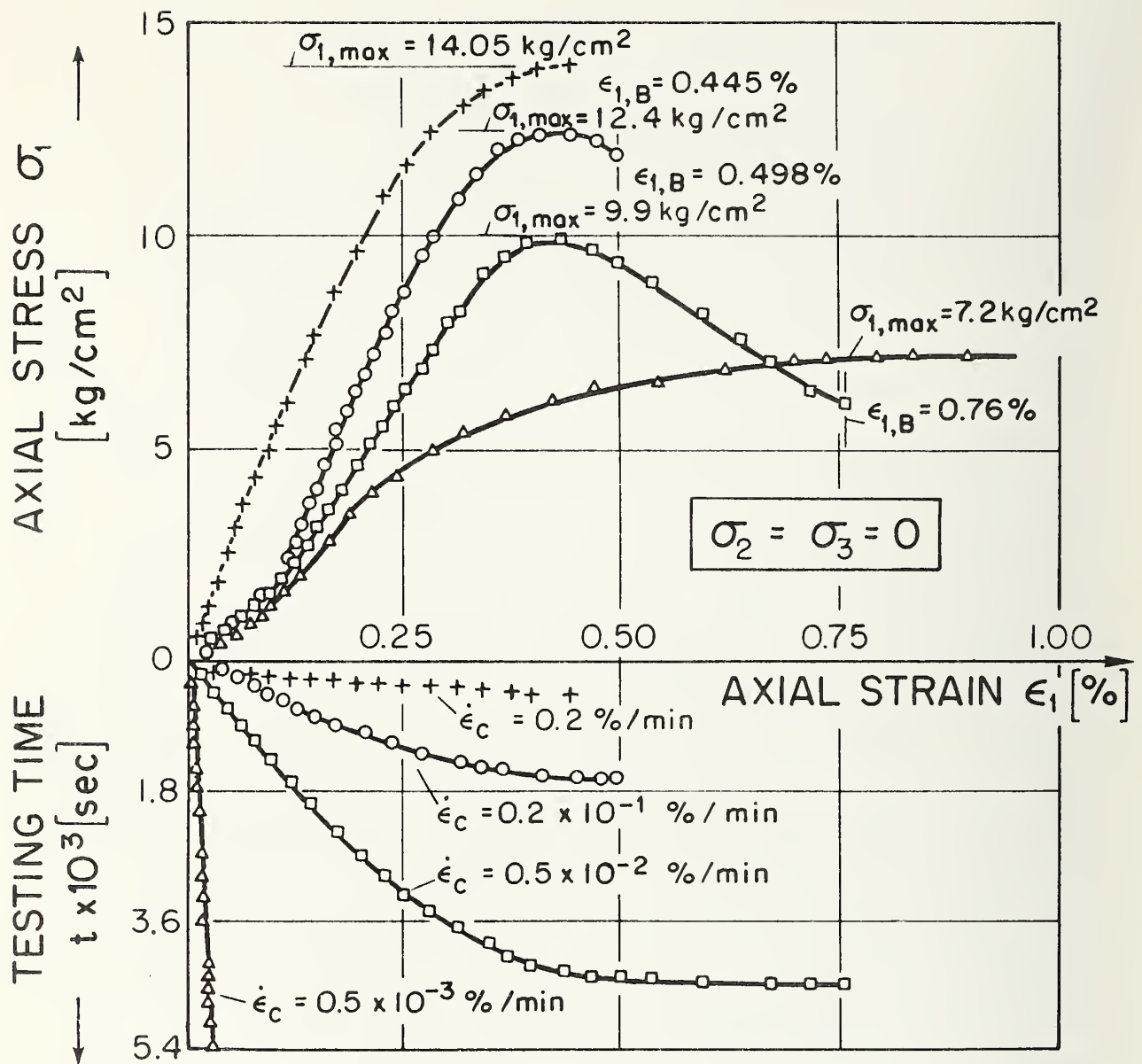


FIGURE 2.5. VARIATION IN STRESS-STRAIN RESPONSE WITH RATE OF LOADING (AFTER KOENZEN, 1975)

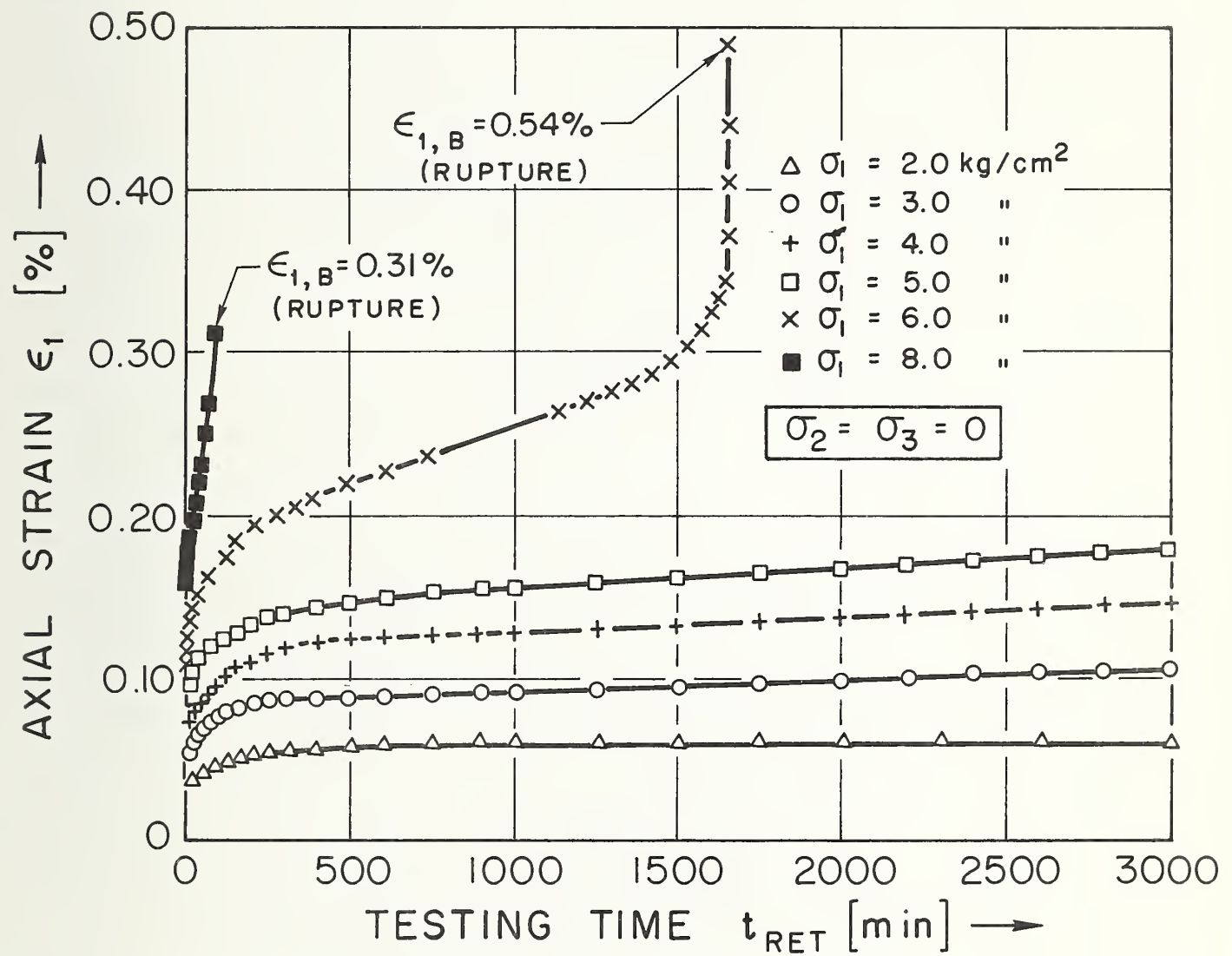


FIGURE 2.6. RESPONSE OF GROUTED SOIL TO CONSTANT LOAD
(AFTER KOENZEN, 1975)

Aging effects on silicate grouted soils are reported by Warner (1972) and illustrated in Fig. 2.7. In curing the specimens before testing, they were kept totally submerged. The results show that after the initial rapid strength gain within the first ten days, the sample strengths with further aging can decrease or increase depending upon the grout type. In the case of samples cured air-dry, similar effects were observed, although the strength of the submerged cure specimen were less than those of the air-dry cure specimens.

Effect of Confining Stress or Strength

Triaxial tests on silicate stabilized soils which allow the confinement on the sample to be varied have apparently only been published for one previous investigation (Gartung and Kany (1975)). Tests of this type on cement stabilized sands have shown that the strength of these materials comes from both friction and cohesion (Mitchell (1976)). The data suggests that the friction angle of cemented sands is essentially that of the original noncemented sand. The function of the cement is primarily to add a cohesion component to the strength.

The data of Gartung and Kany (1975) on silicate stabilized sands are not so extensive as to allow firm conclusions to be drawn. They suggest the strength envelope for silicate stabilized sands is curved. Interpreted envelopes are shown in Fig. 2.8 for tests run at different rates of strain; the slower the strain rate, the lower the envelope. In any of the cases, however, the strength increases substantially with confining pressure. This means that unconfined compression tests are not adequate to define the strength of silicate stabilized soils.

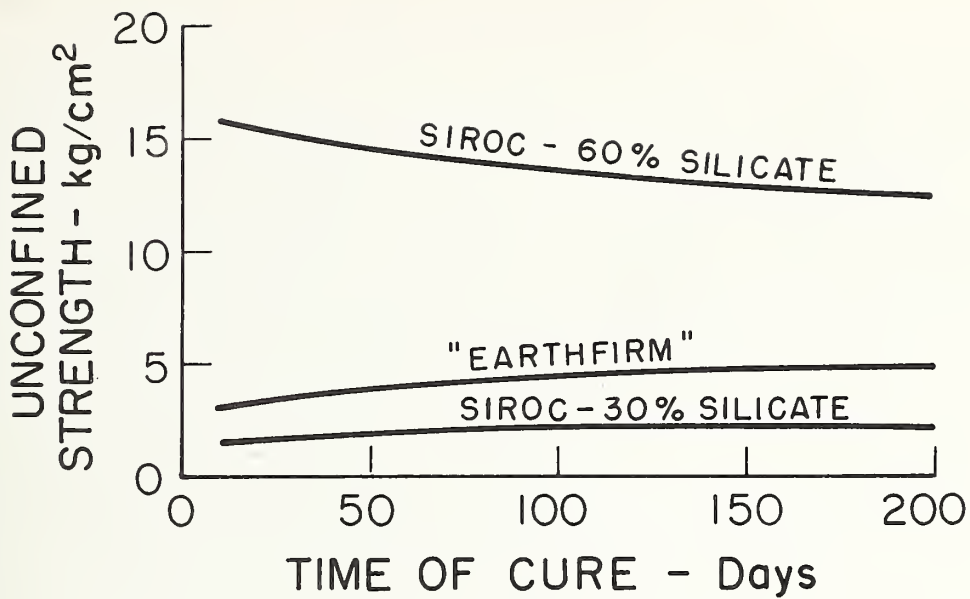


FIGURE 2.7. CHANGE IN UNCONFINED STRENGTH OF GROUTED SOIL WITH CURING (AFTER WARNER, 1972)

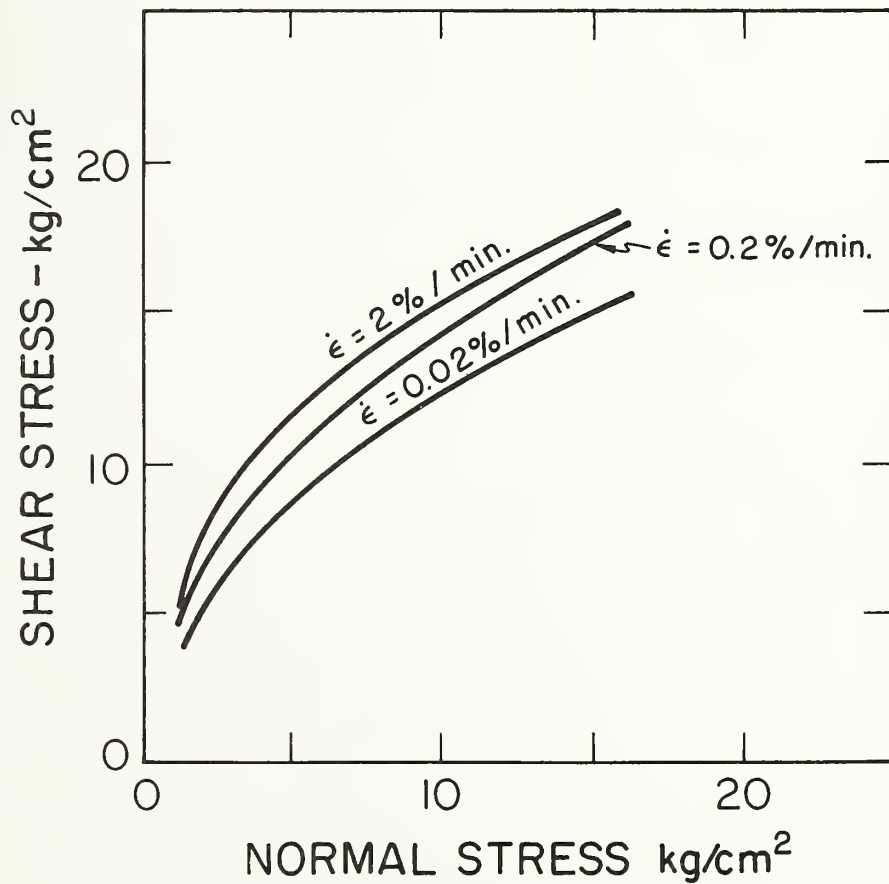


FIGURE 2.8. MOHR ENVELOPES FOR GROUTED SOIL FROM TRIAXIAL TESTS (AFTER GARTUNG AND KANY, 1975)

Stress-Strain Behavior

Most investigations into behavior of stabilized soils have concentrated on the strength aspect. However, in regard to settlement prevention above tunnels, the stress-strain behavior or rigidity is at least as important as strength. Unfortunately, only Koenzen (1975) and Gartung and Kany (1975) report stress-strain behavior for their tests. Typical stress-strain curves for silicate stabilized soils subjected to unconfined compression are shown in Fig. 2.5. The results are for tests performed by Koenzen (1975) at different rates of strain; they show clearly that the stabilized soil decreases in rigidity as the strain rate is lowered. The average slope of the stress-strain curve or modulus before failure drops by a factor of five as the strain rate drops from 0.2%/min to 0.0004%/min. Similar rates of decrease can be shown from the triaxial data of Gartung and Kany (1975).

The creep test results shown in Fig. 2.6 also suggest a continuing increase in deformations under constant load. The results of creep load tests by Koenzen (1975) and Warner (1972) show that even under very low loads, creep straining occurs. In order to correctly predict settlements above grouted zones, the influence of creep as well as load rate needs to be considered.

Effects of parameters other than load rates or sustained loads on stress-strain behavior such as hardener and silicate content, etc., cannot be defined from existing data. This represents a serious gap which limits our abilities to reliably forecast behavior of tunnels in grouted soil. The present investigation is directed towards a study of this problem.

Modeling Observed Stress-Strain Behavior

The foregoing discussion has demonstrated that the stress-strain-strength behavior of a silicate stabilized soil is complex. In order to model the observed behavior Koenzen (1975) has proposed an analytical visco-plastic model which consists of a series of springs, dashpots, and slip elements (see Fig. 2.9). The "elastic" response of the grouted soil is represented by the springs. Plastic behavior is simulated by the slip elements which allow yielding after certain deformation levels are reached. Finally, the dashpots model the viscous response. The model shown in Fig. 2.9 requires five material parameters, all of which can be defined from load tests in the laboratory. This particular model has been shown to reasonably simulate long-time creep response. More complex models can be devised by adding components but they rapidly become unwieldy in terms of the number of parameters needed to define their behavior.

SUMMARY

The review in this chapter has pointed out the fact that there is no developed design method for selecting size, strength, or stiffness of grouted zones around tunnels. Further, it is apparent that there is no established procedure for rationally evaluating what the strength and stiffness of a grouted soil is with respect to what it should be in the ground in order to give a good performance. Unconfined compressive tests are often conducted, but neither the stress conditions, stress path nor load rates used in this test are representative of those under actual tunneling conditions. At present, past experience is largely the design guide with little assurance that this can be economically or safely extrapolated to new conditions.

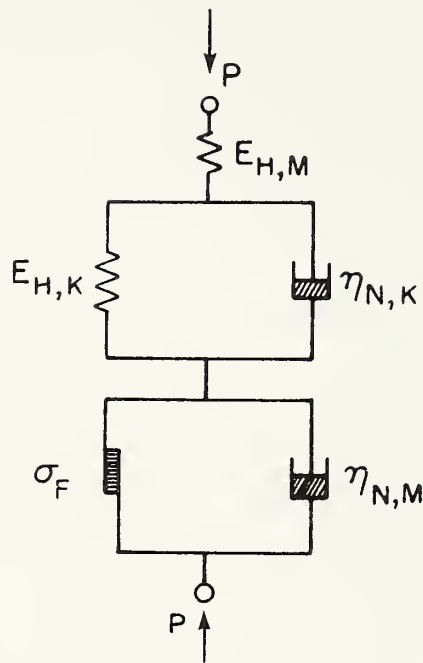


FIGURE 2.9. SIMPLIFIED VISCOELASTIC MODEL FOR GROUDED SOIL (AFTER KOENZEN, 1975)

The review of the behavior of silicate-stabilized soils has shown that there are a large number of factors which affect the response of these soils to load. While much information on silicate stabilized soils is available, the data is insufficient as to stress-strain response, effect of confining pressure and rate of loading influences. A particular deficiency lies in the fact that no method or procedure has been developed to determine what type of test should be used to evaluate silicate-stabilized soil response for grouted tunnel design.

CHAPTER III

LABORATORY TEST PROGRAM

In the preceding chapter it was noted that the review of published test data for grouted soils reveals a distinct nonuniformity of testing procedures and a lack of data on the stress-strain behavior of grouted soils. With these facts in mind, the laboratory test program for the first year of research was designed with the following objectives:

1. Establish a reliable procedure for creating and testing grouted samples.
2. Perform a test program designed to develop an understanding of the important variables that influence grouted soil stress-strain and strength response.
3. Interpret the test results and develop parameters for use in finite element parametric studies of grouted tunnel behavior.

The following paragraphs describe the progress towards these objectives.

LABORATORY PROCEDURES FOR GROUTING

SOIL SAMPLES

In order to allow maximum flexibility in modeling various grouting environments, it was considered that the laboratory equipment for creating grouted soil samples should allow:

1. Use of grouting pressures from very low to 830 kN/m^2 (120 psi).
2. Use of saturated and unsaturated soil sample conditions prior to grouting.
3. Development of a uniform sample.

Before designing equipment to achieve these purposes, existing methods were reviewed.

Existing Techniques to Create Grouted Samples

Little published information is available on methods for grouting soil samples in the laboratory and in order to learn what others were doing, personal contacts were pursued. Basically, two different methods were found in use. In the simplest, grout is mixed in an open container and sand is dumped into the grout; after set-up of the grout, samples may be trimmed. This method does not allow grouting under pressure nor saturation of the soil prior to grouting and was not considered suitable for this investigation.

The other method for creating grouted samples offers more flexibility and eliminates the disadvantages associated with the simplest technique. In this procedure, a column of soil is prepared in a steel or lucite tube; the soil can be dry or saturated as desired.

Grout is injected into the soil in the tube under either a constant pressure control or a constant flow control. The soil sample is extruded from the tube after grout set and is ready for testing. This procedure, with a few modifications, was adopted for the present work.

Techniques Used in Present Investigation

In this investigation both the flow control and pressure control grout injection techniques for preparing samples were tried. The pressure control method was found to be much simpler than the flow control method and to meet all necessary experimental criteria. By fixing the grouting pressure, it was found that flow was also reasonably constant unless the grout underwent a partial set during injection, a problem only present in very unusual circumstances. Further details of testing procedures finally adopted for the work are described as follows.

The equipment employed is depicted in Fig. 3.1. It consists of (1) an enclosed grout pot where the grout components are added and mixed, (2) four upright 9 cm diameter and 71 cm long lucite sample tubes, and (3) a hydraulic system for passage of the grout from the pot into the sample tubes. The sample preparation procedure begins with placement of sand and end filters into the lucite tubes. The end filters consist of a 5cm (2 in.) thick pea gravel layer bounded by wire mesh screens. The bottom filter is installed in the lucite tube before any sand is placed. Build up of the sand follows and any of several procedures may be used. In the tests reported herein, the sand was poured into the tube in 7.5cm (3 in.) lifts and rodded to a dense configuration by tamping the lift 30 times using a 1cm (0.4 in.) diameter wooden dowel. At about 5cm (2 in.) below the tube top, the upper gravel-screen filter is added. At this stage, the tube top plate is clamped into place and the apparatus is ready for water saturation or grout treatment.

If presaturation of the sample is desired, the next step is to fill the grout pot with water. The water is pushed from the pot through the grout lines and into the sand samples by introducing air pressure on the top of the water in the pot via a pressure port on top of the pot. Almost all samples tested were prepared using the presaturation technique.

After the water saturates the sand samples, the bottom valve of each sample tube is closed to retain the water in the sand, and the grout pot and hydraulic lines are emptied of water. The grout components are then poured into the grout pot and mixed using a stirring mechanism (see Fig. 3.1).

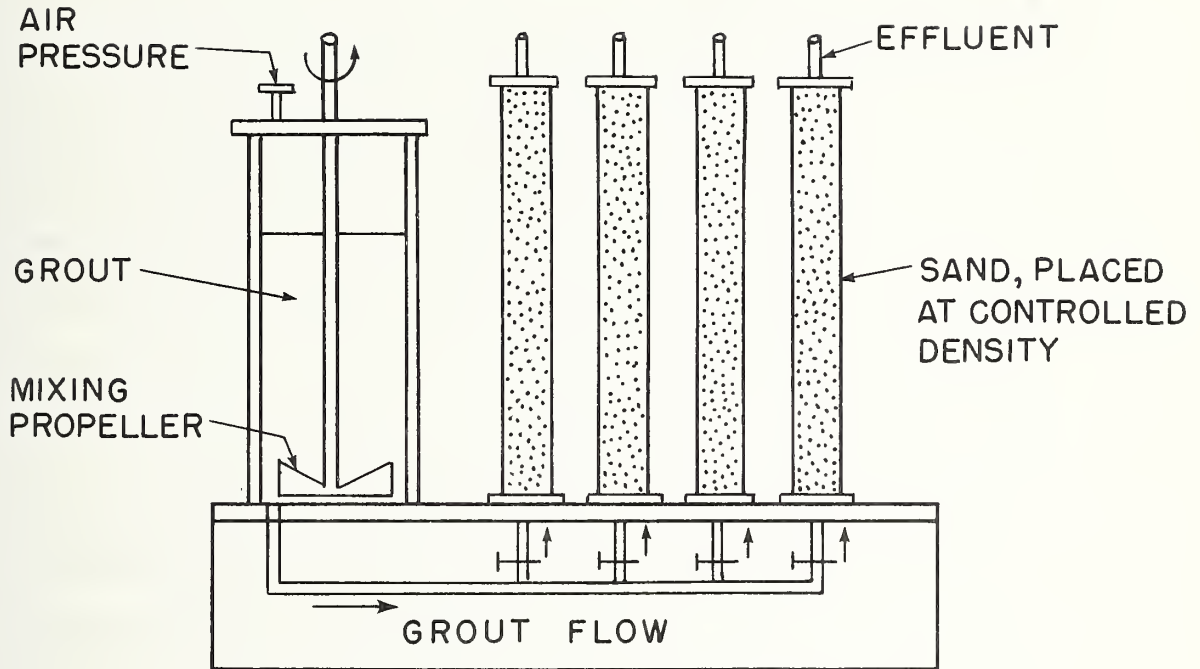


FIGURE 3.1. SCHEMATIC OF GROUTING APPARATUS

The stirring is continued throughout grouting to insure good mixing and to prevent any tendency towards grout flocculation. Grouting of the sand samples proceeds in the same manner as the injection of water. Each tube of soil is grouted independently.

During the early phases of this investigation, the grouted soil samples were extruded from the sample tubes after grout set by jacking. Subsequent concern over possible disturbance of the samples by the jacking led to the use of split sample forming tubes. The new tubes, now employed in every test, are split by a small gap down the entire length on one side only. When grouting a sample, the gap is closed by means of pipe clamps tightened at intervals along the tube. Sealing of the gap is accomplished by applying adhesive tape along the gap on inside of the tube. After the sample is grouted and the grout sets, the pipe clamps are released; because of the elasticity of the lucite tube, it springs open to restore the gap. This small amount of radial movement releases all restraint on the sample and it slides freely out. The grouted samples are thereafter cut into the lengths required for testing. The top and bottom 7cm or so, of the samples are always discarded.

TESTING METHODS

The test procedures used in the present investigation involved primarily constant rate of strain unconfined and triaxial loading and in a few instances constant load creep tests. Particular care was taken in documenting stress-strain behavior at both low and high strain levels. All samples tested were 7.1cm (2.8 in.) in diameter and 17cm (6.5 in.) in length.

Age of the samples at the time of testing was varied from one to 110 days, although the majority were tested in the range of three to eight days. In storing samples, the grouted soil was left in the lucite sample tubes and capped with polyethylene sheeting. The sheeting and the grout-filled gravel end filters maintained the moisture content of the samples. The rate of strain used in the constant rate of strain tests was typically taken as 0.15%/min. Other strain rates were used to evaluate the effect of this parameter in a few tests.

The triaxial load tests were performed in a standard triaxial apparatus. The photograph in Fig. 3.2 shows the triaxial cell in the loading frame; load and deformation are recorded electronically and fed into the digitizing unit seen on the right of the photograph. The loading frame is a specially adapted unit which can be used for stress control or strain control tests. It is hydraulically operated so that there are no vibrations to disturb the sample during testing. Volume change is measured for each sample using a water-filled burette which is connected via a saturated plastic tube to the bottom of the sample. This procedure is consistent with that used by Koenzen (1975) and Gartung and Kany (1975).

In the initial phases of the test program, attempts were made to measure water contents of the grouted samples. The exact meaning of the water content in a chemically stabilized soil is, however, not clear. In the initial grout mix there is a considerable amount of water, e.g., 64% of the 30% silicate Siroc grout mix is water. This water in the grout is largely locked in during the initial chemical reactions. Heating a sample to determine water content presumably drives off free water from the sand but also some of the water from the solidified grout.

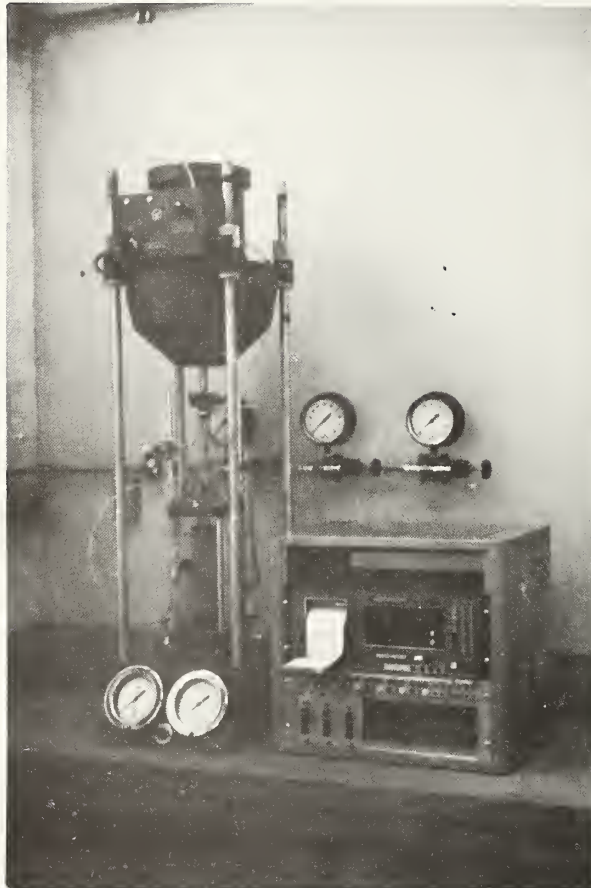


FIGURE 3.2. LOADING AND RECORDING APPARATUS
WITH SAMPLE IN PLACE FOR TESTING

Unfortunately, the degree of contribution of each component cannot be determined and thus the measured water content has no specific meaning.

TEST MATERIALS AND SAMPLE DENSITIES AND PERMEABILITIES

One grout type and two sands were used in the laboratory test program.* Grain size curves for the sands are shown in Fig. 3.3; Monterey sand No.16 is a uniform medium sand while Monterey sand No. 30 is a uniform fine sand. Both sands have predominantly rounded particles and there are no silt or clay size particles present.

The grout used is known by the trade name Siroc and is commercially marketed and readily available to any contractor. Its base is sodium silicate solution and the reactive or hardener is formamide. Calcium chloride is added as desired to accelerate gelling. Water makes up the remainder of the grout. Mix designs are suggested in a manual published by Raymond International (1972). Mixes and their gel times as used in this investigation are shown in Table 3.1. This type of grout is in common use in the United States and has been studied by Koenzens (1975) and Gartung and Kany (1975) in Germany.

The grout components were obtained from local sources. The sodium silicate is available from Philadelphia Quartz Company.

Properties and components of the silicate solution are as follows:

8.9% Na₂O by weight
28.7% SiO₂ by weight
62.4% Water by weight
41° Baume @ 20°C

*An extensive series of laboratory tests were also performed on samples from field grouting trials. Different types of grouts were used in this program, the results of which are described in Chapter Five of this report.

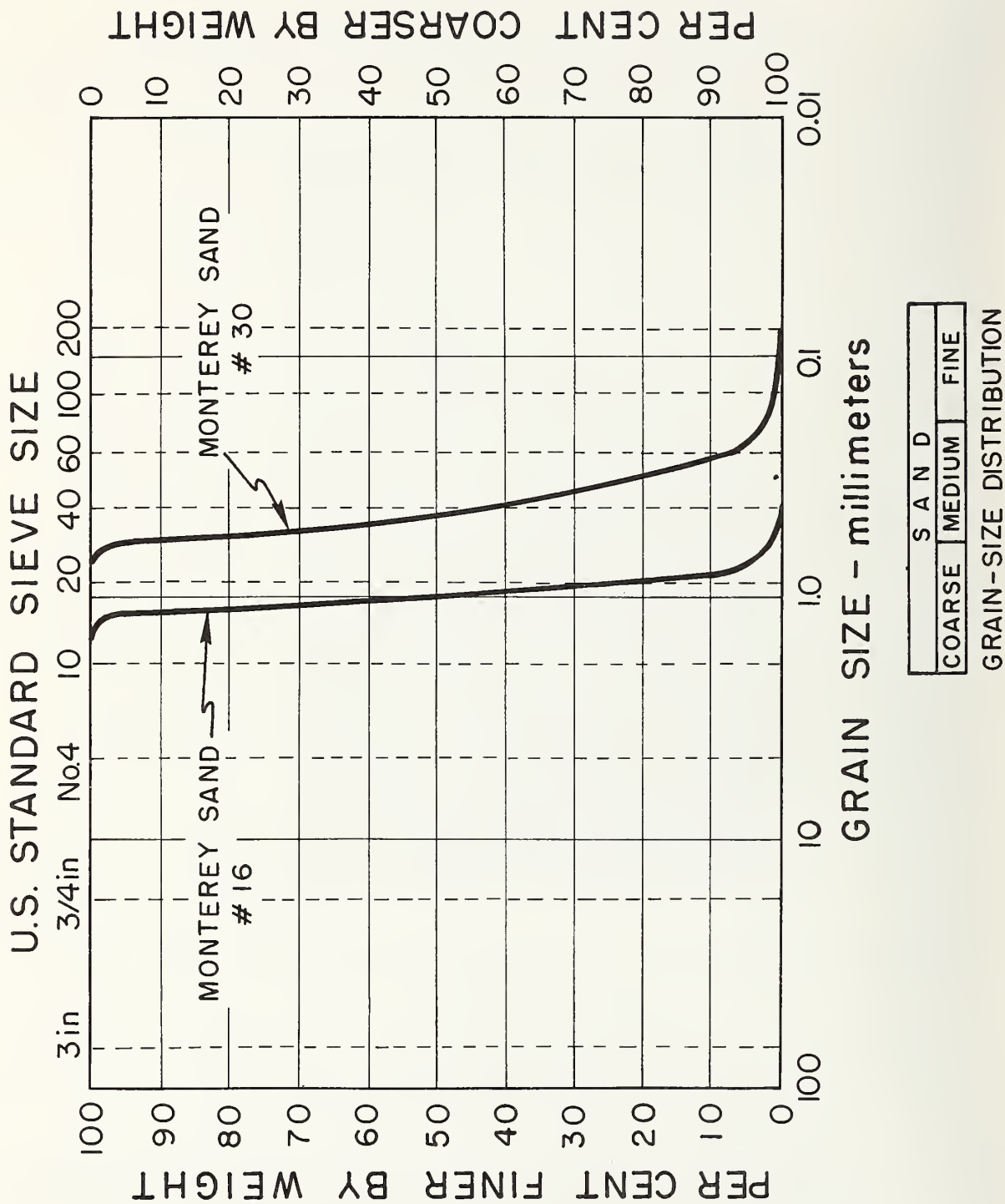


FIGURE 3.3. GRAIN SIZE CURVES

TABLE 3.1. GROUT CONSTITUENTS USED IN LABORATORY TESTS

Percent Silicate	Percent Formamide	Percent WATER	g/l CaCl ₂	Approximate Gel Time--Hours
30	6	64	9.36	1
30	6	64	0	12
50	6	44	0	12
50	9	41	0	10
70	6	24	0	12
70	12	18	0	4

Note: Percent = Percent by Volume

As discussed previously, the sand was poured into the forming tube in three inch lifts and rodded into place. Sample densities were very consistent when prepared by this process. Average density for the Monterey #30 and Monterey #16 sands before grouting were 1.58 gm/cc and 1.62 gm/cc respectively. After grouting, the respective average densities were 1.98 gm/cc and 2.02 gm/cc. For this increase in density, approximately 95 percent of the void space in the sand samples should be filled with grout.

Permeabilities of a number of grouted samples were measured by means of a standard constant head test. The values ranged from 1×10^{-5} cm/sec to 1×10^{-6} cm/sec and are consistent with those reported by Koenzen (1975) for silicate stabilized soil. The permeability of the samples presumably results from flow through the grout itself and the 5 percent of void space not filled by the grout.

TESTING PROGRAM

The first year program was aimed at determining the influence of the following variables on grouted soil behavior:

1. Confining pressure
2. Grout component concentrations
3. Sand grain size
4. Large strain
5. Age
6. Constant load vs. constant strain-rate loading

A total of 83 triaxial and unconfined shear tests were performed during the course of the laboratory work. An additional 31 tests are reported on in Chapter 5 in connection with the field grouting effort.

Important parameters for each laboratory test are given in Table 3.2, along with the observed stress and strain at failure. In the triaxial tests, confining pressures of 0, 69 and 138 kN/m² (0, 10, 20 psi) were employed. Sodium silicate, formamide and calcium chloride percentages* used were 30, 50, and 70; 6, 9 and 12; and 0 and 2 respectively. Age of the samples at testing was varied from 1 to 110 days.

Also noted in Table 3.2 is the type of sample tube forming used, i.e., split or non-split. Comparative results on samples obtained from both types of tubes provides useful information as to the effect of sample disturbance caused during extrusion from the non-split tubes.

RESULTS OF TEST PROGRAM

The data obtained from the tests consists of stress-strain curves, volumetric change curves and strengths. In the following discussion the general stress-strain response will be covered first, the strength behavior second and the initial tangent modulus values for the stress-strain curves third.

General Stress-Strain Response

Effects of Confining Pressure, Chemical Concentration and Large Strains.

In Figs. 3.4, 3.5, and 3.6, typical results from a series of constant strain-rate triaxial tests on stabilized Monterey No. 16 sand, are shown;

*Percent by volume of grout solution.

TABLE 3.2 RESULTS OF LABORATORY TESTS, FIRST YEAR PROGRAM

TEST #	TYPE OF GROUT	PERCENTAGE OF CONSTITUENTS IN MIX		CURING TIME DAYS	CONFINING PRESSURE (PSI)	SAND NUMBER	TYPE OF TUBE	STRAIN RATE IN/MIN	PEAK STRESS (PSI)	STRAIN AT FAILURE %
		SILICATE	CALCIUM CHLORIDE PRESENT							
1	SIROC	30	6	1	0	16	NONSPLIT	0.011	14.1	7.69
2	"	"	"	1	20	"	"	"	90.9	11.67
3	"	"	"	3	0	"	"	"	18.1	1.49
4	"	"	"	4	10	"	"	"	57.2	5.90
5	"	"	"	4	20	"	"	"	118.1	7.08
6	"	"	"	8	22	"	"	0.0021	91.6	9.85
7	"	"	"	9	22	"	"	0.0021	99.1	8.04
8	"	"	"	3	20	"	"	0.011	107.5	9.93
9	"	"	"	3	20	"	"	0.011	95.8	4.61
10	"	"	"	3	20	"	"	0.011	103.9	9.63

TABLE 3.2 - CONT.

TEST #	TYPE OF GROUT	PERCENTAGE OF CONSTITUENTS IN MIX			CURING TIME DAYS	CONFINING PRESSURE (PSI)	SAND NUMBER	TYPE OF TUBE	STRAIN RATE IN/MIN	PEAK STRESS (PSI)	STRAIN AT FAILURE %
		SILICATE	FORMAMIDE	CALCIUM CHLORIDE PRESENT							
11	SIROC	30	6	YES	3	20	16	NONSPLIT	0.011	104.1	6.97
12	"	"	"	"	3	20	"	"	"	98.3	8.75
13	"	"	"	"	4	20	"	"	"	100.4	10.10
14	"	"	"	"	4	20	"	"	"	106.7	7.74
15	"	"	"	"	4	20	"	"	"	99.9	6.36
16	"	"	"	"	4	20	"	"	"	99.1	7.29
17	"	"	"	"	3	0	"	"	"	35.5	1.25
18	"	"	"	"	3	10	"	"	"	68.0	8.07
19	"	"	"	"	3	20	"	"	"	122.5	8.96
20	"	"	"	"	4	0	"	"	"	36.2	0.98
21	"	"	"	"	4	10	"	"	"	96.2	10.08
22	"	"	"	"	4	0	"	"	"	39.0	1.0
23	"	"	"	"	4	10	"	"	"	83.3	10.56
24	"	"	"	"	4	20	"	"	"	123.5	7.8

TABLE 3.2 - CONT.

TEST #	TYPE OF GROUT	PERCENTAGE OF CONSTITUENTS IN MIX			CURING TIME DAYS	CONFINING PRESSURE (PSI)	SAND NUMBER	TYPE OF TUBE	STRAIN RATE IN/MIN	PEAK STRESS (PSI)	STRAIN AT FAILURE %
		SILICATE	FORMAMIDE	CALCIUM CHLORIDE PRESENT							
25	SIROC	30	6	YES	2	20	30	NONSPLIT	0.011	88.3	6.6
26	"	"	"	"	2	10	"	"	"	54.9	5.8
26	"	"	"	"	2	0	"	"	"	14.5	0.93
28	"	"	"	"	2	0	"	"	"	22.5	0.61
29	"	"	"	"	3	10	"	"	"	59.9	4.7
30	"	"	"	"	3	20	"	"	"	93.0	6.4
31	"	"	"	"	4	20	"	"	"	85.1	5.7
32	"	"	"	"	4	0	"	"	"	20.5	0.52
33	"	"	"	"	3	0	"	"	"	41.4	1.29
34	"	"	"	"	3	0	"	"	"	40.9	1.24
35	"	"	"	"	3	0	"	"	"	45.5	1.10
36	"	"	"	"	5	0	"	"	"	37.0	1.51
37	"	"	"	"	5	0	"	"	"	30.3	1.14
38	"	"	"	"	5	0	"	"	"	29.3	1.51
39	"	"	"	"	6	0	"	"	"	33.8	1.05
40	"	50	"	"	7	0	"	"	"	107.4	1.90

TABLE 3.2 - CONT.

TEST #	TYPE OF GROUT	PERCENTAGE OF CONSTITUENTS IN MIX			CURING TIME DAYS	CONFINING PRESSURE (PSI)	SAND NUMBER	TYPE OF TUBE	STRAIN RATE IN/MIN	PEAK STRESS (PSI)	STRAIN AT FAILURE %
		SILICATE	FORMAMIDE	CALCIUM CHLORIDE PRESENT							
41	SIROC	50	6	NO	7	0	30	NONSPLIT	.011	129.3	1.98
42	"	"	"	"	7	0	"	"	"	126.0	1.97
43	"	70	"	"	7	0	"	"	"	91.2	3.87
44	"	"	"	"	8	0	"	"	"	86.2	4.70
45	"	50	"	"	9	0	"	SPLIT	"	205.2	1.37
46	"	"	"	"	9	0	"	"	"	212.4	1.42
47	"	"	"	"	9	0	"	"	"	203.8	1.16
48	"	"	"	"	15	0	"	"	"	242.8	1.35
49	"	"	"	"	18	10	"	"	"	219.5	1.28
50	"	"	"	"	14	0	"	"	CONSTANT LOAD	100.0	--
51	"	"	"	"	15	0	"	"	CONSTANT LOAD	100.0	--
52	"	30	"	YES	7	0	16	"	"	26.6	0.82
53	"	"	"	YES	7	10	16	"	"	63.0	2.33
54	"	"	"	YES	7	20	16	"	"	104.6	4.83
55	"	"	"	YES	7	0	16	"	"	25.9	0.57

TABLE 3.2 - CONT.

TEST #	TYPE OF GROUT	PERCENTAGE OF CONSTITUENTS IN MIX		CURING TIME DAYS	CONFINING PRESSURE (PSI)	SAND NUMBER	TYPE OF TUBE	STRAIN RATE IN/MIN	PEAK STRESS (PSI)	STRAIN AT FAILURE %
		SILICATE	FORMAMIDE							
56	SIROC	30	6	8	10	16	SPLIT	0.011	61.5	2.43
57	"	"	"	8	20	16	"	"	101.8	5.00
58	"	"	"	8	0	16	"	"	24.8	0.56
59	"	"	"	8	10	16	"	"	65.3	2.34
60	"	"	"	8	20	16	"	"	100.9	4.99
61	"	"	"	8	0	16	"	"	8.8	0.48
62	"	"	"	8	10	16	"	"	53.1	5.88
63	"	"	"	8	20	16	"	"	93.4	6.56
64	"	"	"	8	0	16	"	"	7.2	3.04
65	"	"	"	8	10	16	"	"	52.9	6.30
66	"	"	"	8	20	16	"	"	92.4	6.98
67	"	"	"	9	0	16	"	"	9.7	0.50
68	"	"	"	9	10	16	"	"	56.1	5.00
69	"	"	"	9	20	"	"	"	95.6	6.77

TABLE 3.2 - CONT.

TEST #	TYPE OF GROUT	PERCENTAGE OF CONSTITUENTS IN MIX		CALCIUM CHLORIDE PRESENT	CURING TIME DAYS	CONFINING PRESSURE (PSI)	SAND NUMBER	TYPE OF TUBE	STRAIN RATE IN/MIN	PEAK STRESS (PSI)	STRAIN AT FAILURE %
		SILICATE	FORMAMIDE								
70	SIROC	70	6	NO	5	2	16	SPLIT	0.011	103.7	3.93
71	"	"	"	"	5	10	16	"	"	131.3	5.17
72	"	"	"	"	4	20	16	"	"	172.9	6.74
73	"	"	12	"	14	0	16	"	"	371.6	1.21
74	"	"	"	"	13	10	16	"	"	418.3	1.11
75	"	"	"	"	12	20	16	"	"	471.3	1.06
76	"	50	9	"	12	10	16	"	"	165.1	0.81
77	"	"	"	"	14	10	16	"	"	167.2	0.63
78	"	"	"	"	13	20	16	"	"	183.3	0.47
79	"	"	6	"	107	0	30	"	0.011	213.5	0.91
80	"	30	"	"	91	0	30	"	"	34.2	0.68
81	"	"	"	"	91	0	30	"	"	35.1	0.70
82	"	"	"	"	91	0	30	"	"	30.5	0.70
83	"	"	"	"	91	0	30	"	"	30.2	0.66

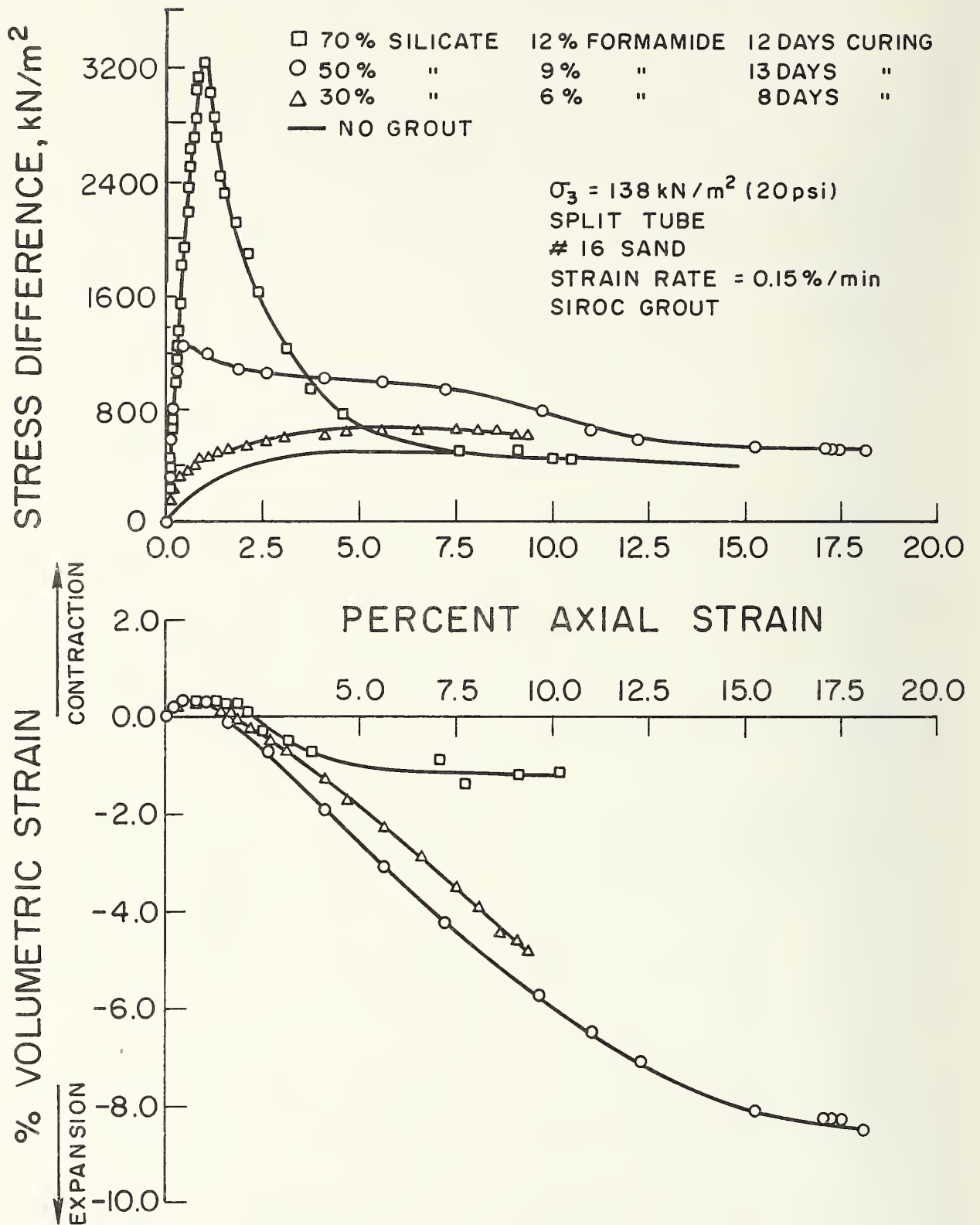


FIGURE 3.4. STRESS-STRAIN BEHAVIOR OF SAMPLES TESTED
 AT $\sigma_3 = 138 \text{ kN/m}^2$

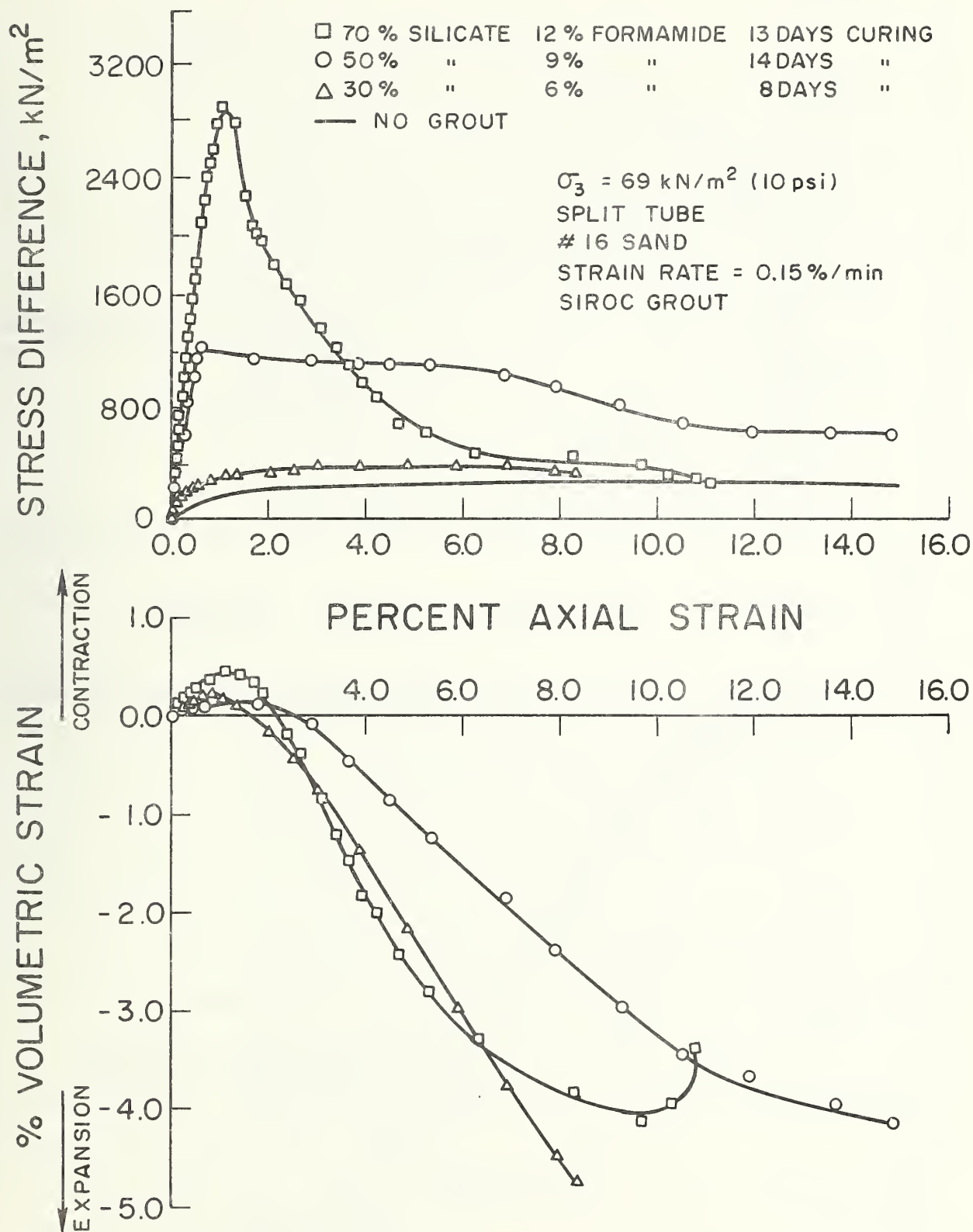


FIGURE 3.5. STRESS-STRAIN BEHAVIOR OF SAMPLES TESTED
 AT $\sigma_3 = 69 \text{ kN/m}^2$

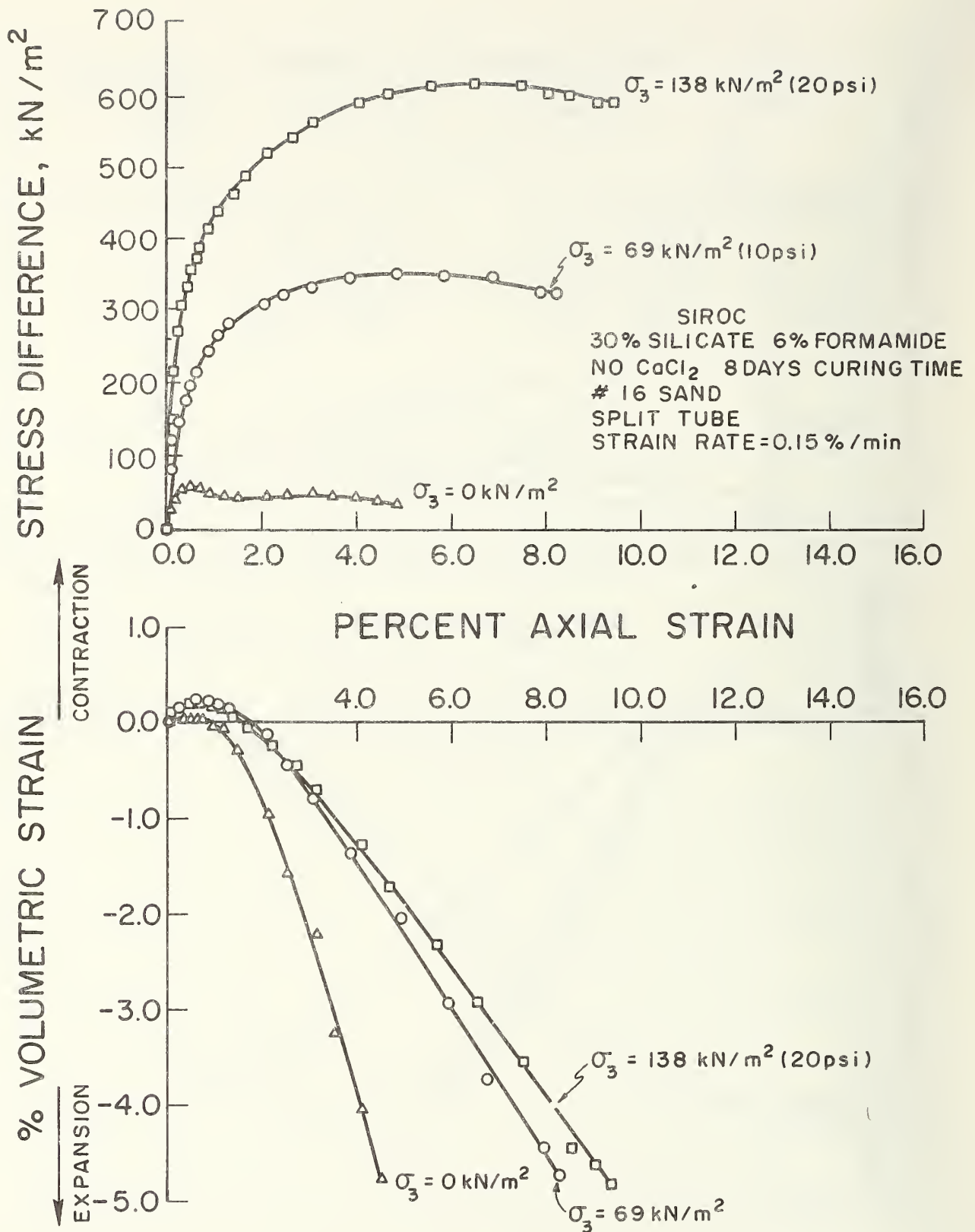


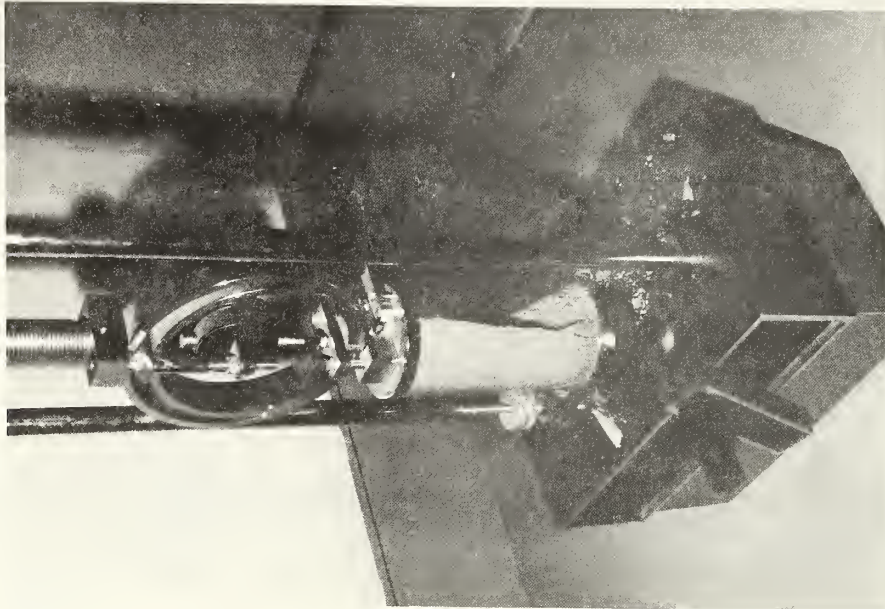
FIGURE 3.6. STRESS-STRAIN BEHAVIOR OF 30% SILICATE SAMPLES TESTED AT VARIOUS CONFINING PRESSURES

principal stress difference and volumetric strain values are plotted against axial strains. These results demonstrate the range of types of behavior which were observed from constant strain-rate tests.

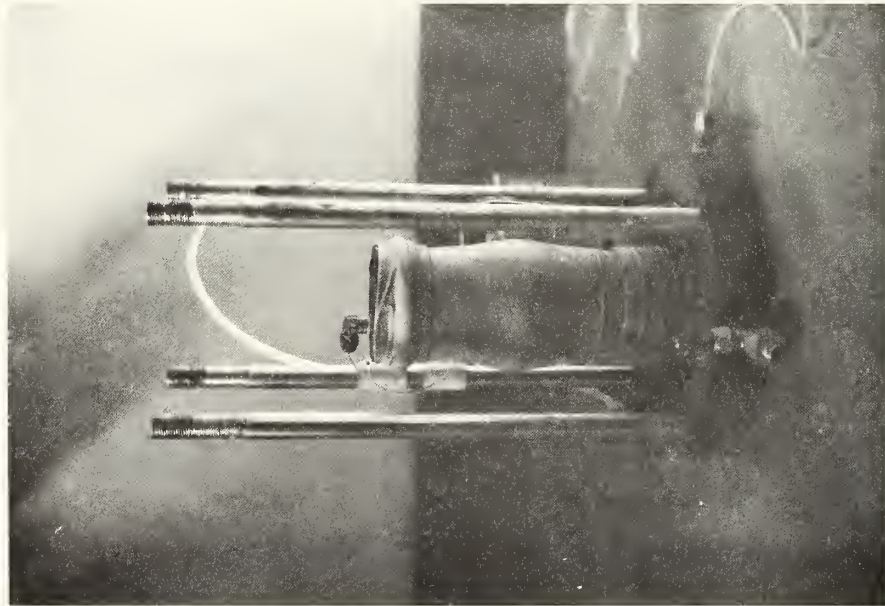
The effects of sodium silicate content in the grout solution are illustrated in Fig. 3.4 by comparing the stress-strain response for 30, 50, and 70 percent sodium silicate samples tested in triaxial compression at a confining pressure of 138 kN/m^2 (20 psi). For reference, the ungrouted sand behavior at this confining pressure is also shown. Clearly, as the sodium silicate content of the grouted samples increases, the stress-strain curve becomes steeper (the sample is stiffer), the stress at failure is larger, the strain at failure is smaller, and the post failure behavior exhibits a more brittle response. It is particularly interesting that the residual strength at large strains ($\epsilon > 6\%$) of all of the grouted samples tends to be the same as that of the ungrouted sand. This behavior suggests that once the grout bonds are completely broken on the failure plane, the residual strength is simply that of the sand to sand friction. Several photographs of failed samples are shown in Fig. 3.7; bulging of the samples occurred at low silicate contents while at higher silicate contents a sharp failure plane formed. These modes of failure are consistent with the observed relative stress-strain behaviors.

The volumetric strains measured in the tests indicate that near failure, all of the samples began to expand, a behavior characteristic of dense, ungrouted sand. It is not clear if this is simply a reflection of the sand component of behavior or a characteristic tied to the breaking of the grout bonds. This aspect is now under further study.

The results shown in Fig. 3.5 are the same as those of Fig. 3.4, except that the confining pressure used in the tests is 10 psi instead of 138 kN/m^2 (20 psi). Trends in Fig. 3.5 are the same as those in Fig. 3.4, only the stresses at failure are lower as would be expected because of the lower confining stresses.



(b) Ductile Failure



(a) Brittle Failure

FIGURE 3.7. EXAMPLES OF FAILURE MODES OF GROUTED SAMPLES

In Fig. 3.6, a series of triaxial tests on 30% silicate samples demonstrates clearly the effects of confining pressure on behavior; results for tests performed at confining pressure of 0, 69, and 138 kN/m² (0, 10, 20, psi) shown. As the confining pressure increases, the failure stress and initial stiffness of the grouted soil increases. It is also interesting that while the unconfined sample fails in a brittle mode, showing a significant if not total, loss in strength after failure, the confined samples demonstrate a strong residual component in strength. The residual component in strength for the confined samples is essentially equal to that of the ungrouted sand.

In summary, the results in Figs. 3.4 - 3.6 show that, as expected, chemical concentrations have a significant influence on behavior. They also show that confining pressure plays an important role; higher confining stresses result in higher peak and residual strengths and higher soil stiffnesses. This is particularly important since grouted zones are usually buried in the ground and are subjected to confinement by the surrounding soil.

Effect of Age

All of the test results in Figs. 3.4 - 3.6 are for samples of approximately the same age; curing times are in the range of 8 to 13 days. Unconfined compression tests were also performed on samples aged over longer periods of time. The effects of aging are illustrated by the stress-strain curves in Fig. 3.8 for 50 percent silicate samples tested at ages of 7 and 107 days. The results show that the older sample is almost twice as strong and has an initial tangent modulus more than twice that of the younger sample. It is thus clear that age is an important factor

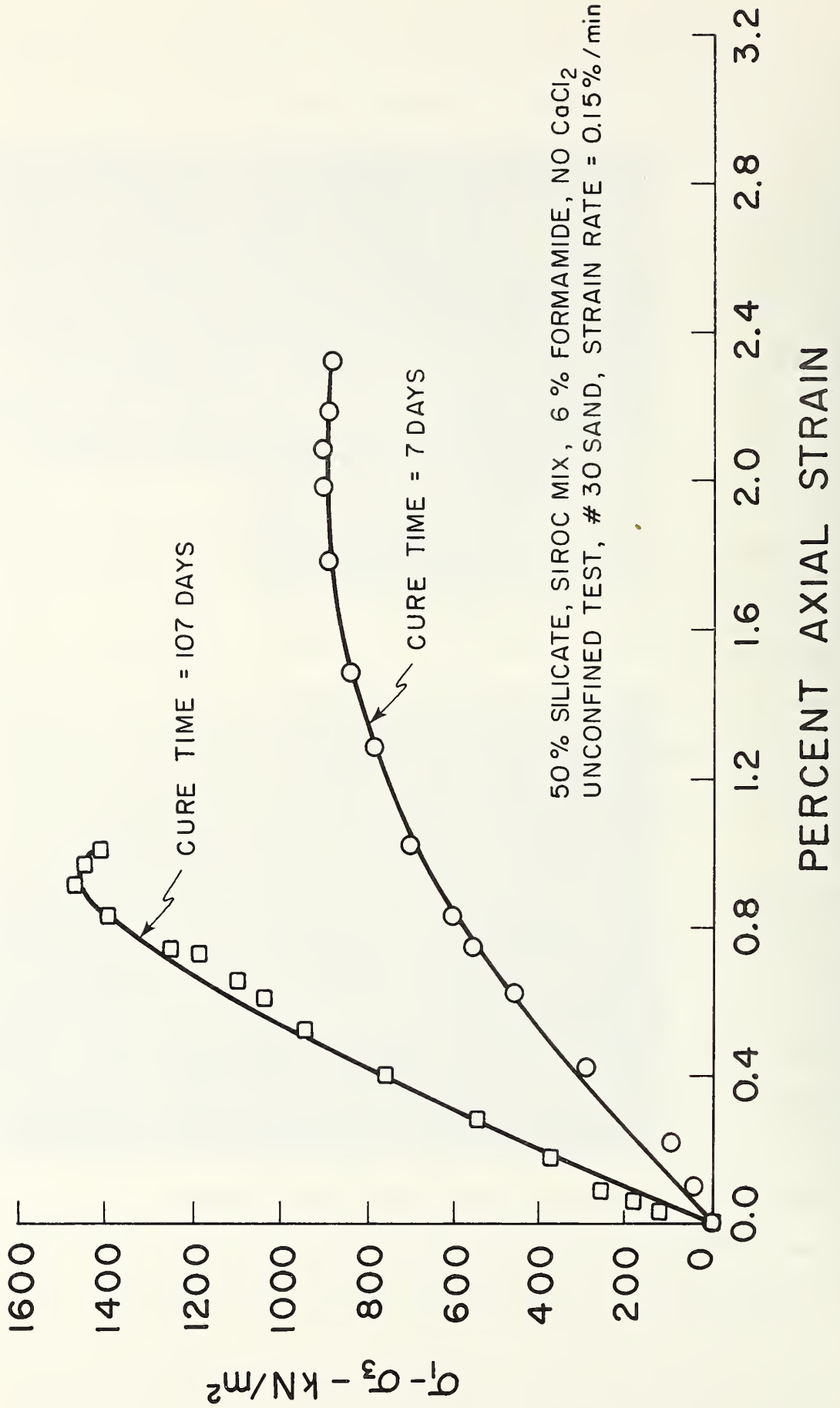


FIGURE 3.8. EFFECT OF CURE TIME ON STRESS-STRAIN RESPONSE

which must be considered in developing a stress-strain response for silicate stabilized soil.

Effect of Constant Load

As was noted in Chapter II, silicate stabilized soils tend to creep under constant load. Two tests of this type were performed in the first year program in order to determine the degree of the effect on the stabilized soils of this investigation. Both the samples were stabilized with the 50% silicate mix and were loaded in unconfined compression to one half of the failure load determined in the constant strain rate tests performed at a strain rate of 0.15% per minute.

The deformation-time response curves are depicted in Fig. 3.9 and they show a behavior identical to that described in Chapter II by Koenzen (1975). There is an immediate deformation under initial load application, followed by a slow seemingly stable creep period but terminated by creep rupture after about 8 to 12 hours. According to Koenzen (1975) and Warner (1972), this is characteristic of most grouted soils. In unconfined compression the constant loads may need to be as low as 20% of those from quick loading tests in order to prevent creep rupture under constant loading conditions. Thus, the present tests are consistent with previous results and it is apparent that, in addition to the other variables which influence grouted soil behavior, time effects need strong consideration in developing a method for selecting design parameters. Future work in this study will be devoted to this end.

Strength of Grouted Samples

Peak strength values for all tests performed are listed in Table 3.2. In the following discussion the influence of key variables is isolated.

GROUT MIX: 50% SIL
 06% FORMAMIDE
 0% CaCl₂

LOAD ≈ 50% AVG. UNC. COMP.
 FAILURE LOAD
 = 690 kN/m²

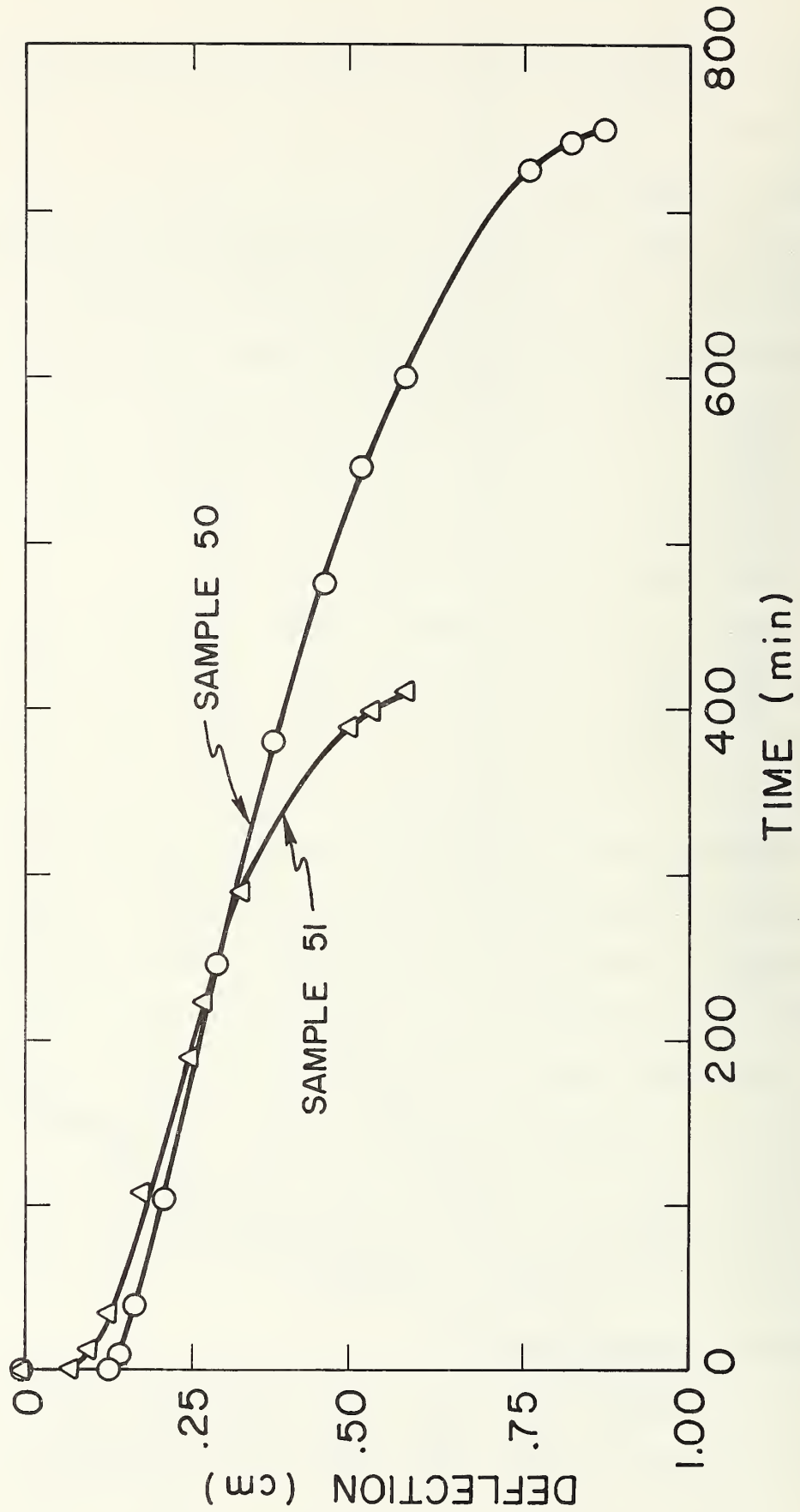


FIGURE 3.9. RESPONSE OF SAMPLES TO CONSTANT LOAD

Effect of Confining Pressure on Strength.

The effect of confining pressure on strength is best depicted via a plot of the values of $(\sigma_1 - \sigma_3)_{\text{failure}}$ vs. $(\sigma_1 + \sigma_3)_{\text{failure}}$ from the tests. This type of plot is similar to a Mohr diagram except that a Mohr circle is represented by a single point, the coordinates of which are the maximum shear stress at failure, $(\sigma_1 - \sigma_3)_f$, and the maximum principal stress sum, $(\sigma_1 + \sigma_3)_f$. A straight line connecting points on this diagram is indicative of a straight line Mohr envelope; the slope of the line is $\sin\phi$ and the intercept is $2 \times (\text{cohesion}) \times \cos\phi$.

In Fig. 3.10, all of the results are shown from triaxial tests performed on samples of Monterey No. 16 sand stabilized using a 30 percent silicate grout. Different data symbols are used to distinguish samples which were obtained from split and nonsplit tubes and those which included CaCl_2 acceleration and those which did not. Curing time for all samples was between 3 and 7 days. Also shown for reference in Fig. 3.10 is the strength envelope for the ungrouted Monterey No. 16 sand. A total of 40 tests were used to develop this plot; many were duplicates to insure repeatability of the test results.

The data show very consistent trends which may be summarized as follows:

1. The strength of the grouted soil samples increases with confining pressure in a similar sense to that of a simple frictional material.
2. Essentially the same friction angle may be used to characterize the slope of the strength envelope for both the grouted and ungrouted sand. Only a cohesion intercept distinguishes between the various strength envelopes.
3. The addition of CaCl_2 to the grout mix results in a higher cohesive strength than if it is not used, but no change in friction angle (this may be due to different curing rates only).

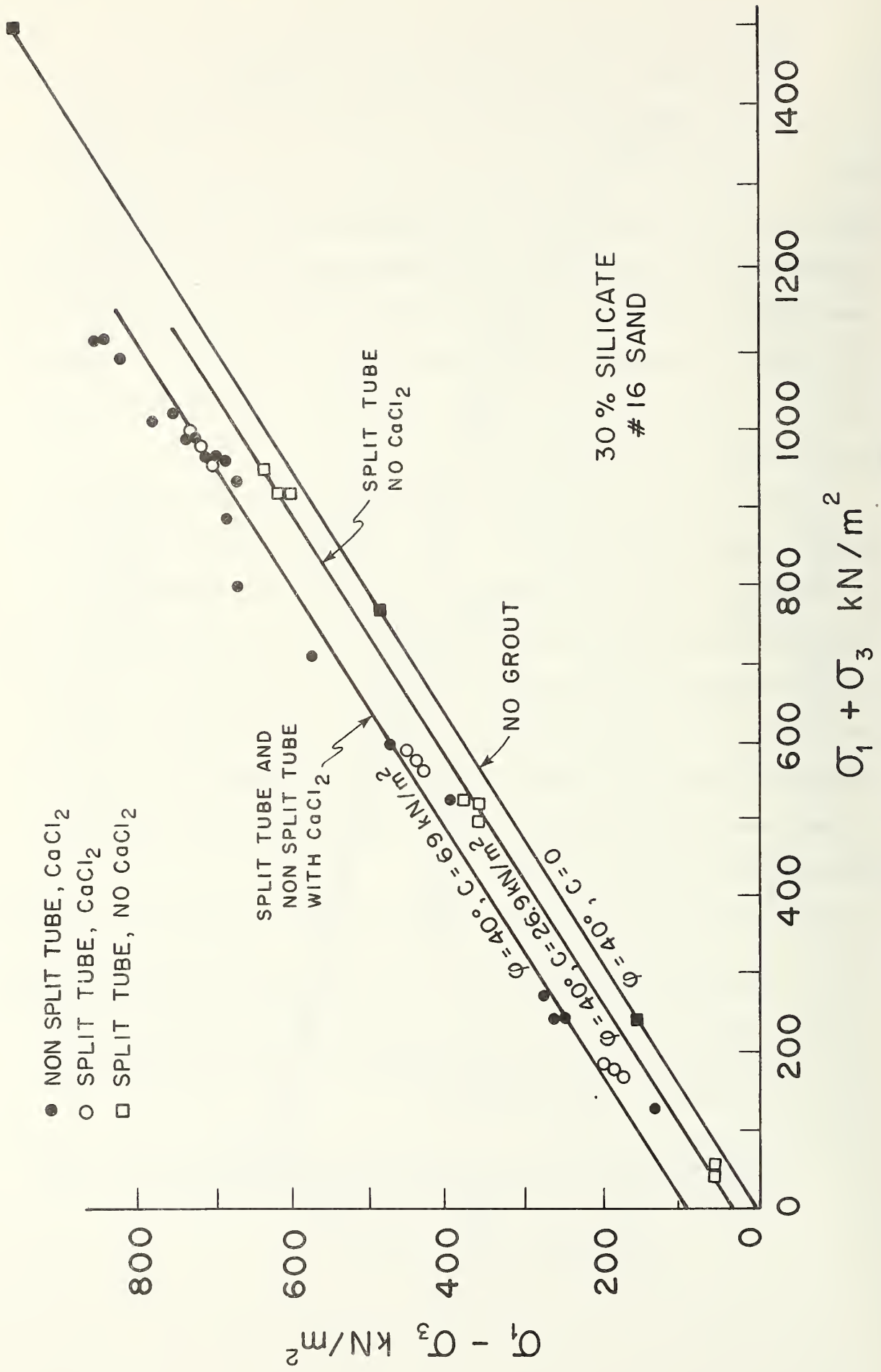


FIGURE 3.10. STRENGTH ENVELOPES FOR 30% SILICATE SAMPLES, MONTEREY #16 SAND

4. There is no apparent difference between samples obtained from split or nonsplit tubes (this is not the case at higher silicate contents).

The finding that the grouted samples demonstrate both frictional and cohesive strength components is not surprising since a grouted sand is a two phase material. That the slope of the strength envelope is the same as the ungrouted sand is probably true only for samples injected with a weak grout mix, such as was used in the case of the results in Fig. 3.10. The friction angle would appear to reflect the amount of the sand strength mobilized, and because the failure strains for the weakly grouted samples are very near those of the sand only samples (see Fig. 3.5 and 3.6), the sand strength could be fully mobilized along with that of the grout, leading to the same friction angle for grouted and ungrouted samples.

Effect of Sand Grain Size on Strength.

Using the same coordinates as in Fig. 3.10, the strength data for 11 triaxial tests on Monterey No. 30 sand stabilized by a 30% silicate grout are plotted in Fig. 3.11. By superimposing the strength envelope from Fig. 3.10 for stabilized Monterey No. 16 sand on Fig. 3.11, it is apparent that there is little difference in the results of tests on the two sands. It thus appears that changing the grain size of a uniformly graded sand has little influence on grouted soil strength.

Effect of Sodium Silicate and Formamide Concentrations on Strength.

In Fig. 3.12, peak strength results of triaxial tests are plotted for Monterey No. 16 sand stabilized with the following grout mixtures:

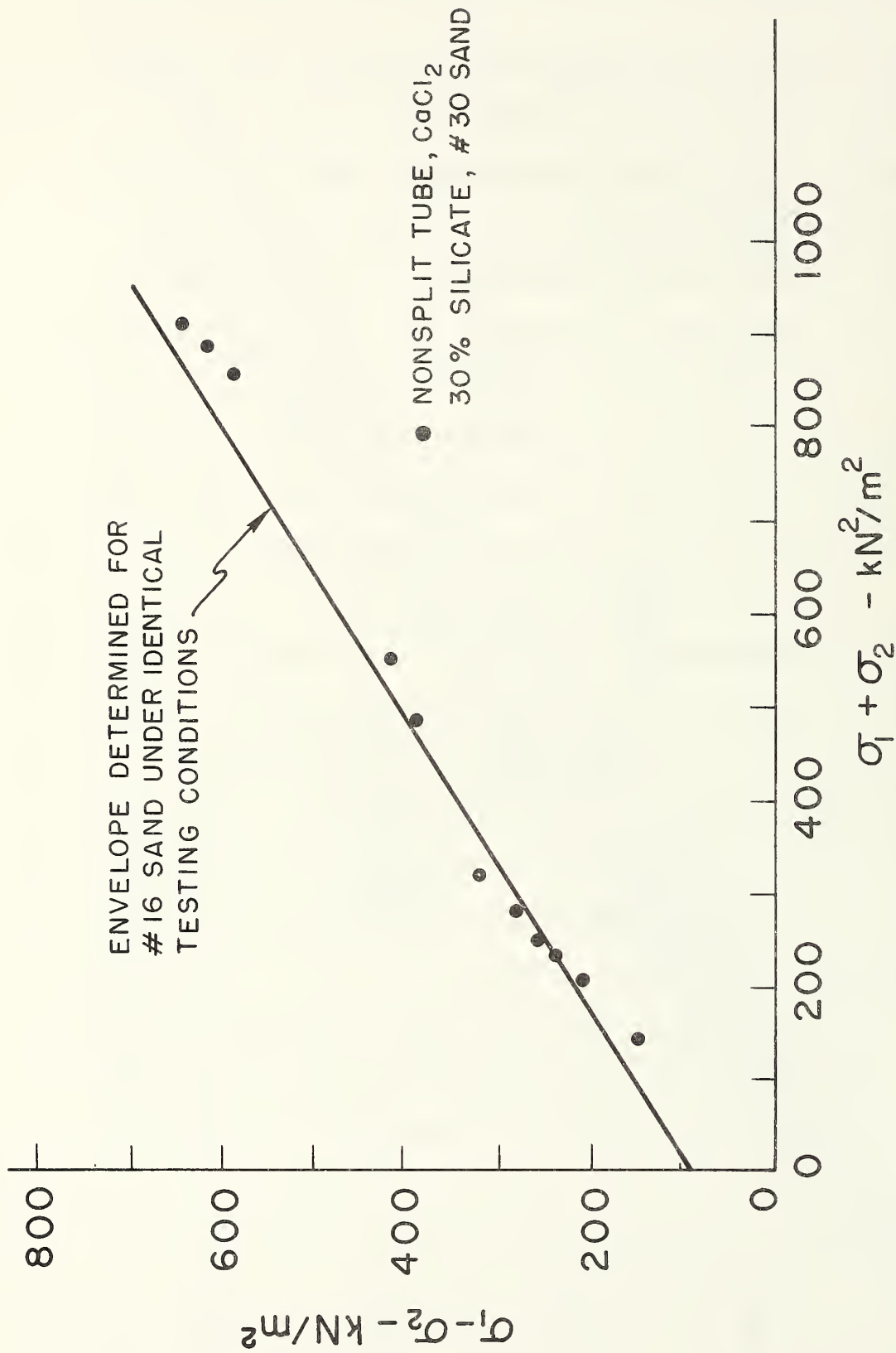


FIGURE 3.11. STRENGTH ENVELOPE FOR 30% SILICATE SAMPLES, MONTEREY #30 SAND

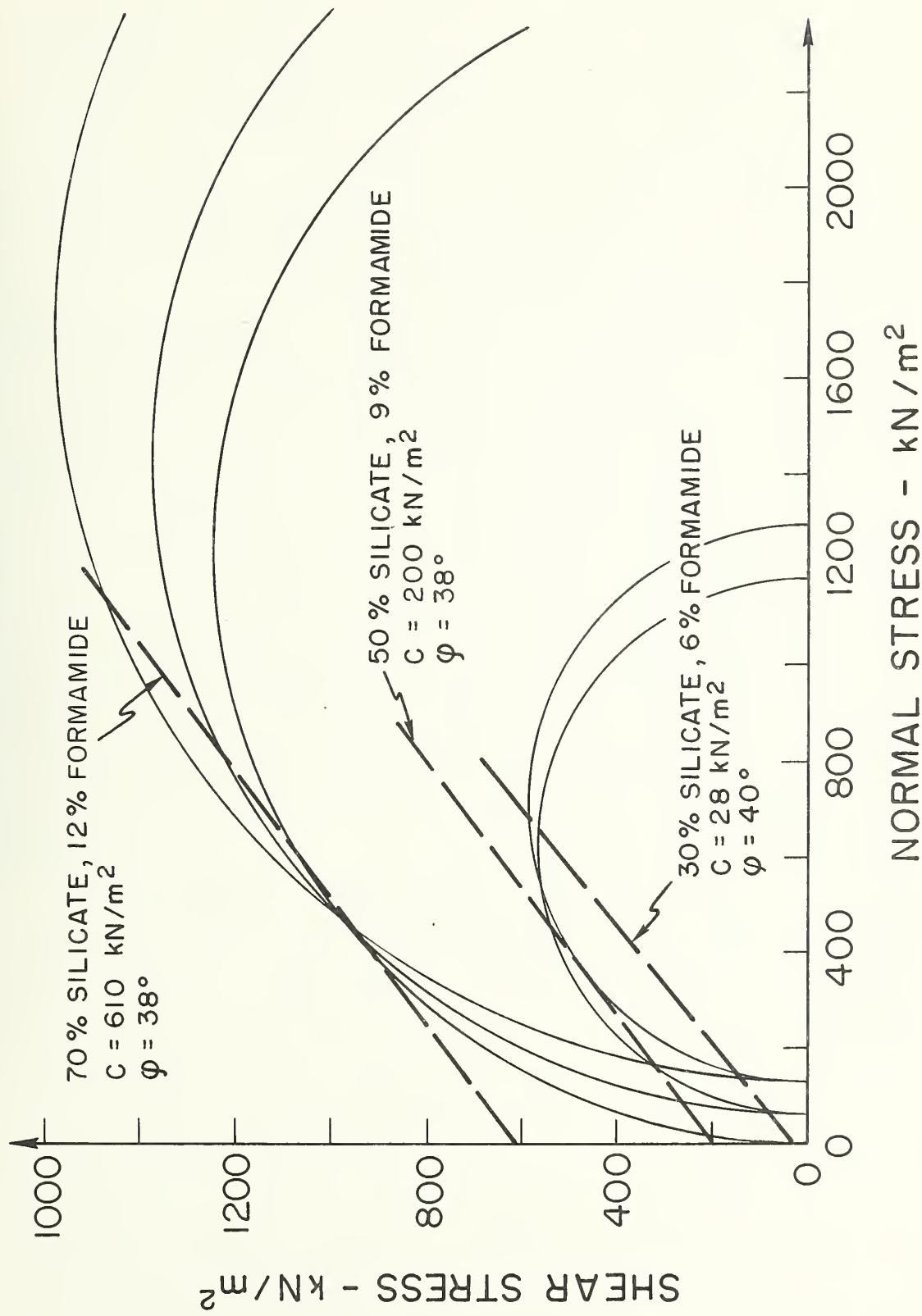


FIGURE 3.12. STRENGTH ENVELOPES FOR 30, 50 AND 70% SILICATE SAMPLES

<u>Sodium Silicate</u>	<u>Formamide</u>	<u>Water</u>
%*	%*	%*
30	6	64
50	9	41
70	12	18

* by volume

No CaCl_2 was used in any of the cases since the acceleration was not needed. Split sample tubes were used in all cases.

The results in Fig. 3.12 demonstrate that: (1) the strength of all the grouted samples increases with confining pressure, regardless of chemical concentrations in the grout; and, (2) the higher the chemical concentrations, the stronger the grouted soil, with the primary influence of higher concentrations to increase the cohesion of the strength envelope while the friction remains reasonably constant. The increase in strength with chemical concentration is not unexpected however, it should be noted that it is not automatic to obtain such an increase. Use of an inadequate amount of hardner with a high percent silicate, or use of insufficient mixing can produce an irregular gel which does not generate the strength it should. For example, the results for tests on the 70% silicate samples with only 6% formamide (see Table 3.2) show that the strengths are less than those of 50% silicate samples with 9% formamide. Six percent formamide is not adequate to gel a 70% silicate solution and thus the beneficial effects of the higher silicate solution are not realized. The effects of insufficient mixing are similar since certain areas of the silicate solution in the soil are not gelled because of insufficient hardner in these areas. To determine the adequacy of mixing and hardner content, a grout solution should be mixed following a standard procedure and set aside in a clear container so that the uniformity of the gel can be visually examined.

In spite of the different results obtained with the different grouts,

all of the results show a strong frictional component of strength, i.e., the strength increases with confining pressure. The friction angle for the higher silicate content samples seems to lie between 30 and 40 degrees. Although these samples fail at very low strains it appears that some of the frictional strength of the sand is mobilized and contributes along with that of the grout. Additional triaxial tests at higher pressures need to be performed to understand this phenomenon better.

The increase in the cohesion intercept with the silicate-formamide percentage of 30-6, 50-9 and 70-12 is demonstrated in Fig. 3.13. Cohesion increases at an increasing rate at higher chemical contents.

Effect of Age on Strength.

The influence of age on the unconfined strength of Monterey No. 16 sand stabilized by the 30 percent silicate grout mix is demonstrated in Fig. 3.14. The greatest gains in strength are obtained early on during aging; however, insofar as the tests have been carried (110 days), the strength has continued to increase.

Effect of Split vs. Unsplit Sample Tubes on Strength.

It was shown in Fig. 3.10 that for a 30 percent grout mix that strength of samples obtained from split sample tubes were essentially the same as those for samples jacked from nonsplit tubes. This finding is not the case, however, for samples with higher chemical concentrations in the grout. At higher chemical concentrations it was apparent that high jacking pressures had to be used to extrude the samples from the nonsplit tubes, whereas the 30 percent silicate samples could be easily pushed from these tubes. A comparison of unconfined strengths for 30 and 50 percent silicate grout mix samples in Table 3.3 shows the effects of use of split vs. unsplit tubes.

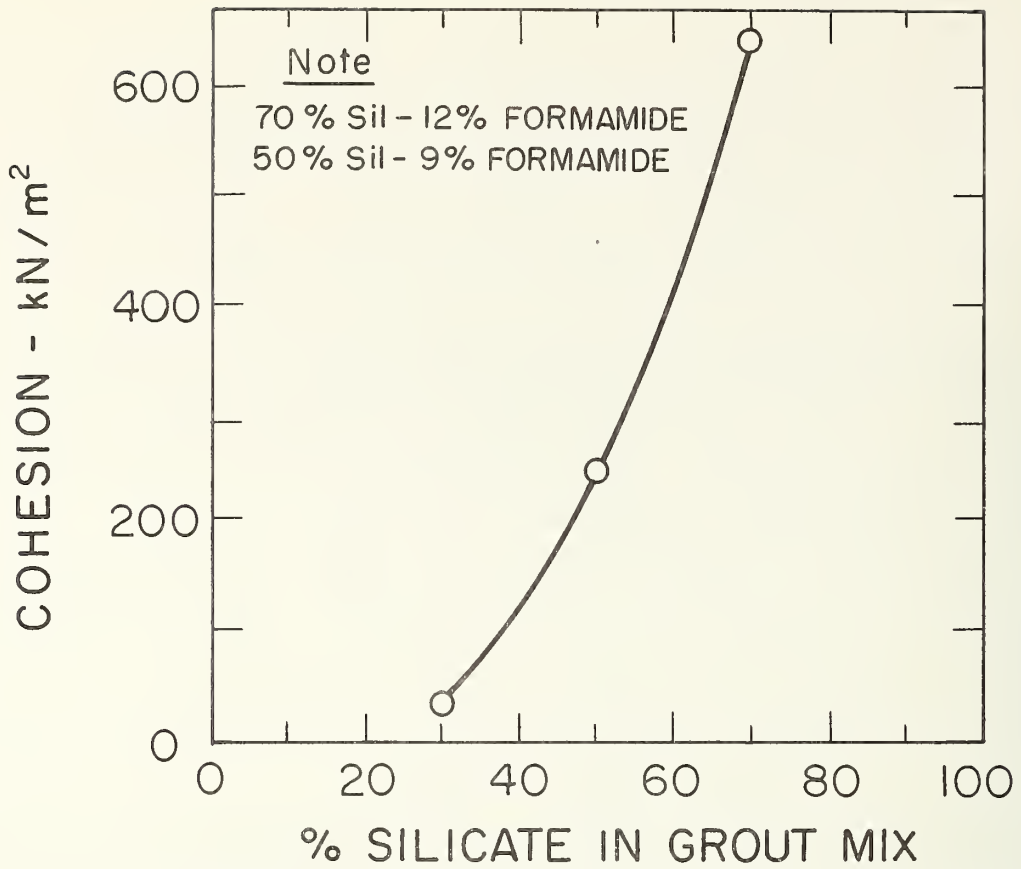


FIGURE 3.13. VARIATION OF COHESION WITH % SILICATE

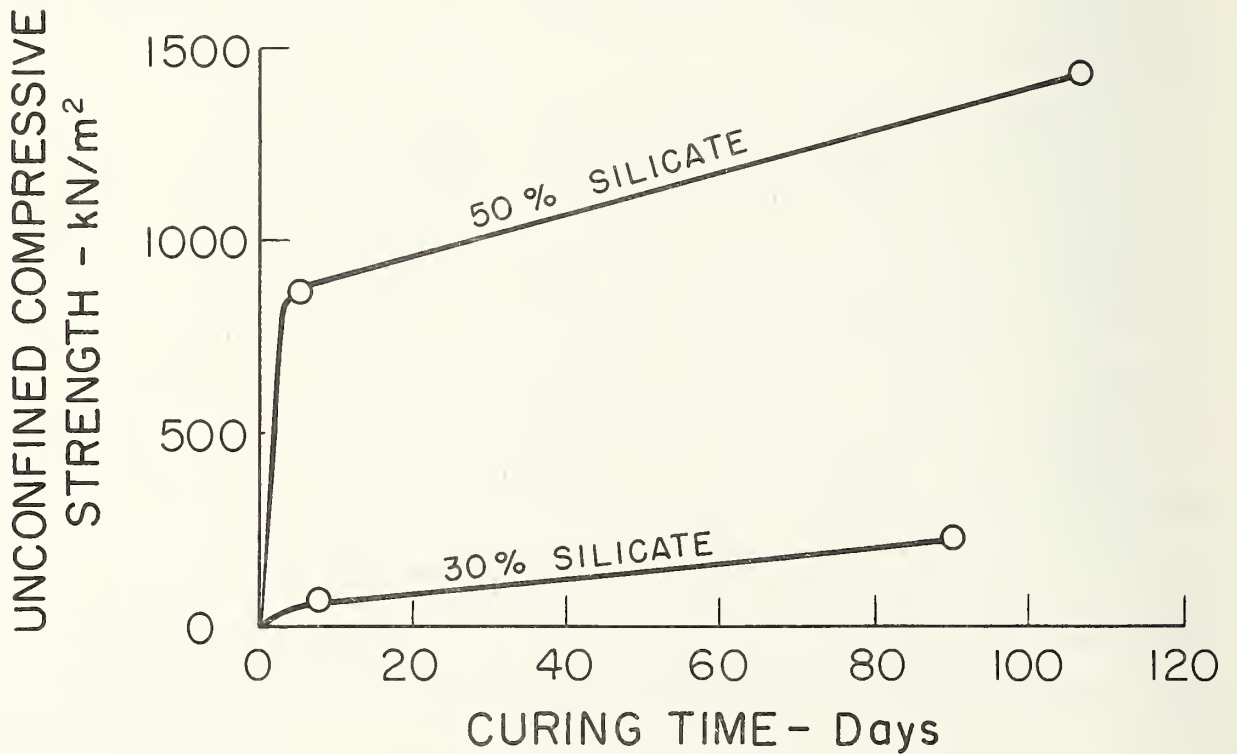


FIGURE 3.14. EFFECT OF CURING TIME ON UNCONFINED STRENGTH

TABLE 3.3 EFFECTS OF TYPE OF SAMPLE TUBE

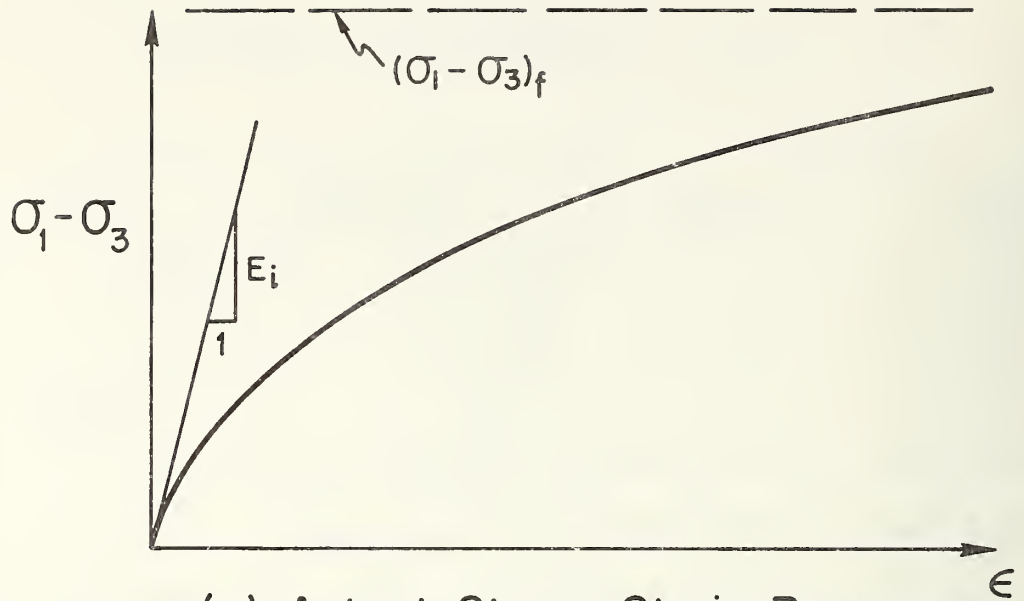
<u>Grout Mix</u>		<u>Average Unconfined Comp. Strength</u>	
<u>Silicate</u>	<u>Formamide</u>	<u>kN/m² (psi)</u>	
<u>%</u>	<u>%</u>	<u>Unsplit Tube</u>	<u>Split Tube</u>
30	6	186 (27)	180 (26)
50	6	793 (115)	1413 (205)

Split sample tubes are now used exclusively in all tests.

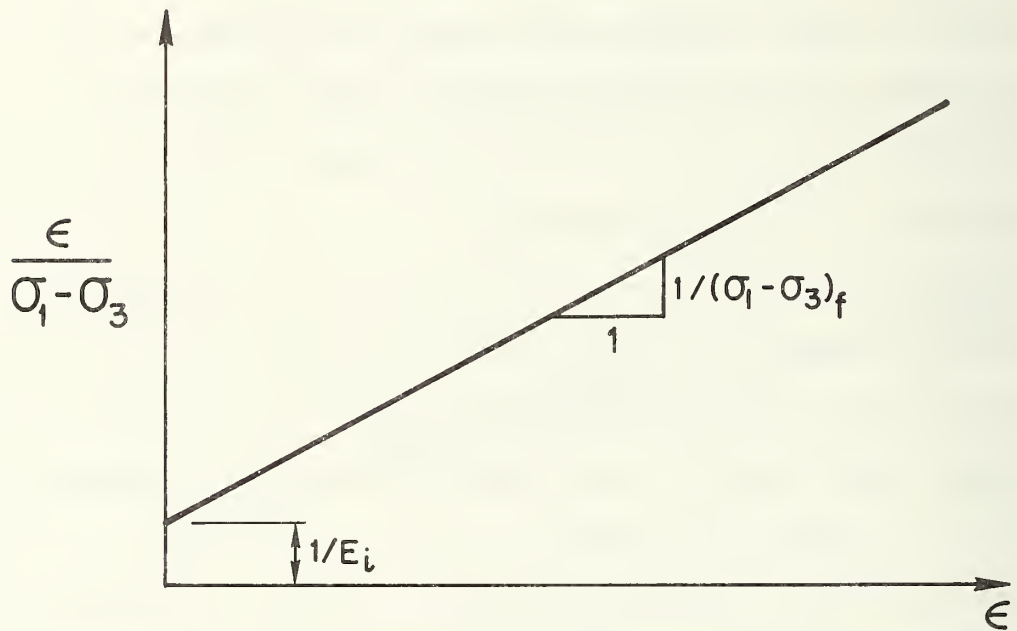
Initial Tangent Modulus Values - Grouted Samples

The portion of the stress-strain response of most importance to design is likely to be that before failure is reached. A useful index for comparing the relative stiffness of the stress-strain behavior before failure is the modulus determined from the tangent to the initial portion of the stress-strain curve, the so called initial tangent modulus, E_1 . This parameter is widely used in soil mechanics.

Unfortunately, the direct determination of the initial tangent modulus by drawing a tangent to the initial portion of the curve is a highly subjective process. A more consistent technique has been described by Duncan and Chang (1970). Briefly, this involves transposing the stress-strain curve to a straight line as shown in Fig. 3.15 by plotting the results as (axial strain)/ $(\sigma_1 - \sigma_3)$ vs. axial strain. The resulting transformed straight line is extrapolated to zero axial strain and the inverse of the intercept value at this point is the initial tangent modulus. This procedure was applied in evaluation of initial tangent modulus values for the available test results.



(a) Actual Stress-Strain Response



(b) Transformed Stress-Strain Curve

FIGURE 3.15. DETERMINATION OF INITIAL TANGENT MODULUS FROM TRANSFORMED STRESS-STRAIN CURVE

Modulus values for all triaxial tests on split tube samples of Monterey No. 16 sand cured between 8 and 13 days, are shown in Fig. 3.16 plotted vs. the confining pressure, using log-log scales. Different grout mixes are represented as well as the data for ungrouted sand. Conventionally, tests data of this type for ungrouted sand show that the modulus, E_i , increases linearly with the confining pressure on such a plot. This linear relationship is empirically fitted by the equation:

$$E_i = K p_a \left(\frac{\sigma_3}{p_a} \right)^n \quad 3.1$$

in which, p_a = atmospheric pressure, σ_3 = the confining stress, K is the intercept of the line at $\sigma_3/p_a = 1.0$ and n is the slope of the line. For sands, n is commonly 0.5 and K lies between 150 and 800 depending upon density.

The data obtained for the ungrouted sand and shown in Fig. 3.16, follow the conventional linear trend with a slope of 0.5. The data for the grouted sands show similar relationships with slope 0.5 or slightly less. The intercept values, K , are higher for the grouted samples, however, with the K values increasing with chemical concentrations used in the grout. In fact, the modulus values at any given confining pressure tend to have relative magnitudes in the same sense as the strength values discussed in the preceding section. For example, the highest values occur for the samples with 70% silicate grout mix and the lowest values occur for the samples with the 30% silicate grout mix.

Other factors than grout mix components and confining pressures also influence the initial tangent modulus values. Qualitatively the effects are the same as observed for the strength of the grouted samples. Major

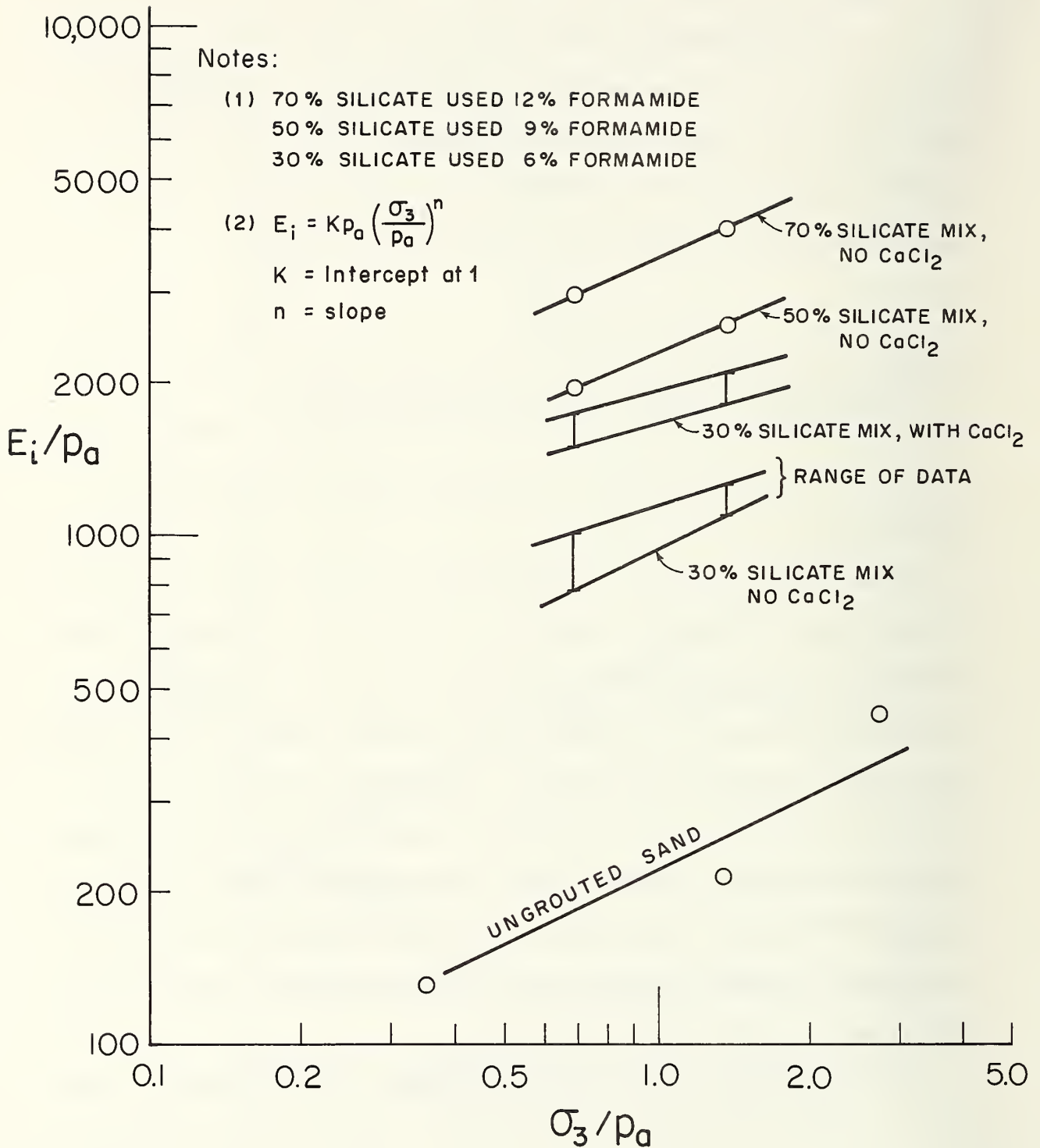


FIGURE 3.16. VARIATION OF INITIAL TANGENT MODULUS VALUES WITH CONFINING PRESSURE

factors would be age of the material, rate of loading, curing environment, etc. Further studies are underway to define these effects.

SUMMARY

The laboratory test program has progressed as planned. Equipment has been developed which allows creation of stabilized soil samples which can simulate a variety of grouting environments. Numerous duplicate tests have shown that reliable and repeatable results can be obtained.

Over 80 tests have been performed in studies of a number of the key variables which influence grouted soil behavior. The data give a uniquely detailed insight as to the effects of chemical concentrations in the grout mix, confining pressure and large strains. Strength and modulus values are defined in terms of a conventional soil mechanics framework.

The results of this first year effort and those of previous investigations reviewed in Chapter 2 show that the engineering behavior of grouted soil is complex. However, a fuller understanding of this behavior is arising from the work and it appears that an analytic modeling technique for the stress-strain response can be developed. Further testing will be devoted to a better definition of behavior under the actual stress paths and time spans encountered in typical tunneling operations.

CHAPTER IV

FINITE ELEMENT CODE DEVELOPMENT AND PARAMETRIC STUDIES

In Chapter 2 it was noted that there is no design methodology for choosing sizes strengths and stiffnesses of grouted zones which are intended to limit movements above tunnels. The lack of a design approach to the grouted tunnel problem probably results from the fact that until only very recently there were no analytical methods which could reasonably simulate the complex facets of the problem. The finite element method, however, offers a tool which has the capability to consider most of the important variables in grouted tunnels, including nonhomogenous soil conditions, complicated loading and geometry, and involved material response. Nonhomogeneous subsurface conditions are the norm in urban areas with an additional twist added by the presence of the grout zone. The use of noncircular tunnels and different grout zone shapes, the presence of other tunnels nearby, the increase of gravity loading with depth, and the location of the tunnel near the ground surface all contribute to the complexity of the geometry and loading. The nonlinear, stress-dependent, inelastic stress-strain behavior of soils and grouted soils necessitate their representation by involved constitutive relations.

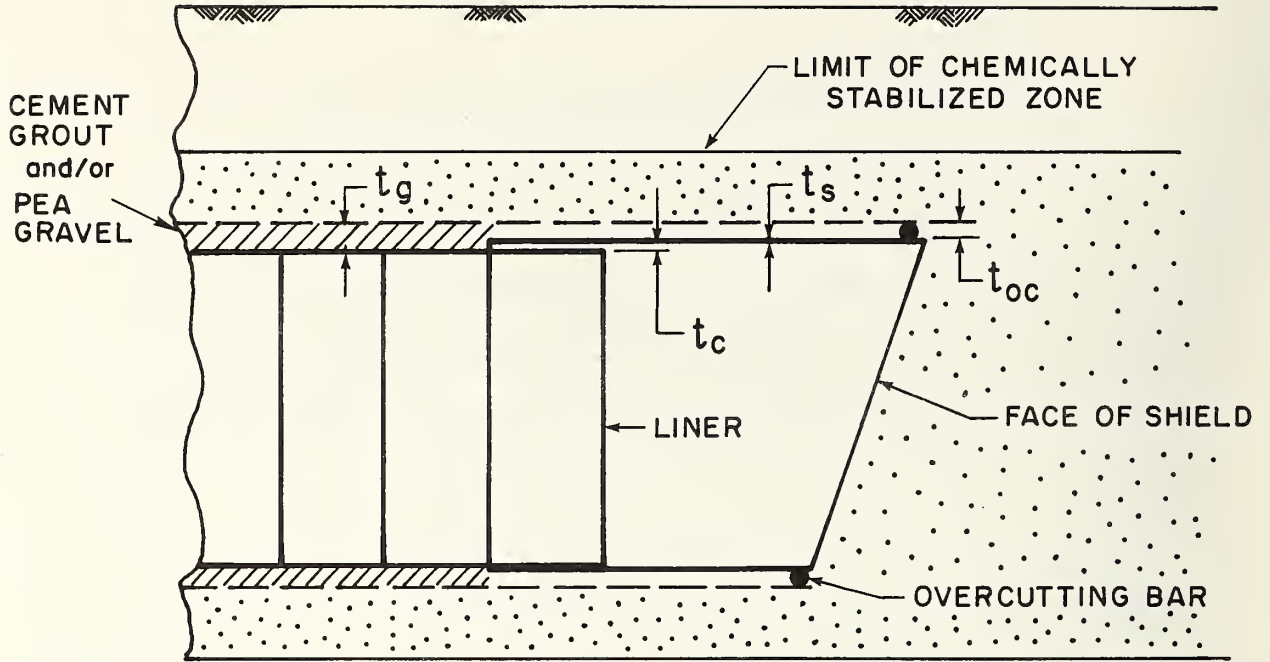
This chapter describes the development of a general purpose finite element code for analysis of the grouted tunnel problem. The code contains plane strain and axisymmetric options, which allow economic study of the major variables influencing grouted tunnel behavior. To demonstrate the capability of the code, the results of a series of analyses are presented herein, demonstrating the effects of grout zone size, stiffness and strength on surface settlements above the tunnel. In Chapter 6, the code is applied to a complicated case history from the Washington Metro.

DEFINITION OF THE PROBLEM TO BE ANALYZED

In Fig. 4.1, the process of shield excavation and liner support of a tunnel in chemically stabilized soil is depicted. The purpose of the stabilization in limiting surface movements is to prevent movements towards the face of the shield during shield passage and to limit radial movements around the shield and liner, which tend to close the annular gap left after passage of the shield. The annular gap may be as small as 7cm if the shield is well aligned but may reach 20cm if the front of the shield is pitched upwards along the tunnel axis. An upward pitch of the shield is not uncommon due to thrust forces created during a shove; this is called "plowing" in tunneling vernacular.

As is apparent from Fig. 4.1, the stress and deformation system around the tunnel is three-dimensional. However, it is uneconomical, and not even particularly desirable at the present stage to make three-dimensional finite element studies of tunnels in chemically stabilized soils given our present lack of knowledge about grouted soil behavior. In this investigation, plane strain and axisymmetric idealizations of the problem are used.

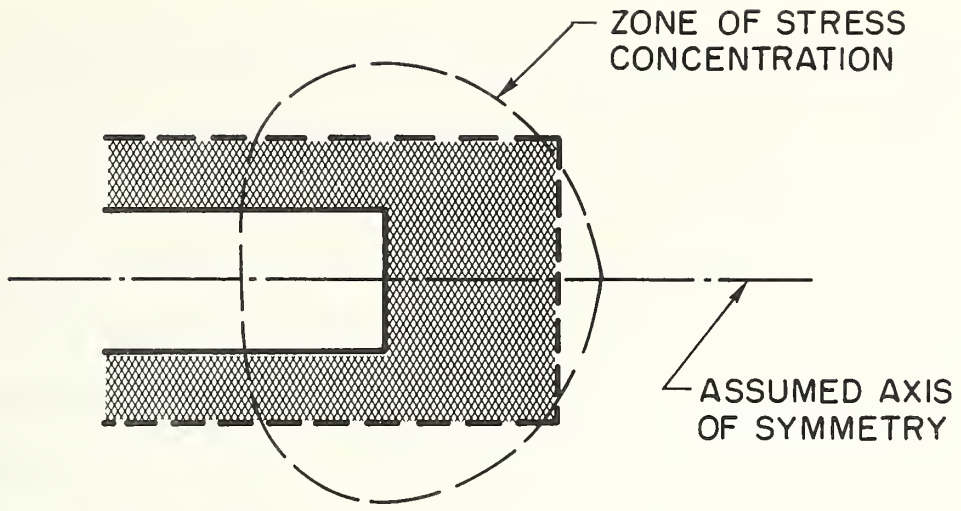
Plane strain analyses allow study of a section cut across the tunnel axis; in this case, surface effects are included and effects of soil stabilization on critical surface settlements can be evaluated (see Fig.4.2). A plane strain analysis is conservative in the sense that it does not recognize the support provided by the liner which is already in-place behind the shield. It is unconservative in the sense that it does not account for movements towards the excavation face which can lead to surface settlements. Fortunately, in reasonably stable systems, the effects of



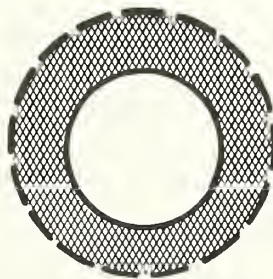
- t_g^* = thickness of annular gap left by process of shield excavation and liner erection = $t_{oc} + t_s + t_c$
 t_s = thickness of tail of shield
 t_{oc} = thickness of overcutting bar
 t_c = thickness of clearance left for erection of liner within shield

* t_g is also strongly influenced by shield orientation; if shield pitches upward, t_g can be significantly increased

FIGURE 4.1. DEVELOPMENT OF GAP BEHIND A TUNNEL SHIELD



AXISYMMETRIC ANALYSIS



PLANE STRAIN ANALYSIS

FIGURE 4.2. CONDITIONS FOR FINITE ELEMENT ANALYSES

movements towards the face are small and, on balance, the plane strain type analysis should predict conservative estimates of surface settlements and represent a useful design tool.

In order to fully document the effects of the stresses induced ahead of the tunnel face, an axisymmetric idealization of the problem is also used in this study (see Fig. 4.2). This case can model the three dimensional system around the advancing tunnel face using no more unknowns than required for the plane strain case. However, the axisymmetric representation cannot simulate the horizontal surface above a shallow tunnel, and instead applies primarily to deep tunnels where surface effects are small.

DESCRIPTION OF FINE ELEMENT CODE CAPABILITES

In developing the finite element code for this investigation, it was considered desirable to handle the following items:

1. Nonuniform initial stress fields
2. Nonhomogeneous soil conditions
3. Arbitrary shapes and sizes of stabilized zones
4. Arbitrary geometry and surface loads
5. Nonlinear, time-dependent material response
6. Usual and unusual excavation sequences
7. Groundwater, dewatering and seepage effects
8. Liner restraint on annular gap closing
9. Effects of shield "pitch"
10. Both plane strain and axisymmetric conditions

As of the writing of this report all these capabilities have been built into a finite element code except the time-dependent material

response; work is underway on this aspect. In the following paragraphs, specific important aspects of the code are discussed.

Type of Element

The finite element program makes use of the isoparametric QM5 quadrilateral element developed by Doherty, Wilson, and Taylor (1969) for both plane strain and axisymmetric analysis. Triangular quadrilateral elements can be handled by the program. The efficiency and response of this element are good when compared to others and it suits the needs of the present study.

Stress-Strain-Models

In the current program, two types of stress-strain behavior can be simulated; (1) linear elastic response; and, (2) nonlinear, stress dependent response. Neither of the models can simulate time dependent response; this capability is being added to the program during the second year of the research. The nonlinear behavior is handled via a pseudo-elastic approach which allows the shear modulus of a material to vary with the magnitudes of the shear and hydrostatic stresses calculated. The bulk modulus is taken to vary only with the level of the hydrostatic stresses. Details of this procedure are given by Duncan and Chang (1970) and Clough and Duncan (1971). The technique has been shown in numerous practical soil mechanics applications involving widely varying soil types to yield reasonable stress-strain response so long as substantial failure does not occur. As will be demonstrated later in this chapter, this behavior aspect is not a major problem for grouted tunnels designed with an adequate factor of safety.

A comparison of the theoretical stress-strain response predicted by the nonlinear elastic model and that observed for grouted soil in a typical series of triaxial tests using confining pressures of 0, 70, 190 kN/m² is shown in Fig. 4.3. The theoretical model can be seen to correctly simulate confining pressure effects and shear stress levels on the stress-strain behavior up to failure. Thus, under the short term types of loading the nonlinear elastic model should reasonably simulate grouted soil behavior. Because the model parameters can be readily determined from conventional laboratory data, it is practical to use.

Simulation of Excavation Effects

The basic procedure for simulation of excavation effects as adopted in the program as follows:

1. Reduction of the stiffness of the material in the areas to be excavated to near zero.
2. Applying a set of forces to the excavation boundaries which are of such a magnitude so as to cancel all boundary normal and shear stress.

The critical aspect of this procedure is in the determination of the excavation forces. In a subsequent section of this report, proof of the accuracy of the techniques used in the present code is presented.

The code allows for several calculation-related refinements during the simulation of excavation. First, the tunnel or opening may be excavated in any incremental sequence desired, via full face or multiple drifts. Second, during any excavation step, the excavation forces may be applied as a series of substeps, chosen by the user. This can be important when nonlinear material response is being modeled since only small loading steps may be acceptable for solution convergence. The breakup of the excavation loads is also important in including effects of liner support

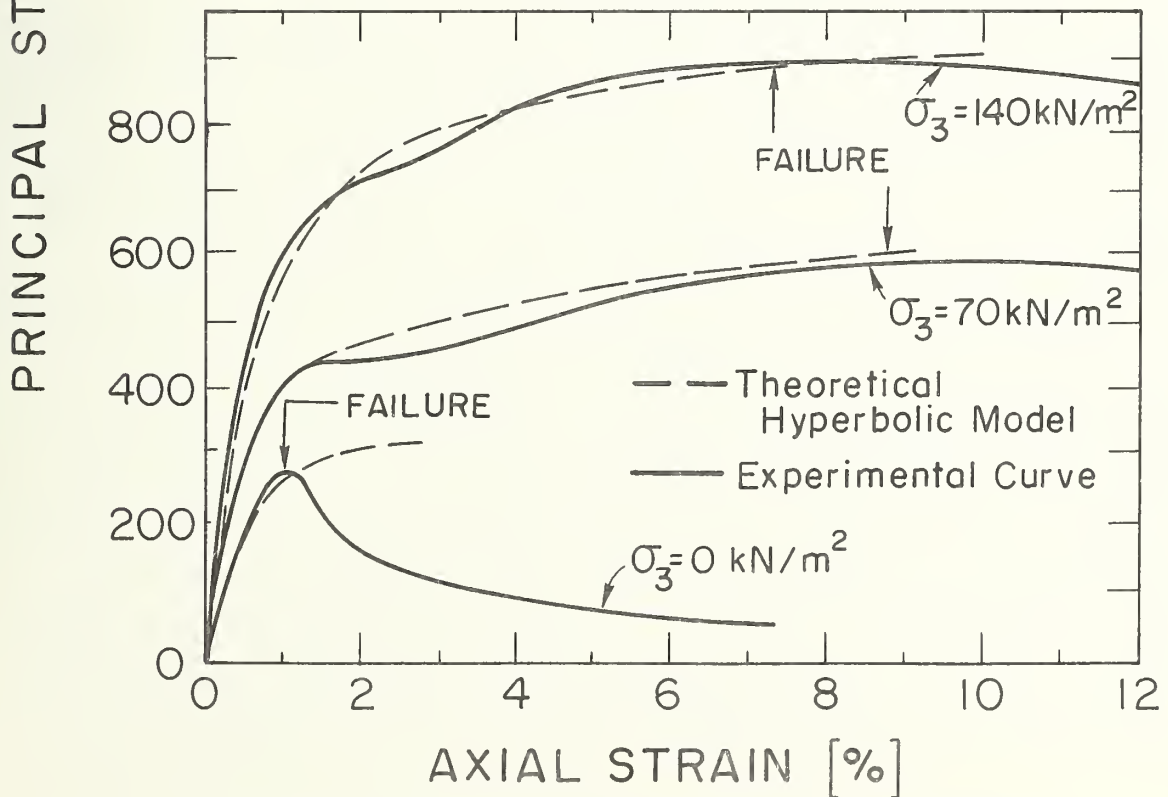
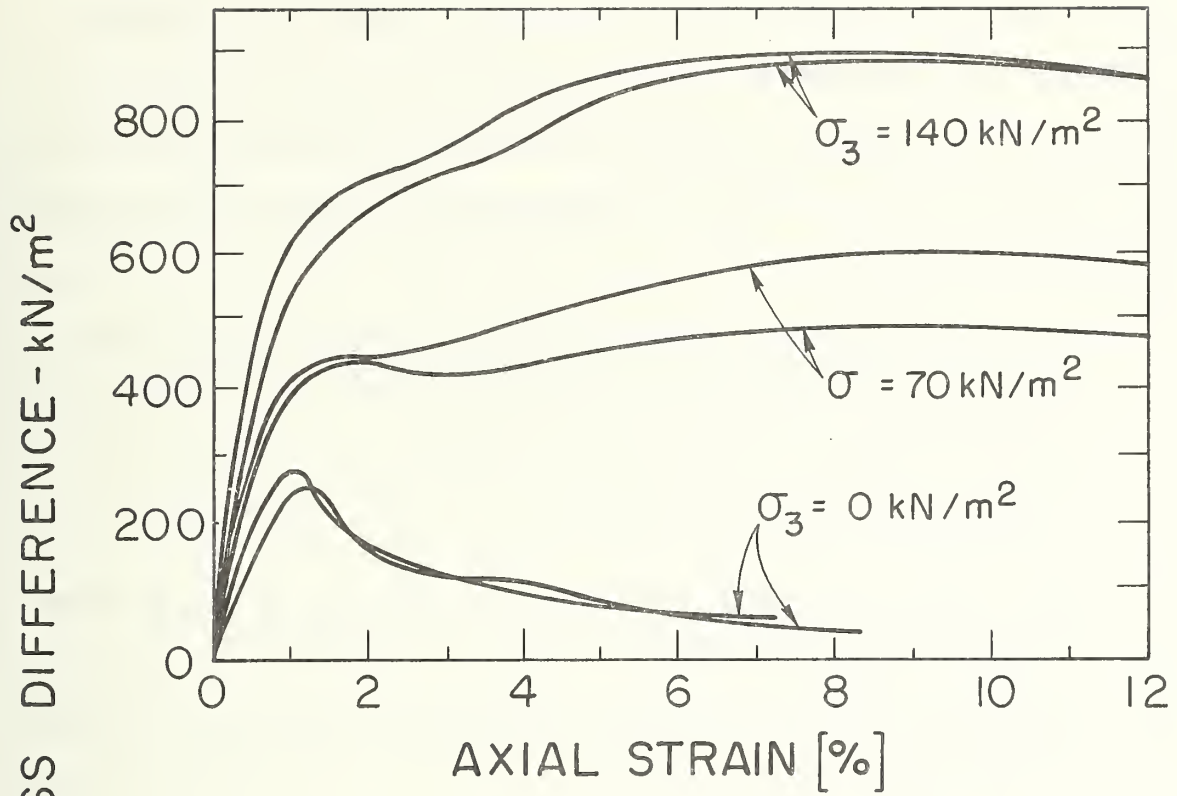


FIGURE 4.3. COMPARISON OF THEORETICAL AND OBSERVED STRESS-STRAIN CURVES

as is described in the following sections of the report. The third calculation refinement included in the code is through the use of iteration, which can be applied to any excavation step or substep. Iteration, which leads to accelerated solution convergence, proceeds in the following manner:

1. Prior to applying an excavation load step, the stress-strain parameters for each element in the finite elements mesh are calculated based upon shear and hydrostatic stress values for each element.
2. The load step is applied and deformations and stresses are calculated.
3. The stresses from Step 2 are averaged with the initial stresses and new stress-strain parameters are calculated based upon the average stresses.
4. The application of the load step is repeated or iterated using the new stress-strain parameters to formulate the element stiffnesses.
5. Steps 3 and 4 are repeated as desired until satisfactory solution convergence is obtained.

Convergence can be defined in terms of the percent change of the stress-strain parameters calculated from successive iterations. This percent change will diminish as iteration proceeds. As a practical matter, convergence is usually rapid with no more than two iterations required.

Accurate calculation of the excavation boundary forces is accomplished by a technique described by Clough and Duncan (1969). To develop the forces, the stresses at each node on the excavation boundary are first determined by interpolation using the known stresses at the centroids of the nearest four elements to each node. The horizontal, vertical and shear stresses are determined using an interpolation function of the type

$$\sigma = a + bx + cy + dxy \quad 4.1$$

in which x and y are the coordinates of the boundary nodal point and a , b , c , and d are interpolation coefficients determined from the stresses of the four surrounding elements. It should be noted that the interpolation elements should be specified in a symmetrical manner around a tunnel opening. During the second year of the research effort, a User's Guide will be produced for the finite element program which will cover details of this nature so as to insure its correct usage.

The excavation forces which are applied to the excavation boundary to reduce stresses to zero are calculated from the nodal stresses determined by the interpolation technique. In calculating the forces, the boundary stresses are assumed to vary linearly between the nodal values. The forces are then determined by integration of the stresses over the boundary area.

The resulting features used to model excavation of the tunnel in the finite element code are accurate and flexible and provide an efficient solution scheme. Essentially arbitrary excavation procedures may be modeled within the context of complex geometric configurations.

Modeling Effects of Liner and Shield Pitch

The radially inward movement of the soil around the tunnel during and after shield passage leads to all important surface settlements. The degree to which these movements will occur is primarily a function of ground conditions, geometry of the tunnel, location of the tunnel relative to the ground surface and other tunnels, stabilized soil zone site and properties, and method of tunneling. The method of tunneling will, among other things, determine the size of the annular gap, " t_g " (Fig. 4.1), which must close or be supported by pumped-in pea gravel or cement grout

before closure. If the gap should close entirely before grouting, the liner would support the soil and limit any further movement. The liner serves as an ultimate restraint on inward soil movements.

In the plane strain analysis techniques described thus far, there are no restraints on soil movements into the tunnel. To remedy this situation, an option was added to the finite element program whereby a series of radial springs can be installed inside the tunnel which can serve to limit movements (see Fig. 4.4). These springs are programmed to be activated only if the inward radial movement of a node exceeds a designer specified value, a value which would presumably equal the expected annular gap thickness at a given node. By providing flexibility in modeling gap closing, both desirable and undesirable tunneling methods may be simulated. For example, if the effects of an upward pitch of the shield is to be modeled, the gap opening which must close before the liner springs react would be set at a large value. The stiffness of the springs is taken as that of the liner subdivided by the number of springs to be employed.

In the finite element code, the activation movement for each spring can be different so as to reflect the fact that the gap thickness at different locations around the shield may be different. The springs thus can, in a practical sense, reflect the restraint effects of the liner in cases where large inward soil movements occur. This is essential where the soil stabilization zone does not completely surround the tunnel and collapse of unstabilized soil would occur.

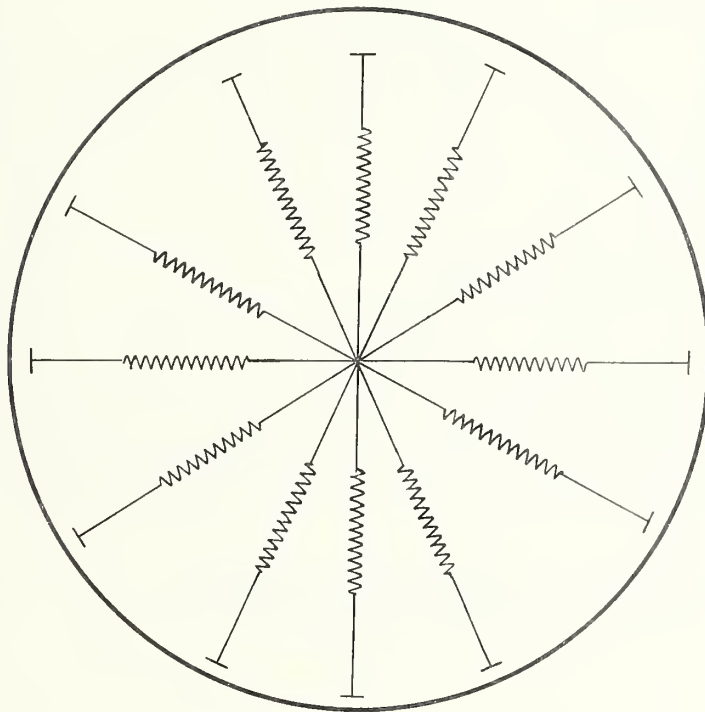


FIGURE 4.4. RADIAL LINER SPRINGS USED TO LIMIT INWARD MOVEMENTS AROUND TUNNEL

TESTING OF THE PLANE STRAIN ANALYSIS CAPABILITY

Following development of the finite element code, analyses were performed to verify the important aspects of it. The method of testing involved comparing finite element calculated results for the problem of a uniformly stressed continuum with a cylindrical hole in it, to those predicted from linear elastic theory for the same problem. Details of the problem are given in Fig. 4.5.

Two different types of test analyses were made, the first treating the problem as an initially unstressed medium subjected to external uniform boundary stresses with the "hole" in the center of the mass made up of elements with very low stiffness values. The second type of test analysis involved originating with a uniformly stressed medium from which elements are excavated to form the cylindrical hole. The first type of analyses were performed to determine if the presence of low stiffness elements in an "excavated" zone influence the predicted results. This is an important aspect in the simulation routine for excavation. The second type of analyses allow the actual excavation routine to be checked. Both types of analyses should yield the same answers if the code is correct.

The finite element mesh used in all the studies is shown in Fig. 4.6. Note that the boundaries of the mesh are located some 30 radii from the hole. This location was chosen by trial. Moving the boundaries in closer results in a savings of elements, but a sacrifice in accuracy. With the boundary at six radii from the hole, there is an additional two percent error in calculated results relative to the case with the boundary at 30 radii from the hole. The excavation sequences used to test the element removal scheme are shown in Fig. 4.6. The excavation is carried

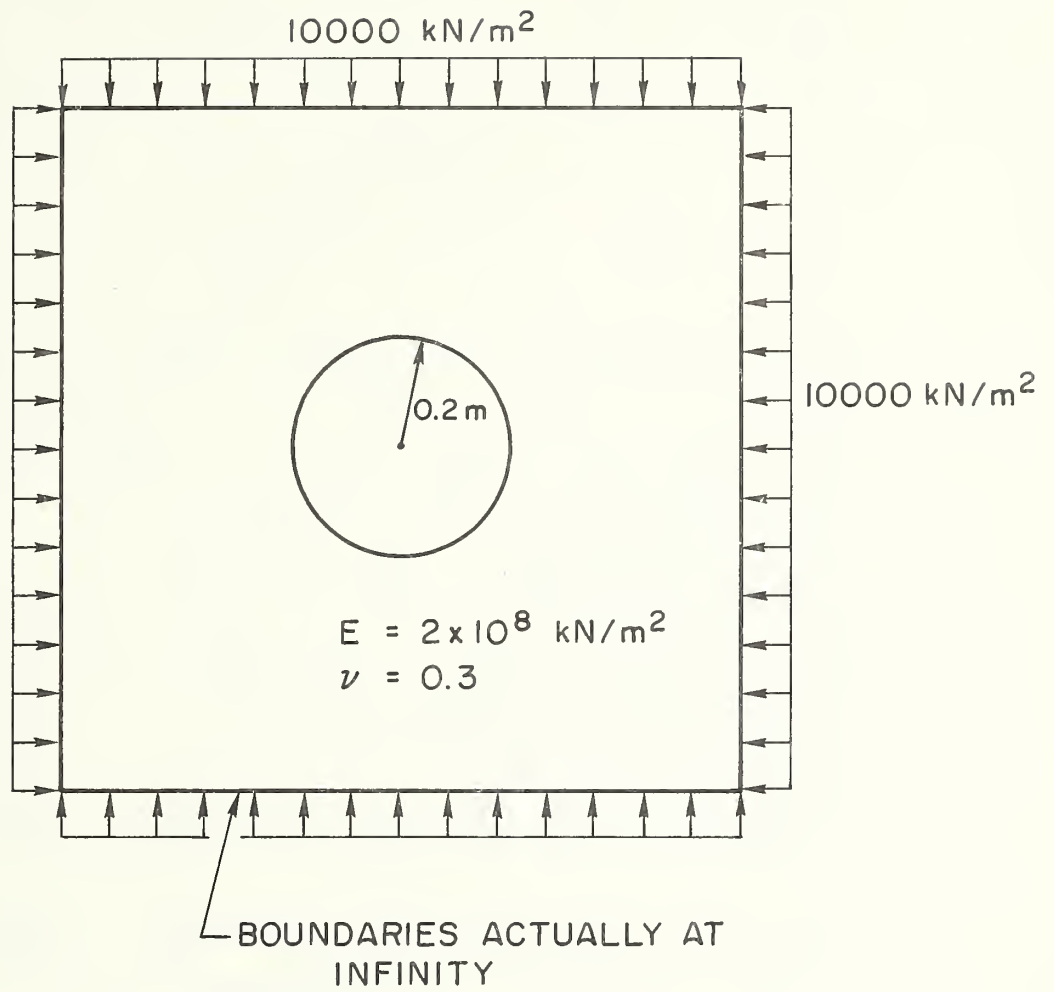


FIGURE 4.5. PROBLEM ANALYZED IN PLANE STRAIN VERIFICATION STUDIES

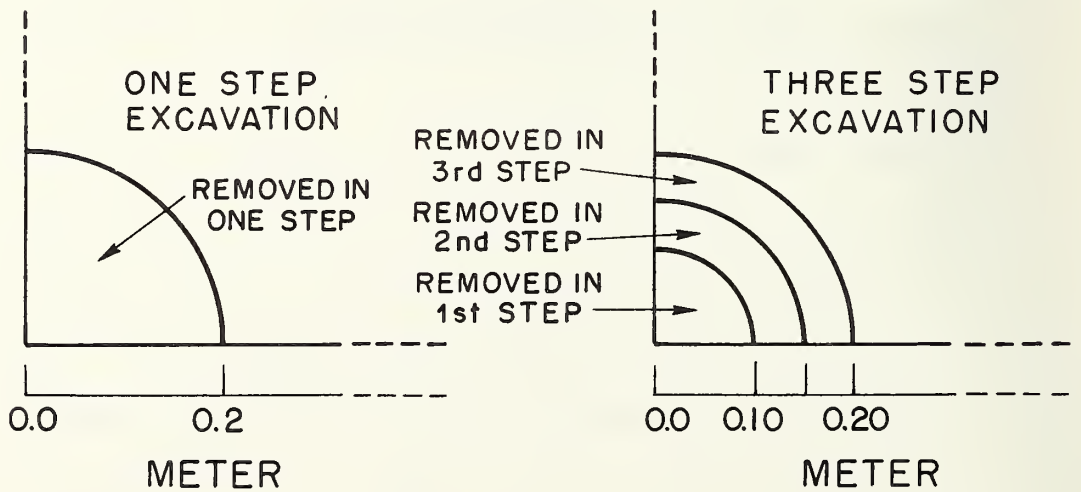
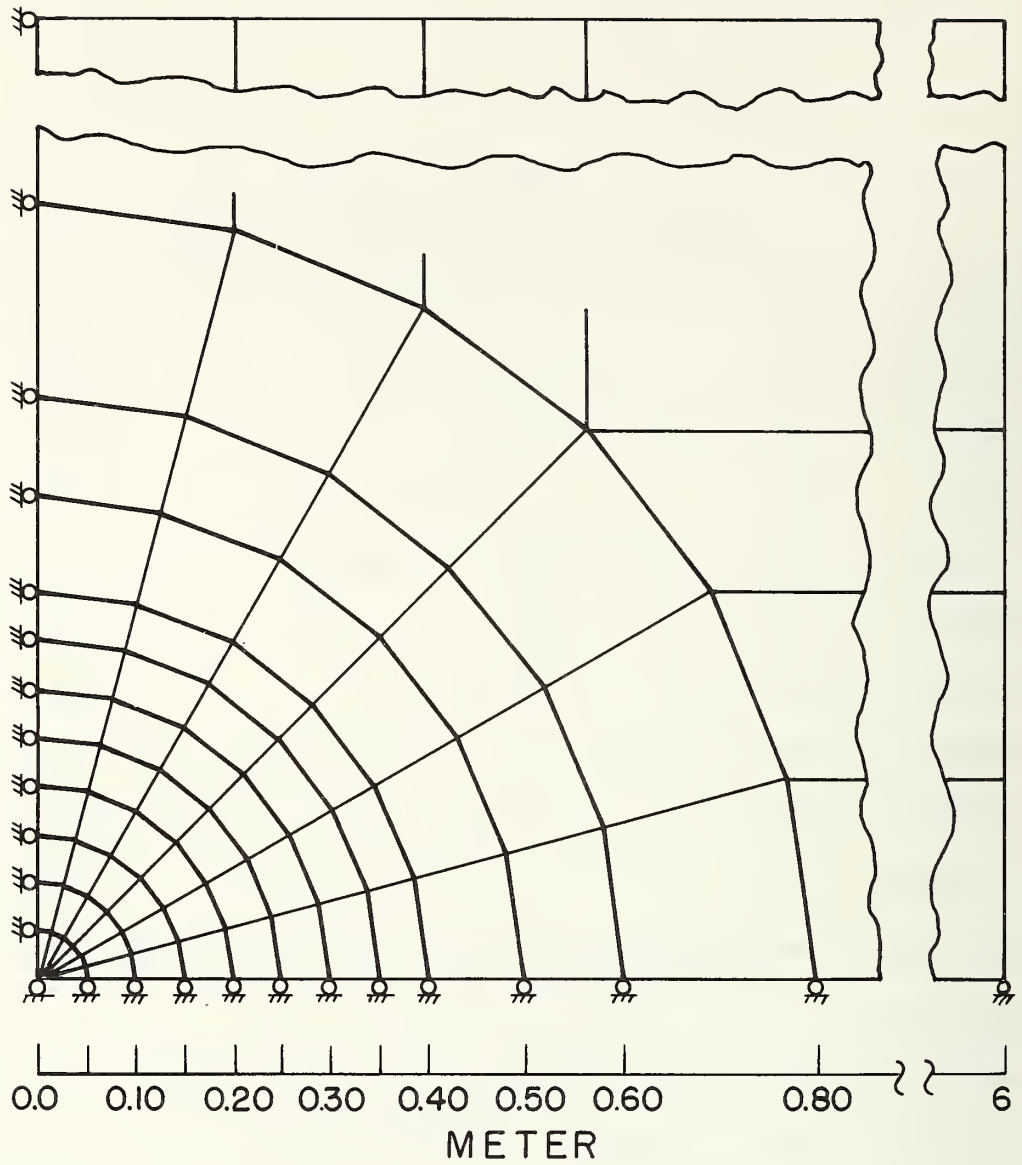


FIGURE 4.6. FINITE ELEMENT MESH FOR PLANE STRAIN VERIFICATION STUDIES

in two different ways; first, in one step all the material was removed; second, the material is removed in three small steps (See Fig. 4.6). Since the problem being analyzed is linear elastic, either simulation should give the same answer. However, the three step case allows a test of the capability of the program to model excavation in stages, a common procedure.

Results - Initially Unstressed Medium With a Cylindrical Hole Subjected to Boundary Stresses

Five runs were made for this case, using modulus values for the "air" elements in the hole ranging from 0.5×10^{-6} to 0.5×10^{-19} times the modulus of the plate. In all cases, the radial and tangential stresses and displacements were within one percent of the theoretical solution results, with the modulus of the air elements having little to no influence. This finding means that (1) the program is working correctly on a general basis and, (2) the representation of "excavated" material by elements with low stiffness values is a satisfactory procedure.

Results - Initially Stressed Medium With Cylindrical Hole Excavated in Stages

The results of these analyses were equally as satisfactory as those of the preceding case. A plot of the theoretical radial and tangential stresses is shown in Fig. 4.7 compared to the finite element results for both the one and three stage excavation simulations. No difference can be discerned for any of the results. The accuracy of the finite element results is better depicted in Tables 4.1 - 4.4 which give percent errors relative to the closed form results for the radial and tangential stresses at various points in the system. The

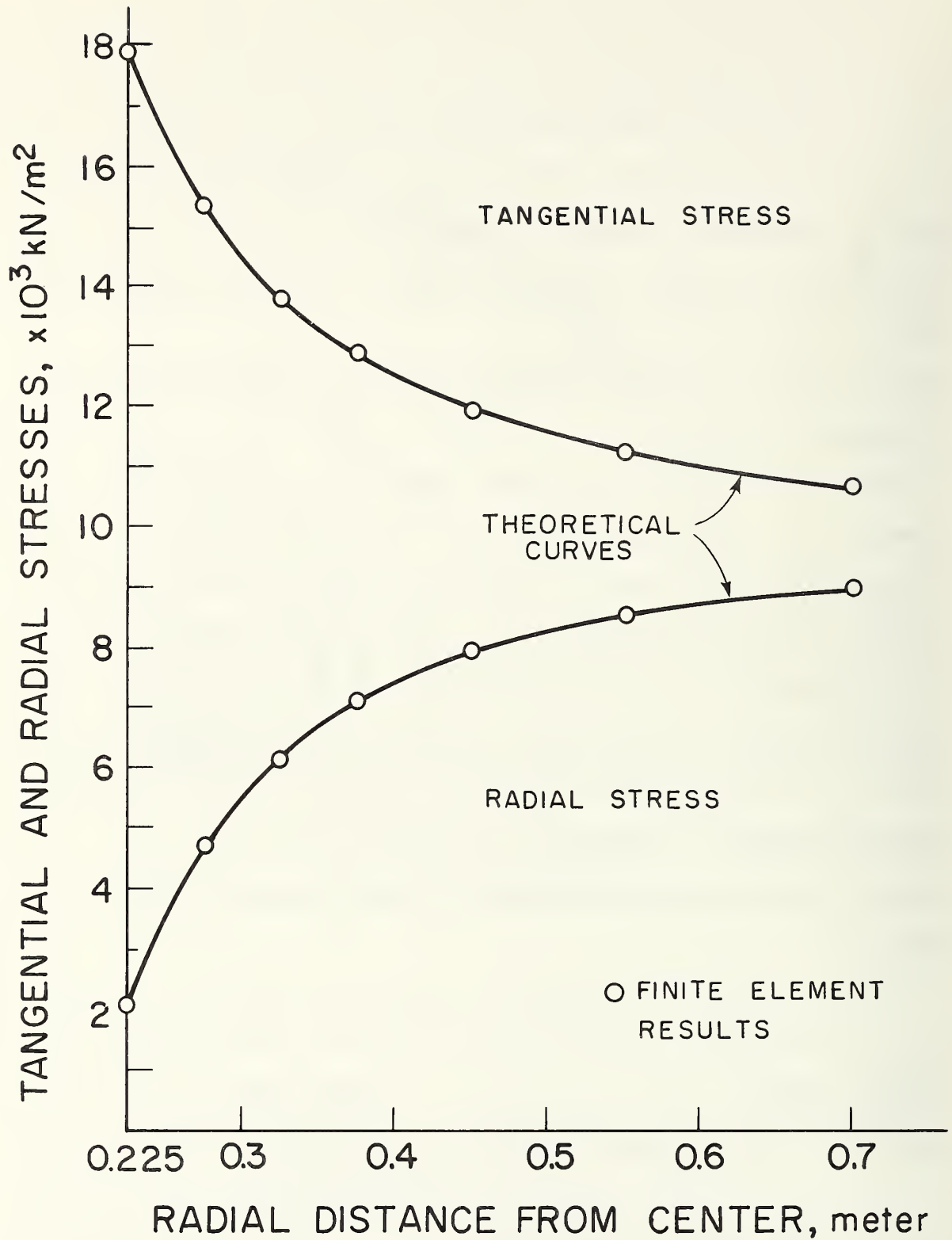


FIGURE 4.7. COMPARISON OF FINITE ELEMENT PREDICTIONS AND CLOSED FORM SOLUTION RESULTS

TABLE 4.1. COMPARISON OF TANGENTIAL STRESSES BETWEEN THEORETICAL AND FINITE ELEMENT RESULTS--ONE-STEP EXCAVATION (kN/m²).

Radius, m	Theory	Finite element results*						Average	% diff from theory	% diff of high from low value
		A	B	C	D	E	F			
0.225	17901	17760	17910	18030	18030	17910	17760	17900	-.01	1.52
0.275	15289	15240	15260	15250	15250	15260	15240	15250	-.26	.07
0.325	13787	13730	13740	13740	13740	13740	13730	13737	-.36	.07
0.375	12844	12760	12780	12830	12830	12780	12760	12790	-.42	.55
0.450	11975	11890	11960	11980	11980	11960	11890	11943	-.27	.76
0.550	11322	11240	11270	11340	11340	11270	11240	11283	-.34	.89
0.700	10816	10750	10750	10880	10880	10750	10750	10793	-.21	1.21

TABLE 4.2. COMPARISON OF RADIAL STRESSES BETWEEN THEORETICAL AND FINITE ELEMENT RESULTS--ONE-STEP EXCAVATION (kN/m²).

Radius, m	Theory	Finite element results*						Average	% diff from theory	% diff of high from low value
		A	B	C	D	E	F			
0.225	2099	2062	2064	1988	1988	2064	2062	2038	-2.91	3.82
0.275	4711	4673	4675	4671	4671	4675	4673	4673	-.81	.09
0.325	6213	6198	6181	6162	6262	6181	6198	6180	-.53	.58
0.375	7156	7158	7121	7092	7092	7121	7158	7124	-.45	.93
0.450	8025	8009	7982	7952	7952	7982	8009	7981	-.55	.72
0.550	8678	8699	8615	8600	8600	8615	8699	8638	-.46	1.15
0.700	9184	9175	9225	9013	9013	9225	9175	9138	-.50	2.35

* Elements around periphery of hole

TABLE 4.3. COMPARISON OF TANGENTIAL STRESSES BETWEEN THEORETICAL AND FINITE ELEMENT RESULTS--THREE-STEP EXCAVATION (kN/m²)

Radius, m	Theory	Finite element results*						Average	% diff from theory	
		A	B	C	D	E	F			
0.225	17901	17740	17680	17990	17990	17990	17680	17740	17803	-.55
0.275	15289	15150	15270	15150	15150	15150	15270	15150	15190	-.65
0.325	13787	13690	13690	13700	13700	13700	13690	13690	13693	-.68
0.375	12844	12730	12750	12800	12800	12800	12750	12730	12760	-.65
0.450	11975	11870	11940	11960	11960	11960	11940	11870	11923	-.43
0.550	11322	11230	11250	11330	11330	11330	11250	11230	11270	-.46
0.700	10816	10750	10740	10870	10870	10870	10740	10750	10787	-.27

TABLE 4.4. COMPARISON OF RADIAL STRESSES BETWEEN THEORETICAL AND FINITE ELEMENT RESULTS--THREE-STEP EXCAVATION (kN/m²)

Radius, m	Theory	Finite element results*						Average	% diff from theory	
		A	B	C	D	E	F			
0.225	2099	2270	1761	2365	2365	1761	1761	2270	2132	1.57
0.275	4711	4732	4684	4792	4792	4684	4684	4732	4736	.53
0.325	6213	6232	6225	6221	6221	6225	6225	6232	6226	.21
0.375	7156	7186	7153	7134	7134	7153	7153	7186	7158	.03
0.450	8025	8029	8005	7980	7980	8005	8005	8029	8005	-.25
0.550	8678	8713	8632	8618	8618	8632	8632	8713	8654	-.28
0.700	9184	9185	9234	9025	9025	9234	9234	9185	9148	-.39

* Elements around periphery of hole

maximum error is only three percent and this occurs in one isolated case. Generally, the error is less than one percent.

In summary, the following conclusions may be made from the results of comprehensive testing of the plane strain analysis capability of the finite element program:

1. The program performs plane strain analyses correctly, producing results that are in excellent agreement with those predicted by theory.
2. The modeling of empty space by "air" elements of low modulus is valid, leading to results that are stable (insensitive to a variations in material properties specified for the "air" element).
3. Excavation is correctly simulated by the excavation procedure followed by the program.

TESTING OF THE AXISYMMETRIC ANALYSIS CAPABILITY

To verify the axisymmetric analysis capability of the finite element program, several analyses were performed and their results were compared with theoretical predictions. The problem analyzed was that of a thick walled cylinder subjected to uniform external radial pressure. Closed form tangential and radial stresses and radial displacements are given by:

$$\text{tangential stress} = \sigma_{\theta} = p \frac{b^2(a^2 + r^2)}{r^2(b^2 - a^2)}$$

$$\text{radial stress} = \sigma_r = p \frac{b^2(r^2 - a^2)}{r^2(b^2 - a^2)}$$

$$\text{radial displacement} = r \frac{\sigma_{\theta} - \nu\sigma_r}{E}$$

where for the problem analyzed,

$$\begin{aligned} p &= \text{uniform external radial pressure} = 10000 \text{ kN/m}^2 \\ a &= \text{inner radius} = 2\text{m} \\ b &= \text{outer radius} = 10\text{m} \\ \nu &= \text{Poisson's ratio} = 0.3 \\ E &= \text{modulus of elasticity} = 2 \times 10^8 \text{ kN/m}^2 \end{aligned}$$

Three finite element verification analyses were performed: (a) an analysis where elements within the inner radius were assumed to be "air" and uniform boundary pressures are applied on initially unstressed cylinders, (b) and (c) an analysis where the cavity was excavated in one step and two steps respectively from an initially uniformly stressed cylinder. The theoretical and finite element predictions are compared in Tables 4.5-4.7 for all three cases. The following may be observed:

1. There is excellent agreement in tangential stress results for all three cases when compared with theory. Percentage errors are less than .4%, with several values that are exactly correct.
2. There is excellent agreement in radial stress results. Percentage errors are, with one exception, less than 1%.
3. There is excellent agreement in radial displacements with zero errors for the first two analyses, and percentage errors less than .05% for the 2-step excavation analysis.
4. There is essentially exact similarity of results for the no-excavation and the one and two-stage excavation cases, thus verifying the validity of the excavation procedure in axisymmetric analyses.

PRELIMINARY PLANE STRAIN PARAMETRIC STUDIES

The preceding sections of this chapter have documented the new code capabilities and the accuracy of the results. In the following paragraphs, the code is applied to a series of hypothetical problems which allow a preliminary definition of the degree of support provided by chemical stabilization of the soil around a tunnel.

Problems Studied

The geometry of the problems analyzed is depicted in Fig. 4.8. The stabilized soil zone surrounds a tunnel which has a diameter of 7m with its crown some 10m below ground surface. Soil is assumed to be a

TABLE 4.5. COMPARISON OF TANGENTIAL STRESSES BETWEEN THEORETICAL AND FINITE ELEMENT AXISYMMETRIC ANALYSIS RESULTS (kN/m²)

Radius, m	Theory	No excavation * Stresses	% diff	One-step Stresses	% diff	Two-step Stresses	% diff
2.05	20330	20320	-.05	20320	-.05	20310	-.10
2.15	19430	19420	-.05	19420	-.05	19410	-.10
2.25	18650	18640	-.05	18640	-.05	18630	-.11
2.35	17960	17960	0.	17960	0.	17950	-.06
2.45	17360	17350	-.06	17350	-.06	17350	-.06
2.55	16820	16820	0.	16820	0.	16810	-.06
2.65	16350	16350	0.	16350	0.	16340	-.06
2.75	15930	15920	-.06	15920	-.06	15920	-.06
2.85	15550	15540	-.06	15540	-.06	15540	-.06
2.95	15200	15200	0.	15200	0.	15200	0.
3.05	14900	14890	-.07	14890	-.07	14890	-.07
3.15	14620	14610	-.07	14610	-.07	14610	-.07
3.25	14360	14360	0.	14360	0.	14360	0.
3.35	14130	14130	0.	14130	0.	14120	-.07
3.45	13920	13920	0.	13920	0.	13910	-.07
3.75	13380	13360	-.15	13360	-.15	13360	-.15
4.50	12470	12430	-.32	12430	-.32	12430	-.32
5.50	11790	11780	-.08	11780	-.08	11770	-.17
7.00	11270	11240	-.27	11240	-.27	11240	-.27
9.00	10930	10920	-.09	10920	-.09	10920	-.09

* Cylinder with hole subjected to boundary stress

TABLE 4.6. COMPARISON OF RADIAL STRESSES BETWEEN THEORETICAL AND FINITE ELEMENT AXISYMMETRIC ANALYSIS RESULTS (kN/m²)

Radius, m	Theory	No excavation *		One-step excav		Two-step excav	
		Stresses	% diff	Stresses	% diff	Stresses	% diff
2.05	501.9	489.4	-2.49	489.4	-2.49	497.1	-.96
2.15	1403	1392	-.78	1392	-.78	1399	-.29
2.25	2186	2178	-.37	2178	-.37	2184	-.09
2.35	2872	2865	-.24	2865	-.24	2870	-.07
2.45	3475	3469	-.17	3469	-.17	3474	-.03
2.55	4009	4004	-.12	4004	-.12	4009	0.
2.65	4483	4479	-.09	4479	-.09	4483	0.
2.75	4907	4903	-.08	4903	-.08	4907	0.
2.85	5287	5284	-.06	5284	-.06	5287	0.
2.95	5629	5626	-.05	5626	-.05	5629	0.
3.05	5938	5935	-.05	5935	-.05	5938	0.
3.15	6217	6215	-.03	6215	-.03	6218	.02
3.25	6472	6470	-.03	6470	-.03	6473	.02
3.35	6704	6702	-.03	6702	-.03	6705	.01
3.45	6916	6914	-.03	6914	-.03	6917	.01
3.75	7454	7426	-.38	7426	-.38	7428	-.35
4.50	8359	8304	-.66	8304	-.66	8306	-.63
5.50	9039	9015	-.27	9015	-.27	9016	-.25
7.00	9566	9529	-.39	9529	-.39	9529	-.39
9.00	9902	9889	-.13	9889	-.13	9889	-.13

* Cylinder with hole subjected to boundary stress

TABLE 4.7. COMPARISON OF RADIAL DISPLACEMENTS BETWEEN THEORETICAL AND FINITE ELEMENT AXISYMMETRIC ANALYSIS RESULTS (10^{-4} m)

Radius, m	Theory	No excavation*		One-step excav		Two-step excav	
		Displmt.	% diff	Displmt.	% diff	Displmt.	% diff
2.0	2.0833	2.0833	0.	2.0833	0.	2.0822	-0.05
2.1	2.0533	2.0533	0.	2.0533	0.	2.0542	-0.05
2.2	2.0331	2.0331	0.	2.0331	0.	2.0321	-0.05
2.3	2.0161	2.0161	0.	2.0161	0.	2.0151	-0.05
2.4	2.0035	2.0035	0.	2.0035	0.	2.0025	-0.05
2.5	1.9948	1.9948	0.	1.9948	0.	1.9939	-0.05
2.6	1.9896	1.9896	0.	1.9896	0.	1.9887	-0.05
2.7	1.9875	1.9875	0.	1.9875	0.	1.9866	-0.05
2.8	1.9881	1.9881	0.	1.9881	0.	1.9873	-0.04
2.9	1.9912	1.9912	0.	1.9912	0.	1.9904	-0.04
3.0	1.9965	1.9965	0.	1.9965	0.	1.9958	-0.04
3.1	2.0039	2.0039	0.	2.0039	0.	2.0031	-0.04
3.2	2.0130	2.0130	0.	2.0130	0.	2.0123	-0.03
3.3	2.0238	2.0238	0.	2.0238	0.	2.0231	-0.03
3.4	2.0362	2.0362	0.	2.0362	0.	2.0355	-0.03
3.5	2.0499	2.0499	0.	2.0499	0.	2.0492	-0.03
4.0	2.1354	2.1354	0.	2.1354	0.	2.1348	-0.03
5.0	2.3646	2.3646	0.	2.3646	0.	2.3641	-0.02
6.0	2.6389	2.6389	0.	2.6389	0.	2.6385	-0.02
8.0	3.2552	3.2552	0.	3.2552	0.	3.2548	-0.01
10.0	3.9167	3.9167	0.	3.9167	0.	3.9163	-0.01

* Cylinder with hole subjected to boundary stress

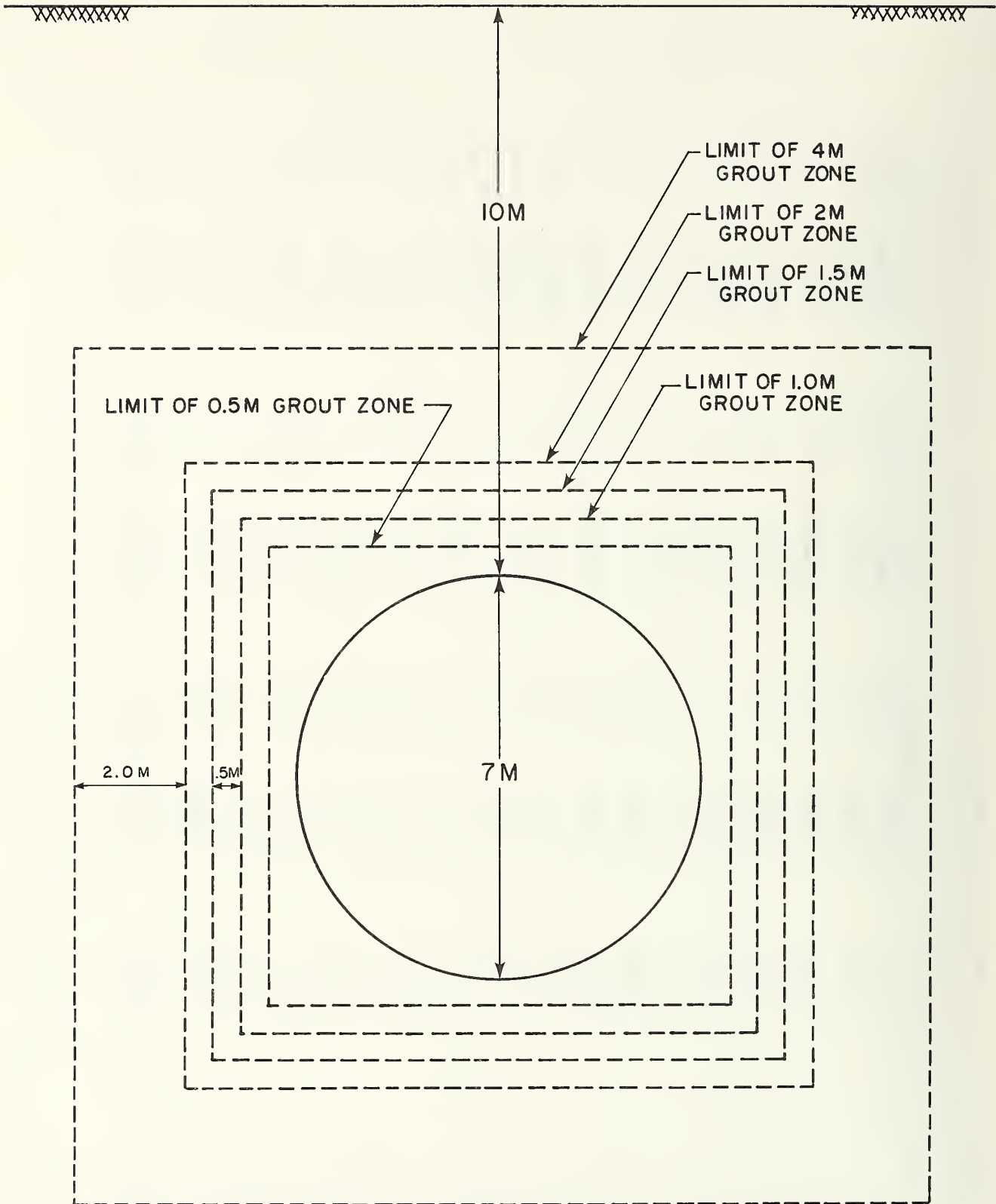


FIGURE 4.8. DETAILS OF PARAMETRIC STUDY PROBLEMS

homogeneous medium sand with no groundwater table present. The stabilized zone is square in shape; its thickness was varied in the studies to determine the influence of this factor. The thickness, defined as the smallest dimension remaining after tunneling (see Fig. 4.8), was varied from 0.5m to 4m, values typical of those used in practice.

Finite Element Representation

The finite element mesh used for the analysis is shown in Fig. 4.9. Only half the problem is modeled in the mesh because of symmetry along the vertical axis through the tunnel. The problem would also have a line of symmetry along the horizontal axis if the initial stresses were taken as uniform; this is not the case because an initial gravity stress field is used with the vertical and horizontal stresses increasing linearly.

The rightmost and bottom boundary of the mesh are placed in the mesh so as to be far enough away to have little to no influence on the calculated results. The right most boundary is located some 12 tunnel radii from the line of symmetry. The mesh consists of 401 elements and 436 nodes.

Material Parameters

Material parameters necessary to define the behavior of the nonlinear stress-strain model used in the program are:

1. Cohesion, c
2. Angle of Internal Friction, ϕ
3. Unit weight, γ
4. Modulus Number, K [$E_i = K p_a \left(\frac{\sigma_3}{p_a} \right)^n$, refer to Chapter III for details]
5. Modulus Exponent, n
6. Poisson's Ratio, ν

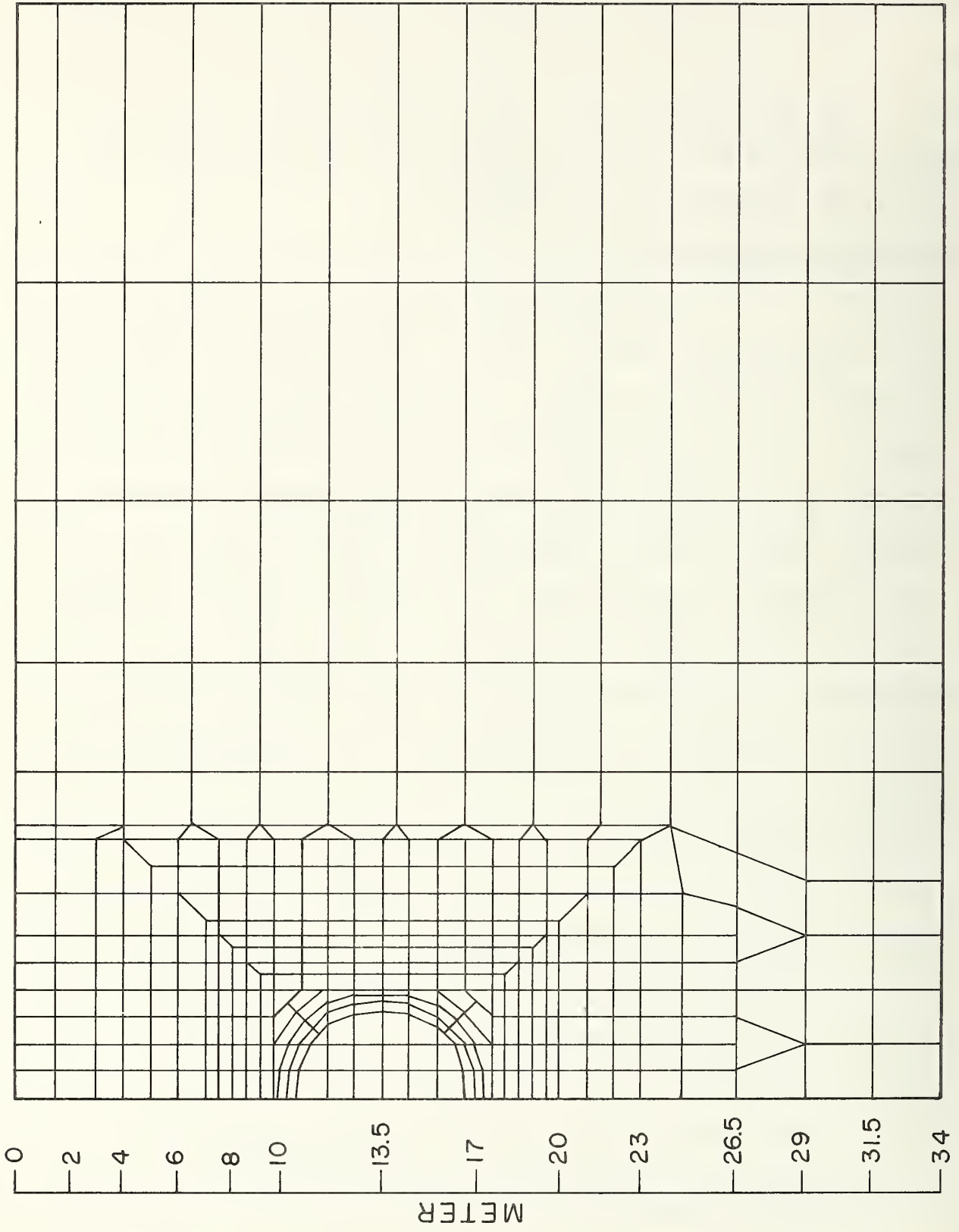


FIGURE 4.9. FINITE ELEMENT MESH FOR PARAMETRIC STUDY PROBLEM

For the ungrouted medium dense sand, parameters for similar materials were obtained from the literature. Parameters for the grouted sand were varied in the different analyses so as to represent a weak, a medium, and a strong stabilization effect. The values of the parameters were selected so as to be consistent with, but well on the conservative side of the results indicated for grouted soil behavior in Chapter III. It was considered unwise to use the peak strengths and stiffnesses found in the relatively short term tests used in most of the laboratory work in view of the longer periods of loading which actually occur in tunneling. In the field, a grouted soil may be loaded over a period of several days before liner support is supplied and brought into contact with the soil. Future efforts will be concentrated on better definition of properties for the actual tunneling problem via the continuing laboratory and field behavior documentation work.

Values of the parameters used in these preliminary studies are given in Table 4.8.

TABLE 4.8.

PARAMETERS USED IN PRELIMINARY GROUTED TUNNEL ANALYSES

Soil Type	Unit Weight kN/m ³	Cohesion kN/m ²	ϕ	K	n	Poisson's Ratio	Coefficient of Lateral Earth Pressure
Sand	19	0	38	400	0.5	0.3	0.5
Weak Stabilized Sand	19	34.5	38	900	0.2	0.48	0.5
Medium Stabilized Sand	19	103.5	38	1200	0.2	0.48	0.5
Strong Stabilized Sand	19	172.5	38	1500	0.2	0.48	0.5

The designations weak, medium and strong stabilized sand correspond to unconfined compressive strengths of 142, 424, and 707 kN/m² respectively. These values derive as a direct result of the friction angles and cohesion values given in Table 4.3.

Loading and Tunneling Conditions

Initial stresses were taken as representative of a gravity stress field. Vertical stresses increase linearly with depth and horizontal stresses were obtained by multiplying the vertical stresses by the lateral earth pressure coefficient of 0.5. Excavation generally was carried out in the program in two stages, with two iterations performed on each stage. This procedure was found to yield convergent results which were in agreement with those obtained using more stages and/or more iterations.

The process of shield tunneling through the grouted zones in the parametric studies was assumed to lead to creation of an annular gap around the liner of 14 cm. Should the gap close, the "liner springs" discussed previously are activated to limit further movements. A 14cm annular gap is likely to occur only in poor tunneling practice, but this situation is felt to best illustrate the effects of grouting. In future studies, other tunneling procedures will be considered.

Results

Typical predicted surface settlement profiles are shown in Fig.4.10. Maximum settlements range from 40 mm for the weakest and thinnest grout zone to 4 mm for the strongest and thickest grout zones. Settlements for the case of no grout are shown in Fig. 4.10 for comparative purposes and reached a maximum of 105mm, more than double that of the weakest grout zone. Movements around the tunnel opening were in no case large enough

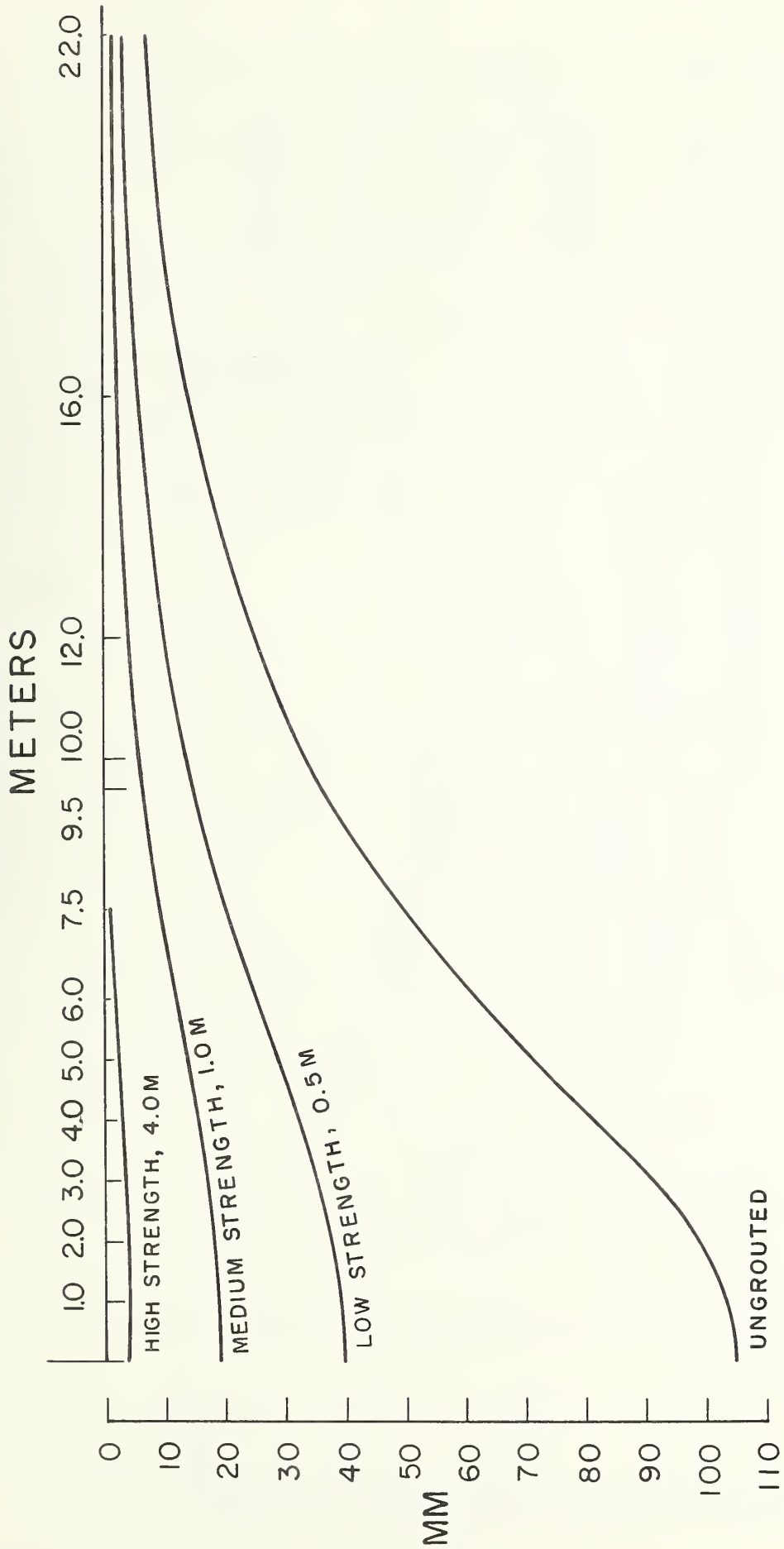


FIGURE 4.10. PREDICTED SETTLEMENTS FROM PARAMETRIC STUDIES

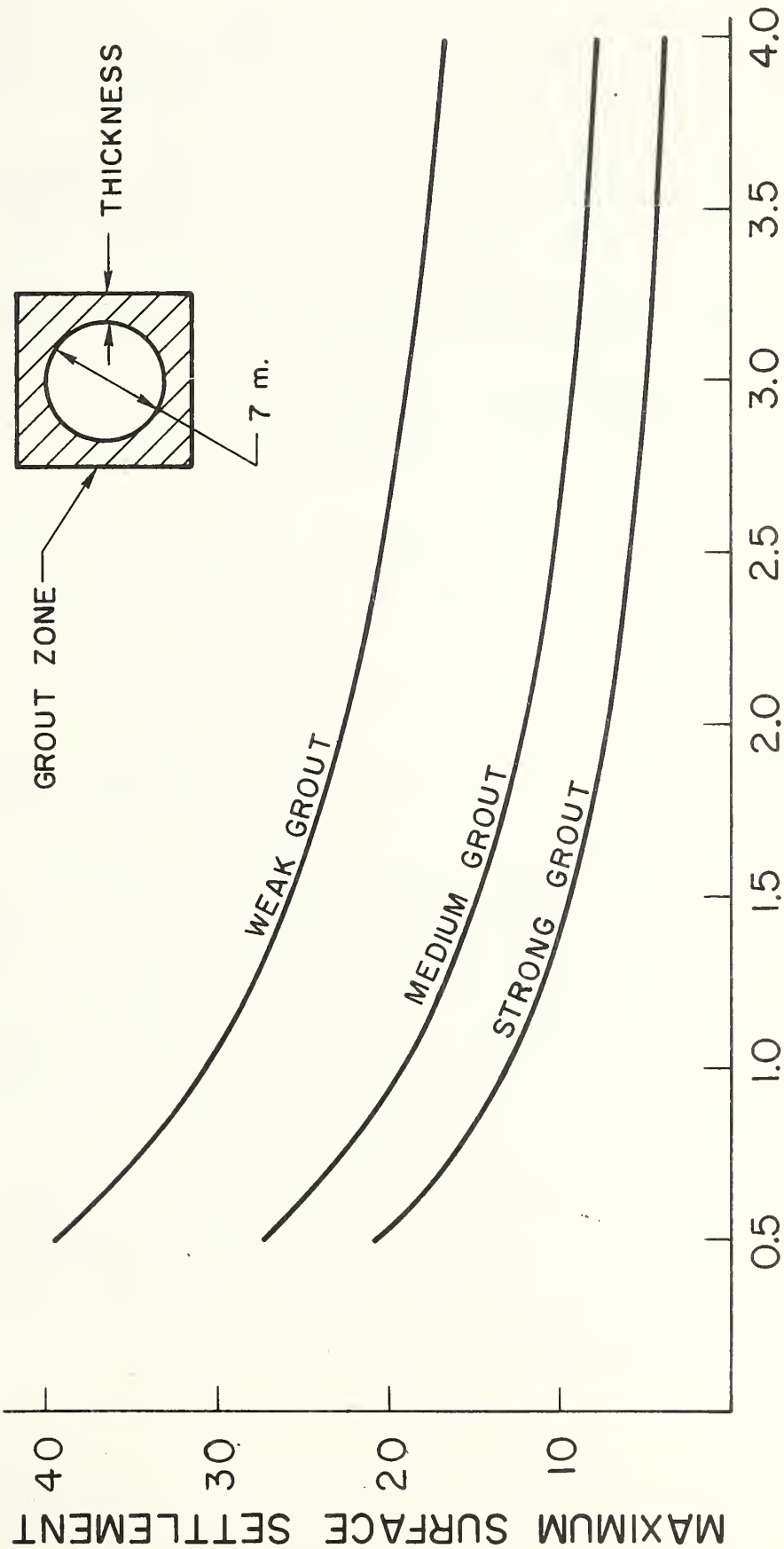
to activate the tunnel "liner springs." The shape of the predicted surface settlement curves is in agreement with that usually observed above tunnels. Magnitudes of the settlements are also quite reasonable, being somewhat less than those reported for ungrouted tunnels.

Plots of the effect of grout zone size and strength/stiffness on maximum surface settlement are shown in Figure 4.11. They show that a given settlement value may be attained through different combinations of grout zone size and strength/stiffness. The choice of a particular combination to be used in practice must eventually be governed by cost considerations. They also show the diminishing effect on minimizing settlement in using larger and larger sizes of grout zones. Similarly, these plots show the diminishing effect on minimizing settlement of increasing the strength/stiffness of grout. For example, for the case of medium strength grout, increasing the size from 0.5 to 1.0 meter reduces maximum settlement by about 8mm, while increasing the size from 1.0 to 1.5 meters reduced maximum settlement by only 5mm. For the 1.5 meter grout zone, an increase by a ratio of 3 from an unconfined compressive strength of 141.5 to 424.4 caused a decrease in settlement of 11mm, while an increase by a ratio of 5 from 141.5 to 707.4 caused a decrease of only 16mm. Obviously, neither the use of very large or very strong grouts is necessarily desirable.

Concerning the effect of grouting on stresses in the soil around the tunnel, the finite element analyses reveal the following:

- (a) When no grout zone is present, massive shear failure of the sand occurs, with failure extending all the way to the surface.

MAX. SURFACE SETTLEMENT



GROUT ZONE THICKNESS - METERS

FIGURE 4.11. EFFECT OF GROUT ZONE SIZE AND STRENGTH ON MAXIMUM SURFACE SETTLEMENT

- (b) When a grout zone is employed, failure in the ungrouted sand occurs only for the weakest and thinnest grout zone; even in this case, only a small zone of failure occurs. The grout is thus very effective in protecting the soil medium around the tunnel from the stresses induced by tunneling.
- (c) Using the weak grout representation, failure in the grout zone is prominent for the 0.5 and 1.5m thick zones. Failure is limited to the inner 0.5m of the grout zone for large sizes.
- (d) When medium strength grout is used, failure in the grout zone occurs only in very limited areas for grout zone sizes of 0.5 to 1.5m, and does not occur at all for sizes of 2.0m and 4.0m.
- (e) No shear failure occurs when high strength grout is used, regardless of the grout zone size.

SUMMARY

A finite element code has been developed which can simulate the effects of tunneling through a grouted zone. The code is extremely flexible and allows the user to model a wide variety of variables associated with the problem. Theoretical tests have been conducted to assure the validity of the code.

Use of the finite element code in a series of parametric studies demonstrated its value in assessing the effects of grouting in stabilizing the soils around a tunnel. Where the grout zones fully surround the tunnel, failure in the ungrouted soil medium adjacent to the tunnel is essentially eliminated for even weak grout representations. Use of moderate to strong grout zones significantly reduces surface settlements. In future work more extensive studies will be performed in order to develop some simplified procedures for selecting necessary grout zone sizes and strengths for limiting surface movements.

CHAPTER V

FIELD GROUTING SITES

The laboratory testing program described in Chapter III has demonstrated many important facets about the behavior of grouted soil. However, the tests were all performed on samples created under ideal laboratory conditions. The obvious question to be raised concerning results so obtained is, "Will the response of a soil grouted under field conditions be the same as that of the ideal laboratory samples?" In order to provide an answer to that question, a series of field trials were set forth in the proposed work for this contract.

The field trials were designed to proceed as follows:

1. Locate a site with reasonably uniform surficial sands.
2. Via a series of shallow injections, create bulbs of grouted soil at the site using different grout types in the bulbs.
3. Excavate the bulbs, cut out a sample of each, and return the samples to the lab.
4. Trim the samples and load test the soil to failure.
5. Inject, in the laboratory, samples of the natural sand from the site with the grouts used in the field.
6. Perform load tests on the laboratory prepared samples.
7. Compare load test results between the laboratory and field grouted samples.

As originally envisioned, there were to be four field trials utilizing four injections of grout each. However, circumstances developed which dictated an alteration of these plans. First, it became apparent that there was little to be learned by grouting four different sites since it has been shown that changes in grain size and sand density have only a small effect on grouted soil behavior. Second, it was quickly obvious that obtaining access to four well suited sites involved tedious and time-

consuming negotiations which detract from the main effort. Third, the opportunity arose to participate in an instrumented grouted tunnel project in Washington, D. C.; this unique and invaluable work was undertaken and it required some of the effort originally budgeted to the field trials (see Chapter VI).

The final solution adopted was to grout at two local sites with more grout mixes than originally planned when four sites were to be used.

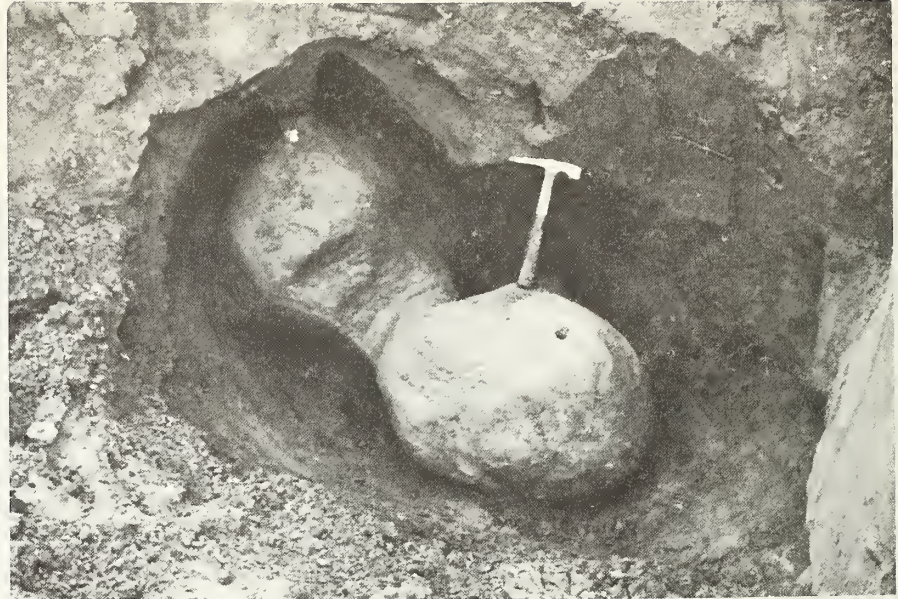
GENERAL DESCRIPTION OF FIELD TRIALS AND RELATED LABORATORY WORK

The field trials were conducted by injecting single or multiple bulbs of grout into surficial sands. Grouting was carried out by personnel of the Pressure Grout Company under the direction of Mr. E. Graf. The method of injection involved jetting a pipe into place and grouting through the pipe. Because the overburden depth was so small, grout pressures were kept small, 100 kN/m^2 (15 psi) or less.

Five different grouts were used at each location; in several instances the gel time of the same grout was varied in separate injections. The stabilized sands were left to cure for two to three weeks, after which each grout bulb was exposed by digging carefully around it. The photographs in Fig. 5.1 and 5.2 show examples of the grout bulbs after excavation. Single bulbs of approximately spherical shape are demonstrated in Fig. 5.1 (a) and (b). A small diameter "neck" can be seen in each of these cases to extend from the bulb to the ground surface. The "neck" is created when the grout pipe is withdrawn and a small amount of grout leaks out into the soil around the end of the pipe. Multi-bulb injection locations are exposed in the photographs in Fig. 5.2.



FIGURE 5.1.1. EXAMPLES OF SINGLE GROUT BULB INJECTIONS.
ALAMEDA TEST SITE



(a) Two Interconnected Bulbs



(b) Six Bulb Injection Where Bulbs Coalesced Into Large Mass

FIGURE 5.2. EXAMPLES OF MULTIPLE GROUT BULB INJECTIONS - ALAMEDA TEST SITE

Photograph 5.2 (a) shows a two-bulb overlap and Photograph 5.2 (b) shows a mass created by the injection of six bulbs. These two injections will be considered further later in this chapter.

After exposing the stabilized sand masses, the bulb or a piece of the bulb was removed to the laboratory in a plastic bag. In the laboratory, cylindrical test specimens of diameter 7.1 cm and length 16.5 cm, were trimmed from the bulk samples and load tested in unconfined compression. The unconfined compression tests were performed at a strain rate of 0.15% per minute. A total of 28 of these tests have been performed to date and approximately 12 more will be done to complete the first phase of this work.

Additional work to be carried out involves testing of samples comparable to the field soils which is now underway. Also, the grout bulbs left in the ground at the test sites will be sampled and tested again after a six to eight month cure time to determine aging effects.

RESULTS OF WORK AT TEST SITE I - ROOSEVELT HIGH SCHOOL

The first test injections were carried out on the grounds of the Roosevelt High School in San Francisco; a location map is given in Fig. 5.3 which pinpoints the site. This site was chosen for the following reasons:

1. The soils are sandy and easily groutable.
2. A complete geotechnical investigation of the site is available courtesy of the City of San Francisco and Harding-Lawson Consulting Engineers. This provides information on natural soil density, grain size distribution and strength.
3. There is easy access because the school is closed for one year for earthquake resistance renovation.

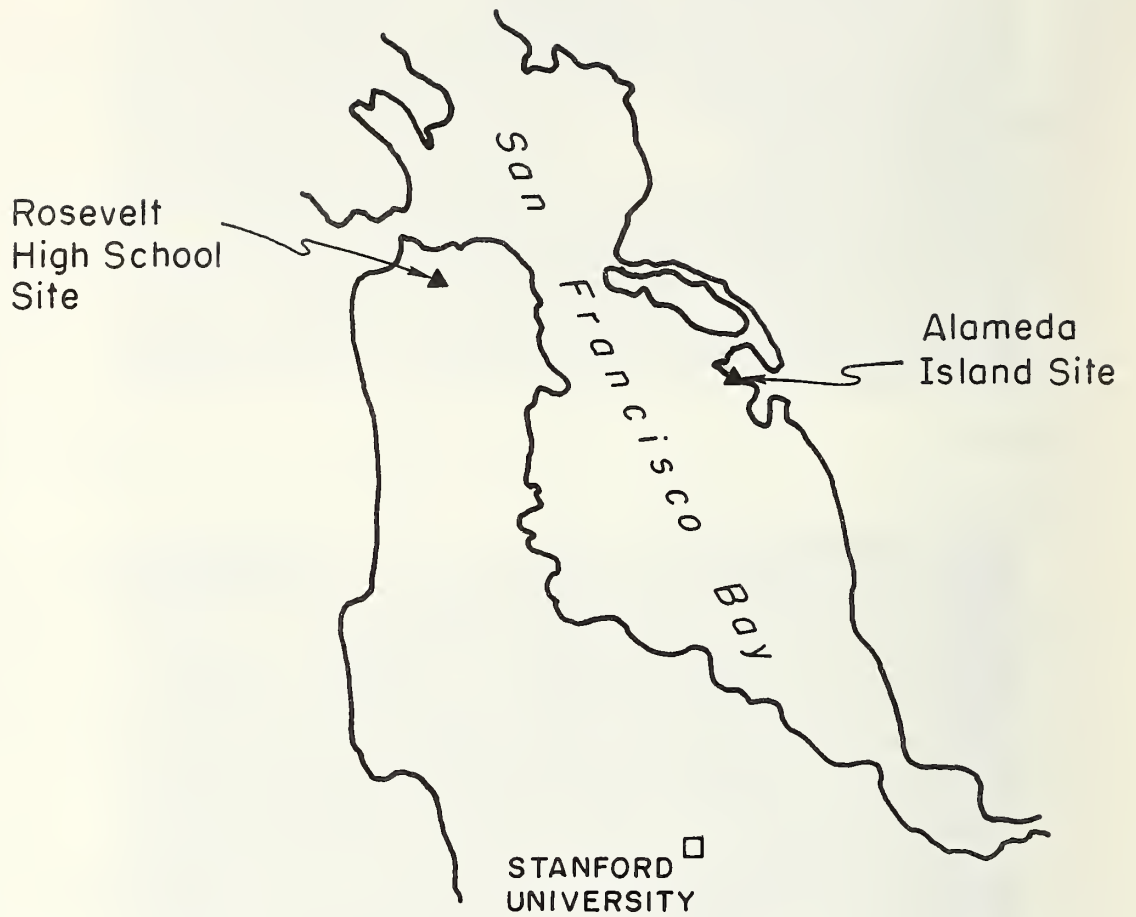


FIGURE 5.3. SITE LOCATIONS OF TEST INJECTIONS

4. Extensive ground stabilization work is being carried out at the site and a substantial number of test results in addition to our own work will be available via Harding-Lawson Consulting Engineers.

Soil Conditions

A typical soil profile at the site is depicted in Fig. 5.4, along with information as to soil densities and basic characteristics. The soils of most interest are in the upper 1.75 m ; the grout bulbs were injected at depths from one to 1.75 m. In this region, the soil is a loose fine sand with some gravel fragments. Below this depth, clean sands are found. Groundwater was not encountered down to a depth of 10 m , although the sand was moist, particularly in the upper five feet.

Grain size curves for the sand in the upper five feet are also shown in Fig. 5.2. Less than 10 percent of the material passes the number 200 sieve, and there was little to no plasticity in the fine fraction.

Test Injections

A plan view showing the layout of the seven test injections at Roosevelt High School is given in Fig. 5.5. Only single bulb injections were made at this site. The different grouts used at the injection points are given in Table 5.1. Five different grout mixes were employed; four of them using a silicate base and one using a urea base. Gel times of two of the silicate grouts were varied from rapid set (0.5 min) to medium set (10 min), in order to examine the influence of this variable.

Excavation of the bulbs went routinely, although considerable effort was required. At each location a hand excavation was made exposing the bulb. Generally, the entire bulb was extracted, placed in a plastic bag and transported to the laboratory.

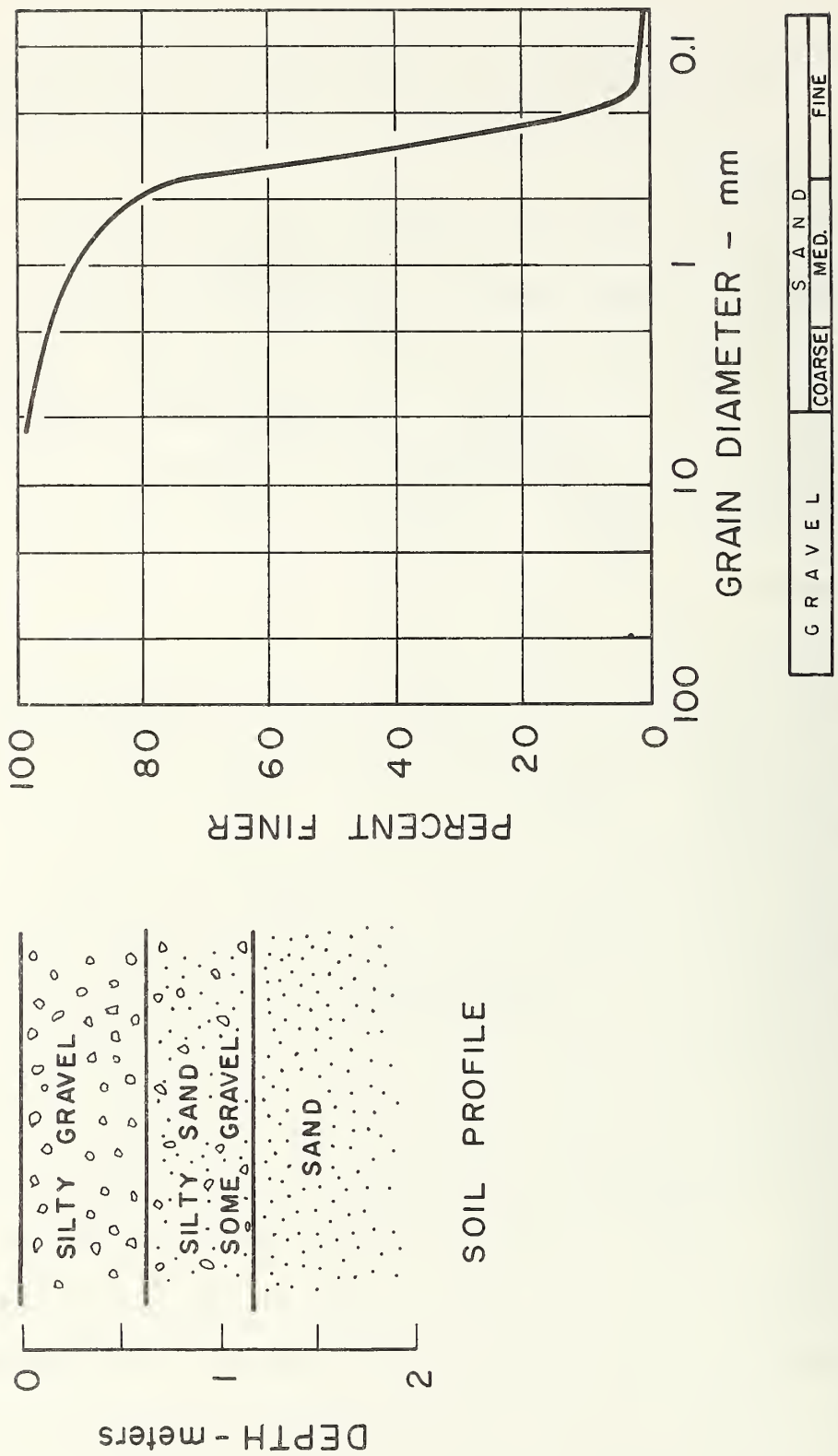


FIGURE 5.4. SOIL PROFILE AND GRAIN SIZE ANALYSIS OF SOIL WHERE GROUT WAS INJECTED, ROOSEVELT HIGH SCHOOL SITE

NUMBERS CORRESPOND TO
GROUT MIXES IN TABLE 5.1.
33 GAL. OF GROUT INJECTED
AS SINGLE BULBS AT EACH
POINT

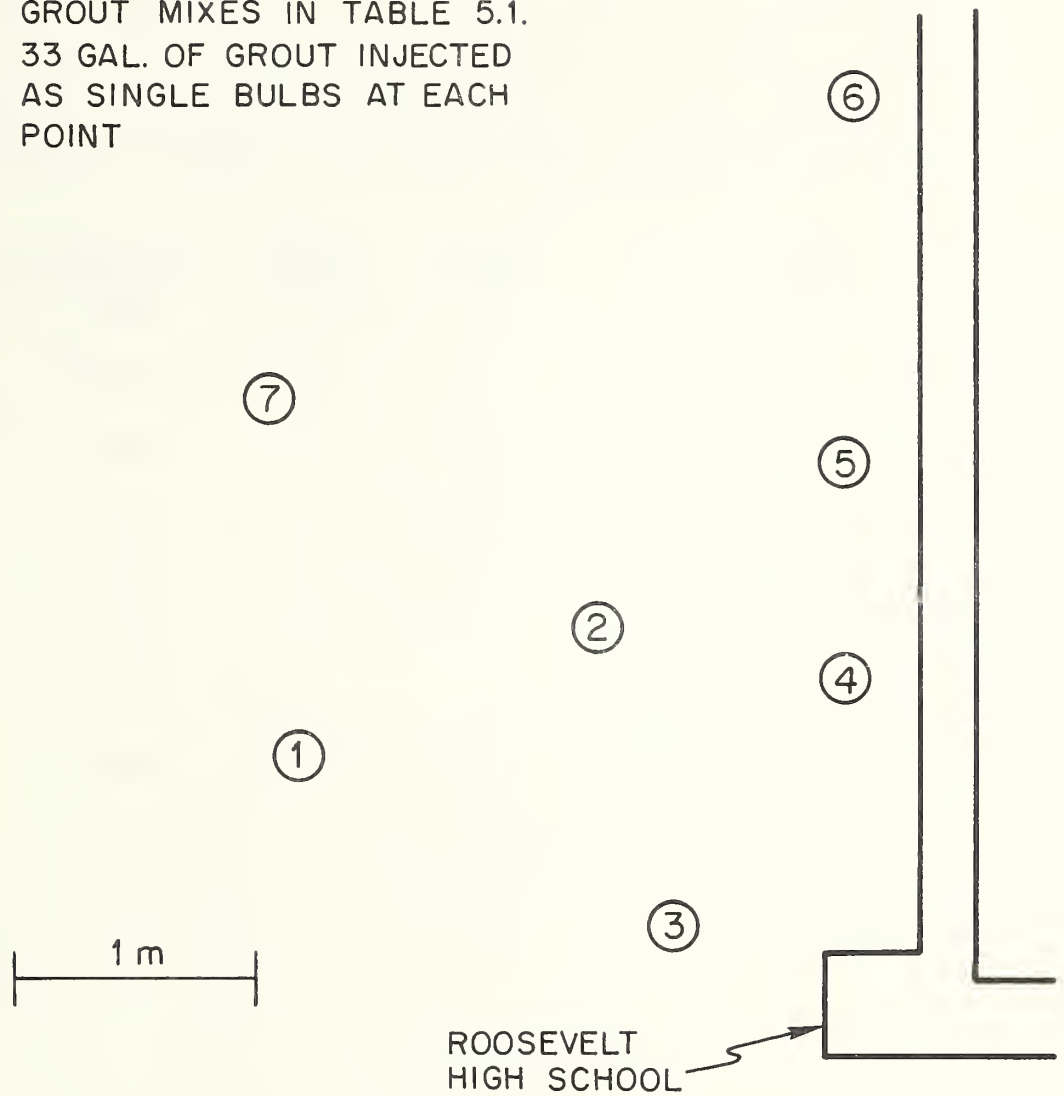


FIGURE 5.5. LAYOUT OF TEST INJECTIONS, ROOSEVELT HIGH SCHOOL SITE

TABLE 5.1

CHEMICAL GROUTS USED AT TEST INJECTIONS, ROOSEVELT HIGH SCHOOL

INJECTION POINT	GROUT NAME	BASE	PERCENT BASE	PERCENT HARDENER	APPROXIMATE GEL TIME MIN	QUANTITY INJECTED GALS
1	T-57	SILICATE	30	*	0.5	33
2	T-57	SILICATE	30	*	10.0	33
3	T-57	SILICATE	40	*	0.5	33
4	SIROC	SILICATE	30	6	30.0	33
5	T-57	SILICATE	40	*	10.0	33
6	UREA	UREA	15	0.5-1	15.0	33
7	SIROC	SILICATE	40	8	30.0	33

* = proprietary

Load Test Results

Samples for the unconfined tests were trimmed from the bulbs by sawing with a hacksaw and shaving with sharpened steel blades. This process was tedious and required a substantial amount of time. Work is now underway to develop a drilling tool to allow one to obtain samples of the correct size quickly and simply.

Eighteen load test results for the field samples from Roosevelt High School are summarized in Table 5.2. For any given grout type there is a fair amount of scatter in the measured strengths, considerably more than seen in the tests of laboratory grouted samples. The scatter is likely due to the fact that the outer portions of the grout bulb were not as strong as the inner portions, because of the difference in grout concentration in the two regions.

Direct comparison of the strengths of the field samples to that of laboratory grouted samples cannot be made until comparable grouting is done for laboratory samples of the field site sands. This is now underway. Relative to the laboratory results of Chapter III, the age and grout mixes of the samples are somewhat different. Only in the case of the Siroc samples is there enough similarity so that a satisfactory comparison can be made. Fig. 5.6 shows a plot of unconfined compressive strength versus age for laboratory tests on Monterey #30, sand stabilized by 30 and 50% silicate Siroc mixes, and, superimposed on this plot are the data for 30 and 40% silicate Siroc mix samples from Roosevelt High School. The test results from the field samples are bracketed by the lab test results indicating that there is reasonable agreement. More precise comparisons will be available as the field sands are grouted in the laboratory.

TABLE 5.2 RESULTS OF LOAD TESTS AT FIELD SITE I - ROOSEVELT HIGH SCHOOL

TEST NO	TYPE OF GROUT	PERCENTAGE OF CONSTITUENTS	(DAY) CURING TIME	CONFINING PRESSURE (PSI)	STRAIN RATE IN./MIN.	PEAK STRESS (PSI)	STRAIN AT FAILURE %	GEL TIME MIN.
1	UREA	15	22	0	0.011	81.1	0.94	30
2	UREA	15	23	0	0.011	79.6	0.61	30
3	T57	15	24	0	0.011	196.5	1.45	30
4	T57	30% SILICATE	23	0	0.011	64.1	0.70	0.5
5	T57	30% SILICATE	23	0	0.011	76.1	0.85	0.5
6	T57	30% SILICATE	31	0	0.011	43	0.48	10
7	T57	30% SILICATE	31	0	0.011	37.3	0.46	10
8	T57	30% SILICATE	31	0	0.011	43.1	0.49	10
9	T57	40% SILICATE	24	0	0.011	108.6	1.06	10
10	T57	40% SILICATE	23	0	0.011	112.0	0.94	10
11	T57	40% SILICATE	23	0	0.011	75.1	0.76	10
12	T57	40% SILICATE	27	0	0.011	64.3	0.77	0.5
13	T57	40% SILICATE	22	0	0.011	48.1	0.60	30
14	SIROC	40% SILICATE	30	0	0.011	171.6	0.78	30
15	SIROC	40% SILICATE	31	0	0.011	152.4	0.68	30
16	SIROC	40% SILICATE	22	0	0.011	211.4	0.73	30
17	SIROC	40% SILICATE	28	0	0.011	127.8	0.57	30
18	SIROC	30% SILICATE	28	0	0.011	84.1		30

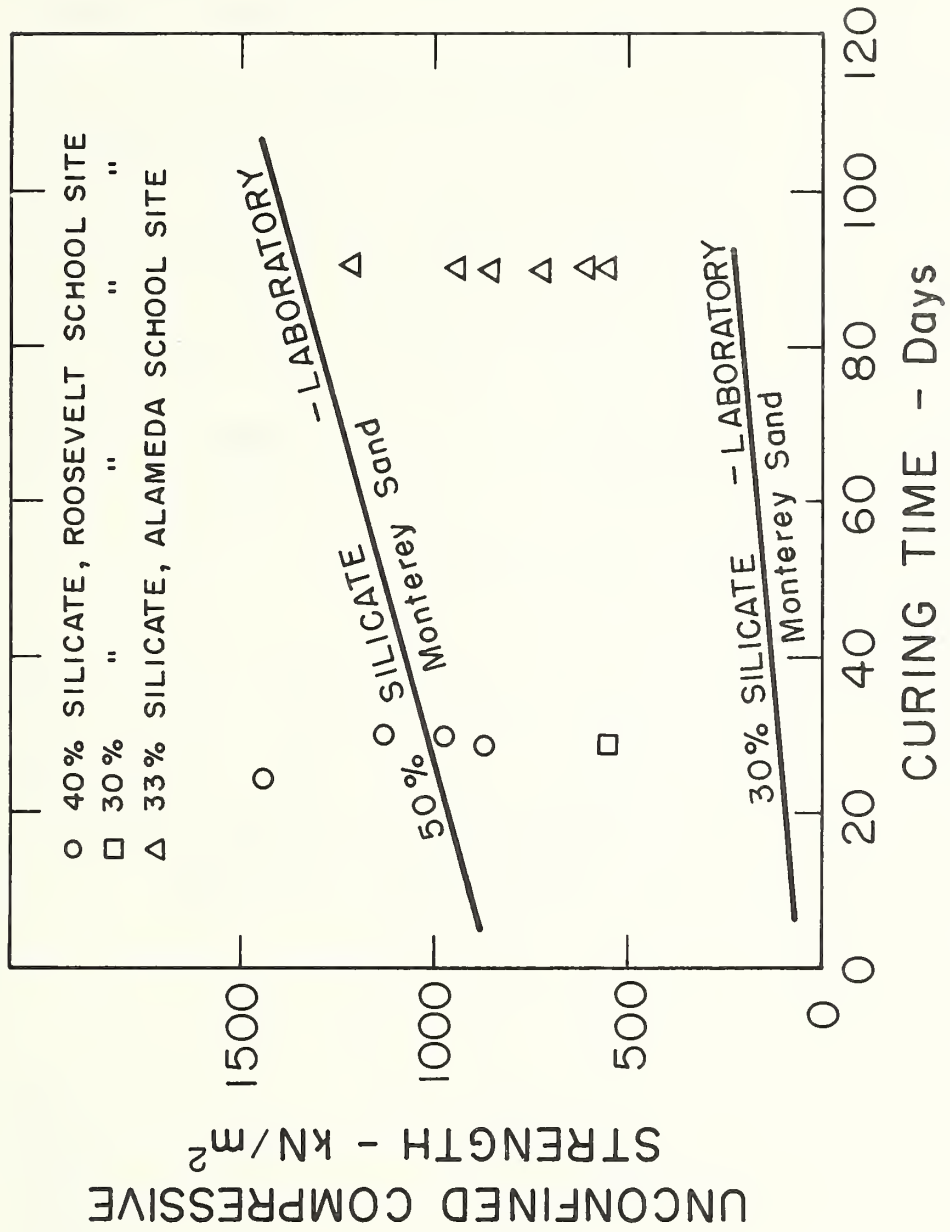


FIGURE 5.6. COMPARISON OF STRENGTHS OF FIELD SIROC SAMPLES TO LABORATORY SIROC SAMPLES WITH MONTEREY SAND

RESULTS OF WORK AT TEST SITE II - ALAMEDA ISLAND

The site of the second grouting trial was located in a hydraulic fill area on Alameda Island near the Oakland International Airport (see Fig. 5.3). This area was chosen because the soils were sandy and groutable and because the water table was within 1.7 m of the ground surface. This allowed grouting in a saturated or near saturated environment. The site is also a completely open area which allowed easy access and which will be available for later testing of grout bulbs that have been left in the ground for later sampling.

Soil Conditions

The subsoil profile at the site is depicted in Fig. 5.7; the upper five feet are uniform clean sands. At about 1.7 m a thin 7 to 10 cm layer of black, organic silt is encountered. This layer is important relative to the grouting since it cannot be penetrated by the grout. Its depth below the surface varies by several inches from point to point in the area of the grouting tests. Below the silt layer a slightly organic sand is encountered which contains considerable shell fragments. The water table generally rises to a height just above the organic silt layer.

Grain size curves for the upper and lower sands are shown in Figure 5.7. All of the curves indicate the sands to be uniform and fine grained; the sand above the water table contains no material finer than #200 sieve while that below the water table contains around 10 percent material finer than the #200 sieve.

Test Injections

A total of five locations were injected with grout as indicated in the plan view in Figure 5.8. Three of the injections used 180

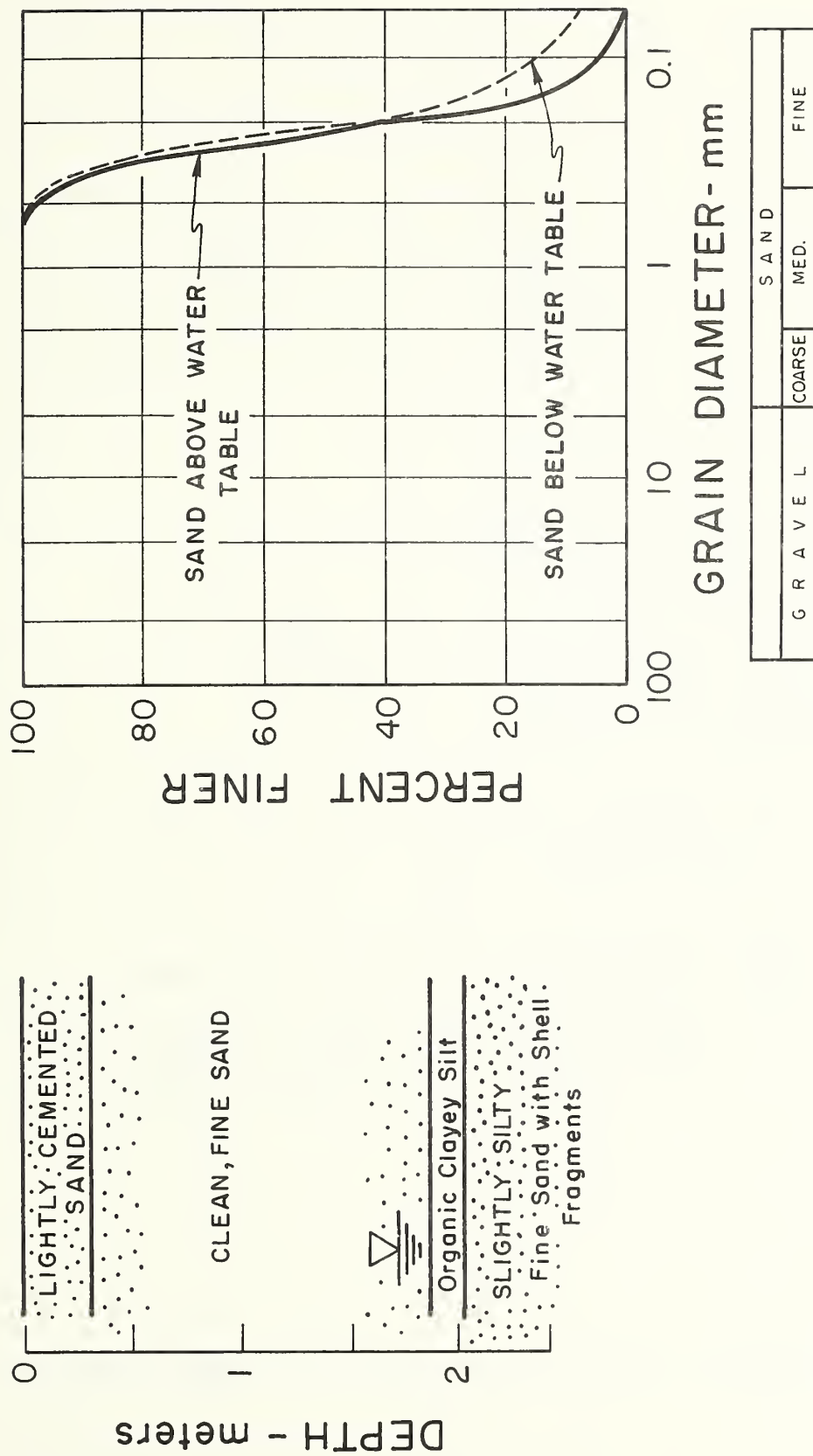
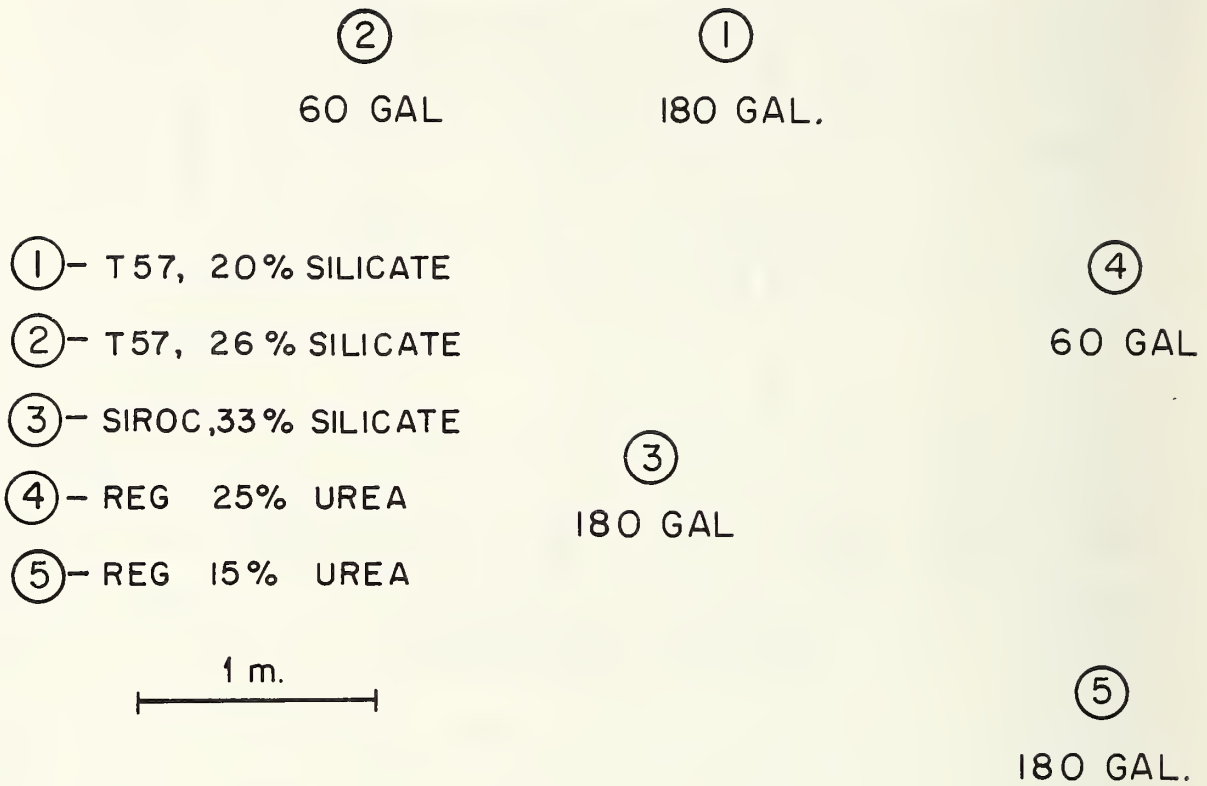


FIGURE 5.7. SOIL PROFILE AND GRAIN SIZE ANALYSES OF SOIL WHERE GROUT WAS INJECTED, ALAMEDA ISLAND SITE



Note: 60 Gal. injections are single bulbs.

180 Gal. injections are six 30 gal. multiple bulb arrays as below.



FIGURE 5.8. LAYOUT OF TEST INJECTIONS, ALAMEDA ISLAND SITE

gallons and two used 60 gallons. The 60 gallon injections were intended to create one large bulb while the 180 gallon injections were performed in a series of stages so as to create three slightly overlapping small bulbs with centers about four feet below the surface and three other overlapping bulbs with centers at about six feet below the surface. The upper three bulbs were expected to be located in the moist sand above the thin silty clay seam found in exploratory borings at about 1.7 m. The lower three bulbs were to be created in the saturated slightly organic sand layer below the silty clay seam. Details of the grouts used are given in Table 5.3.

Pictures of the two 60 gallon injections were described previously in Figure 5.1. These injections produced essentially ideal spherical bulbs. However, the three 180 gallon injections resulted in a differing product in each case. At injection point 1, the grouted soil was too weak to be sampled; this was presumably caused by the low silicate content of the grout mix. Outlining the stabilized zones by means of phenolphthalin indicator showed that the bulbs in this case were relatively spherical and in the proper position. The six individual injections at point 3 coalesced into one large, well defined mass (see the photograph in Fig. 2), instead of separate, but adjoining bulbs. This occurrence was due to the fact that the small silty clay layer thought to be at a depth of 1.6 m dipped slightly in this area to a depth of about 1.8 m, just below the lower bulb injection point. Because the grout could not penetrate this seam, it flowed upward and the upper and lower grout zones mixed instead of remaining as separate bulbs. At injection point 5, the upper bulbs formed essentially as planned. Two of the bulbs were exposed during excavation as shown in the photograph in Figure 5.2 (the third bulb was left in place for later sampling). The lower three bulbs at point 5 did not form properly;

TABLE 5.3. CHEMICAL GROUTS USED AT
TEST INJECTIONS, ALAMEDA ISLAND

INJECTION POINT	GROUT NAME	BASE	PERCENT BASE	PERCENT HARDENER	APPROX. GEL TIME MIN.	QUANTITY INJECTED GALS.
1	T57	Silicate	20	*	30	180
2	T57	Silicate	26	*	30	60
3	Siroc	Silicate	33	6	30	180
4	UREA	UREA	25	0.5-1.0	30	60
5	UREA	UREA	15	0.5-1.0	30	180

* = proprietary

grout seams were clearly present where the lower injections were made, but a uniformly stabilized sand zone was not found. Apparently, the 10 percent fines in this sand were enough to prevent penetration of the grout under the low grouting pressures used in these shallow injections.

Only four of the five injection sites could be sampled because the material at injection point 1 was too weak. Excavation and sampling of the four stabilized zones was routine. Portions of the stabilized zones at points 3 and 5 remain in the ground for later testing.

Load Test Results

Sixteen unconfined load tests have been performed on the samples obtained from Alameda Island test site. Approximately eight more samples are on hand and are being tested, but the results are not available for this interim report.

Results of the tests are summarized in Table 5.4. Comparison of these results to comparably grouted laboratory samples will be carried out as the tests are performed.

For purposes of relating the Alameda data to that of Chapter III, the strength results for the Alameda Siroc 33% silicate samples are plotted on Figure 5.6 along with that for grouted Monterey sand. As with the tests on the Roosevelt field samples, the data for the Alameda sands are scattered more than was found for laboratory prepared samples of Monterey sand. The results for the Alameda Siroc samples are however bracketed by those performed on Monterey sand using Siroc 30 and 50% silicate grout mixes, and thus show generally the same strength trends.

TABLE 5.4 RESULTS OF LOAD TESTS AT FIELD SITE II--ALAMEDA ISLAND

TEST NO	TYPE OF GROUT	PERCENTAGE OF CONSTITUENTS	(DAY) CURING TIME	CONFINING PRESSURE (PSI)	STRAIN RATE IN./MIN.	PEAK STRESS (PSI)	STRAIN AT PEAK STRESS %	GEL TIME MIN.
1	T57	30% Silicate	29	0	.011	5.1	0.23	30
2	T57	30% Silicate	29	0	.011	21.0	0.39	30
3	UREA	15%	29	0	.011	31.7	1.22	30
4	UREA	15%	29	0	.011	20.1	1.04	30
5	UREA	15%	29	0	.011	18.7	0.79	30
6	UREA	15%	29	0	.011	59.3	0.66	30
7	T57	30% Silicate	24	0	.011	3.9	0.67	30
8	T57	30% Silicate	24	0	.011	4.62	0.91	30
9	UREA	25%	24	0	.011	42.6	0.75	30
10	SIROC	33% Silicate	88	0	.011	124.9	1.36	30
11	SIROC	33% Silicate	91	0	.011	104.1	1.87	30
12	SIROC	33% Silicate	92	0	.011	124.8	1.29	30
13	SIROC	33% Silicate	92	0	.011	81.2	1.38	30
14	SIROC	33% Silicate	92	0	.011	178.0	1.44	30
15	SIROC	33% Silicate	92	0	.011	87.4	1.48	30
16	SIROC	33% Silicate	92	0	.011	139.4	2.16	30

SUMMARY

The field grouting trials provide an opportunity to observe the chemical stabilization process first hand as well as a means of comparing the performance of field and laboratory grouted samples. Two of these trials have been carried out; bulbs of grouted soils have been excavated from each site and tests are underway on the field samples.

Results of the tests on the field samples thus far show that scatter in the strength data is larger than in that obtained from samples prepared under ideal laboratory conditions. Future tests will allow direct comparison of strengths of lab samples to field samples. Preliminary work suggests that while differences exist between the results of laboratory prepared and field samples, the differences are not substantial, providing that in the field the grout properly penetrates the soil.

Excavation of the grouted soil masses in the field tests revealed that in areas where soil conditions were well suited to grouting, the grout, in fact, did uniformly penetrate the soil. A small impervious layer within the soil to be grouted at Site II resulted in some migration of the grout to areas not anticipated. This result suggests that secondary grouting after initial grout set is a desirable procedure in practice so that previous grout take can be tested.

CHAPTER VI
DOCUMENTATION OF TUNNEL GROUTING
CASE HISTORIES

The use of chemical stabilization to minimize settlements above tunneling works in the United States is a relatively new idea. Because of this, few case histories are available. However, the documentation of field performance is an important aspect in the development of our understanding of the behavior of grouted tunnels. During the course of both the first and second year of this investigation, efforts have been and are being made to obtain field performance data. Described herein are the data developed thus far, and, for one of the case histories, a detailed finite element study is provided.

Three projects from the Washington Metro have been located for which documentation is reasonably complete. These are described in Table 6.1 along with the type of information available. In order to shorten references to the projects, the reference number given in Table 6.1 will be used for identification hereafter in this report. Performance data for Projects II and III consist only of surface settlements while that for Project I is much more extensive. Finite element studies have been and are being performed for Project I. Of the three projects, only III is complete as of the data of this writing (November 1976).

SOIL AND TUNNELING CONDITIONS AT PROJECT SITES

Longitudinal profiles and cross-sections of the subsurface soils at the three projects are given in Fig. 6.1, 6.2 and 6.3. Soil conditions at all the sites are similar in that each has a layered subsoil profile consisting of sands and clays. The tunnel excavation in all cases passes

TABLE 6.1 WMATA CASE HISTORIES

PROJECT	REFERENCE NO.	AVAILABLE DATA	STATUS
Addison Route Crossing Under Penn Central and Baltimore and Ohio Railroad Tracks *	I	Extensive information being obtained - inclinometer movements, subsurface and surface settlement data for grouted and ungrouted sections.	Still under construction
Pentagon and Branch Route Crossings Under Seventh Street Bridge *	II	Surface settlement data at Seventh Street Bridge location	Still under construction
Name cannot be released at this time because of outstanding legal actions.	III	Surface settlement data at several locations along tunnel route.	Complete

*Data provided courtesy of Hayward-Baker Grouting Company

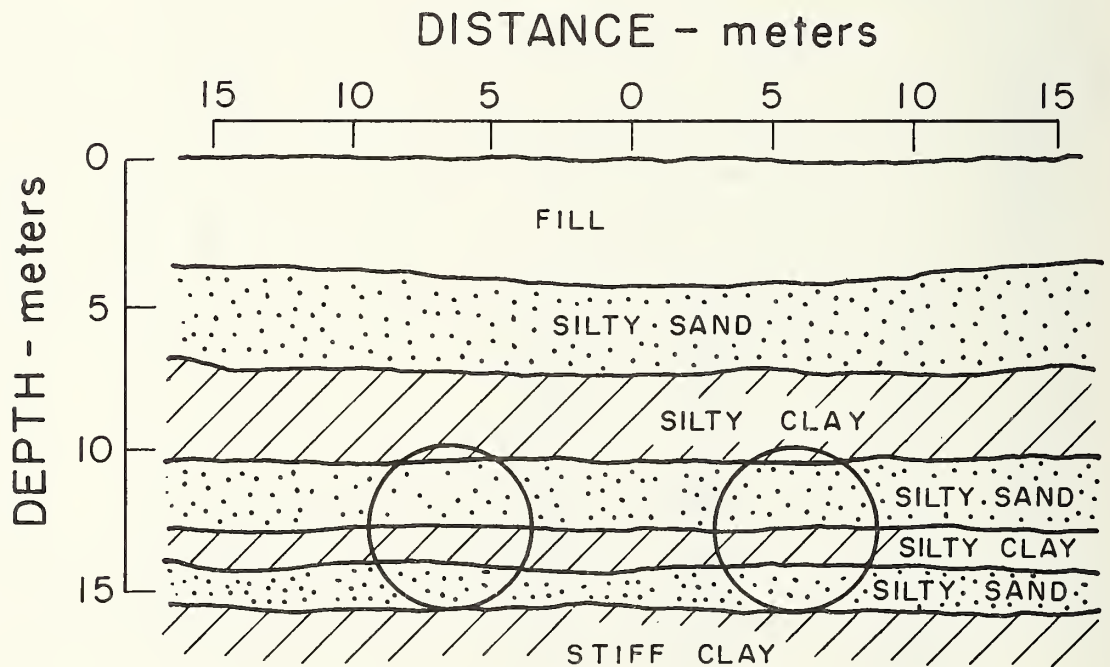
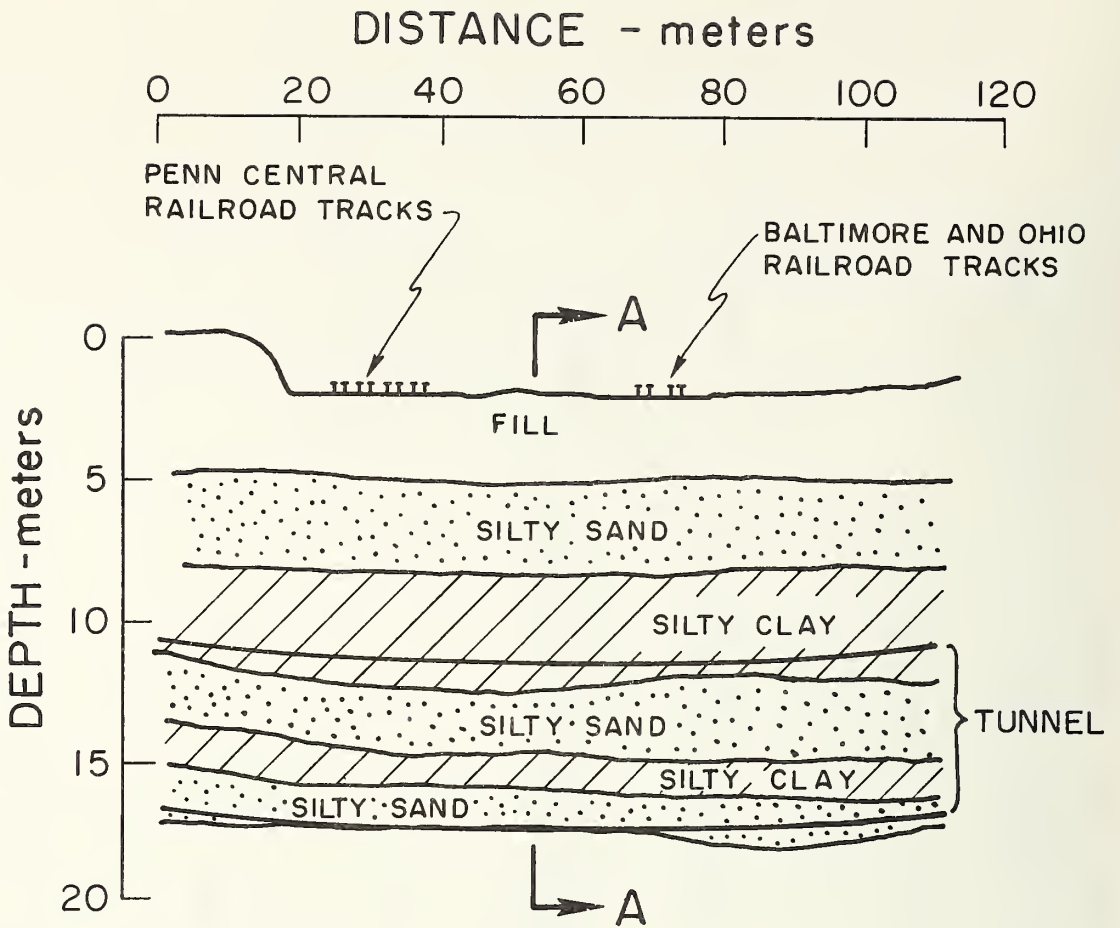
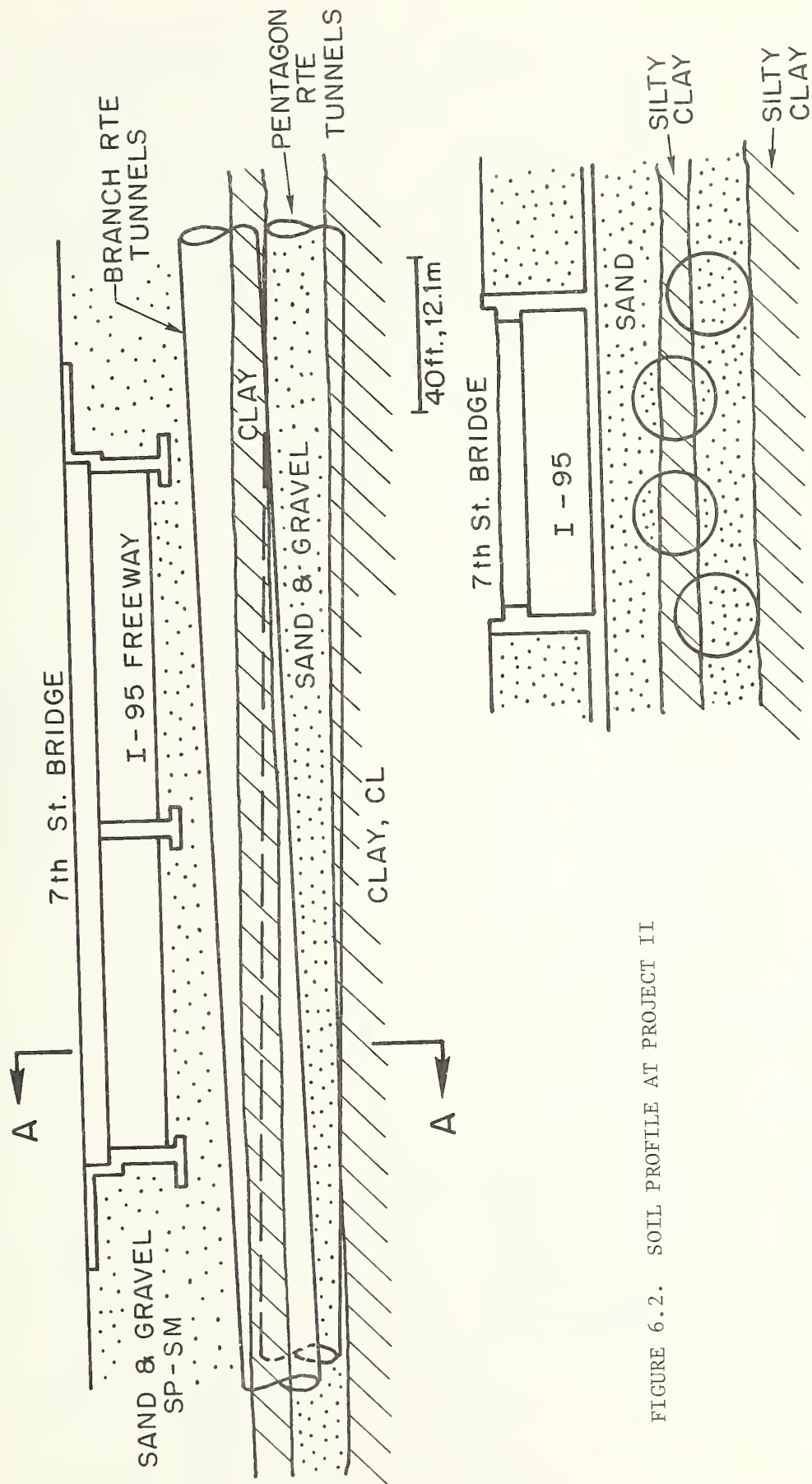


FIGURE 6.1. SOIL PROFILE AT PROJECT I



SECTION A-A

FIGURE 6.2. SOIL PROFILE AT PROJECT II

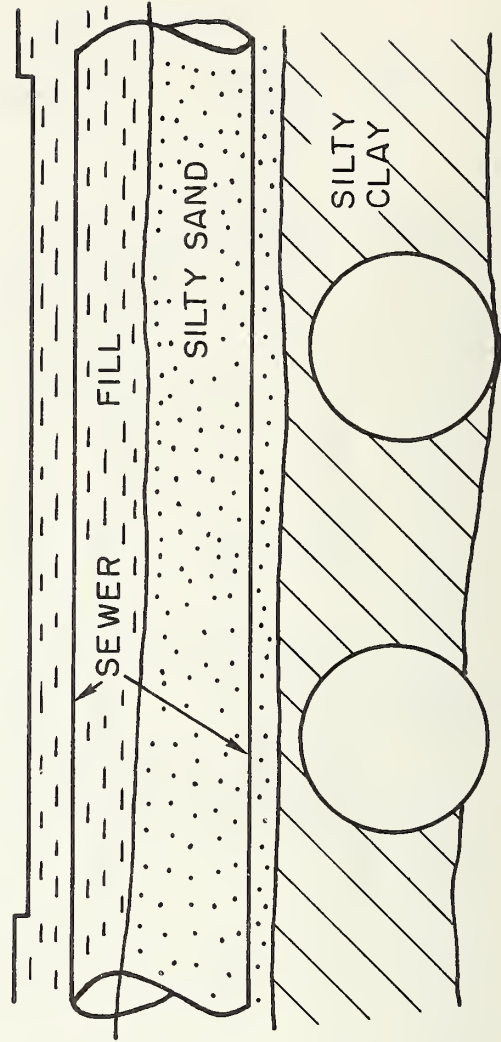
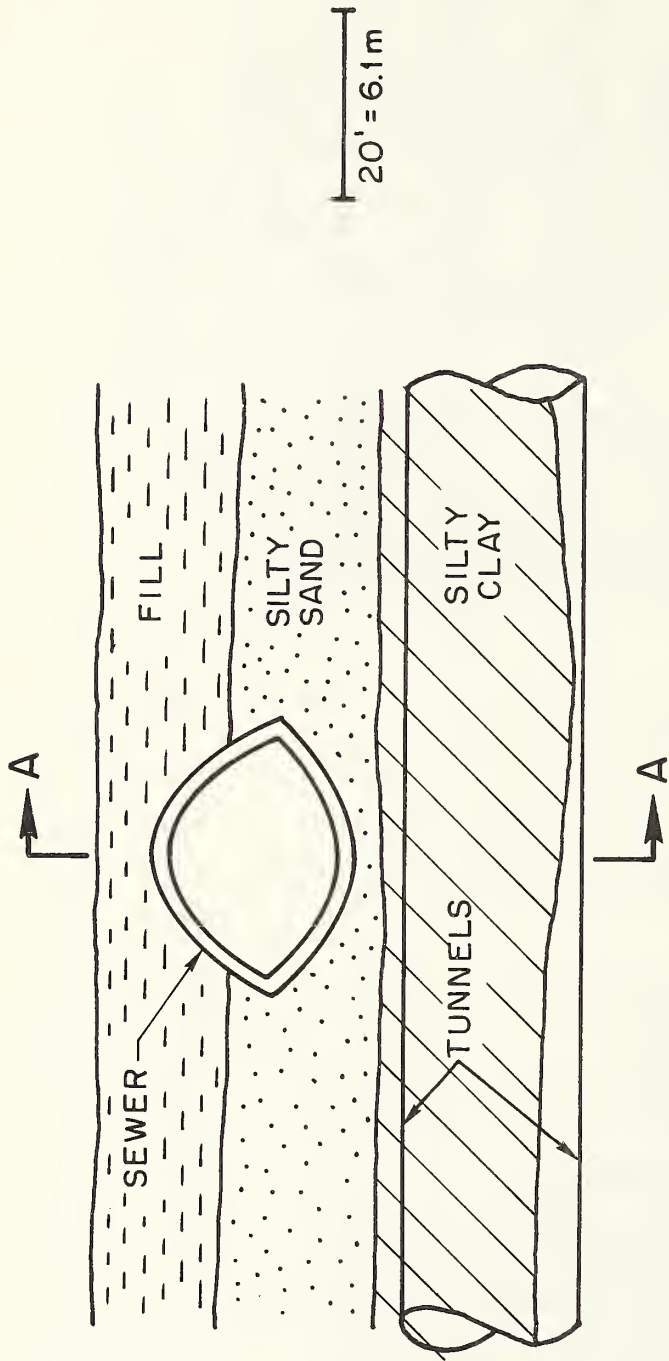


FIGURE 6.3. SOIL PROFILE AT PROJECT III

through both clay and sand layers and is beneath the water table.

The sands at all sites are dense to very dense while the clays vary in stiffness with depth. The upper clay layers are typically medium to stiff while the lower clay layers are very stiff.

Tunnel diameters in all projects are 6.4 m. Projects I and III involve two tunnels while Project III has four tunnels. In all cases the tunnels pass through sands at the tunnel invert with clays in the upper half to the crown of the tunnel. Two of the tunnels at Project II have their crowns cut into an overlying sand layer.

GROUTING SCHEMES

Theoretical grouting zones for each project in longitudinal profile and in cross-section are depicted in Figs. 6.4, 6.5 and 6.6. In the case of Projects II and III, a stabilized zone of approximately 10 foot thickness was developed only in the sand layer above the tunnel crown. Of the four tunnels excavated in Project II, two have their crown in the grouted zone. Neither of the two tunnels in Project III intersect the grouted zone.

The stabilized zone in Project I varied in size (see Fig. 6.4); prior to, between and just after the rail tracks which are being supported by the grouting, a smaller zone, called the moderately grouted section, was used. Only two of the sand layers in this area were stabilized. The heavily grouted section was confined to directly under the railroad tracks; at this location all three sand layers in the soil profile were grouted. The two tunnels at this site pass through the two lower grouted sand layers, but are separated from the upper grouted zone by a 10 foot

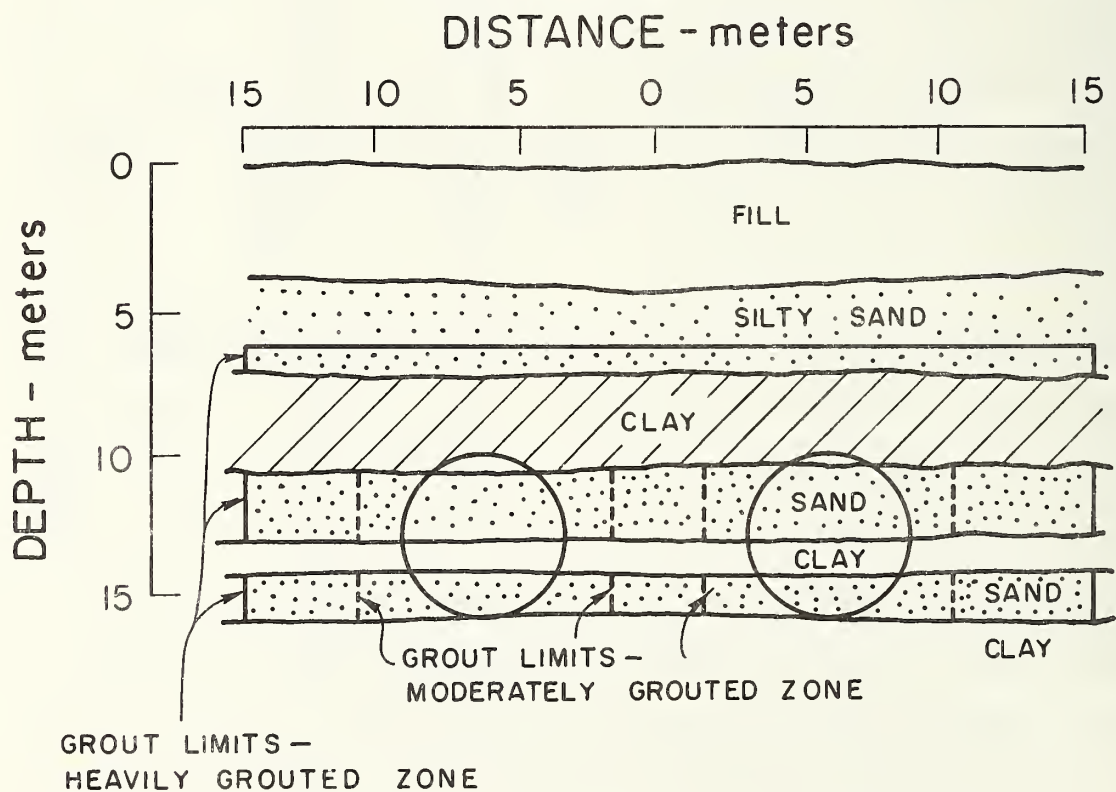
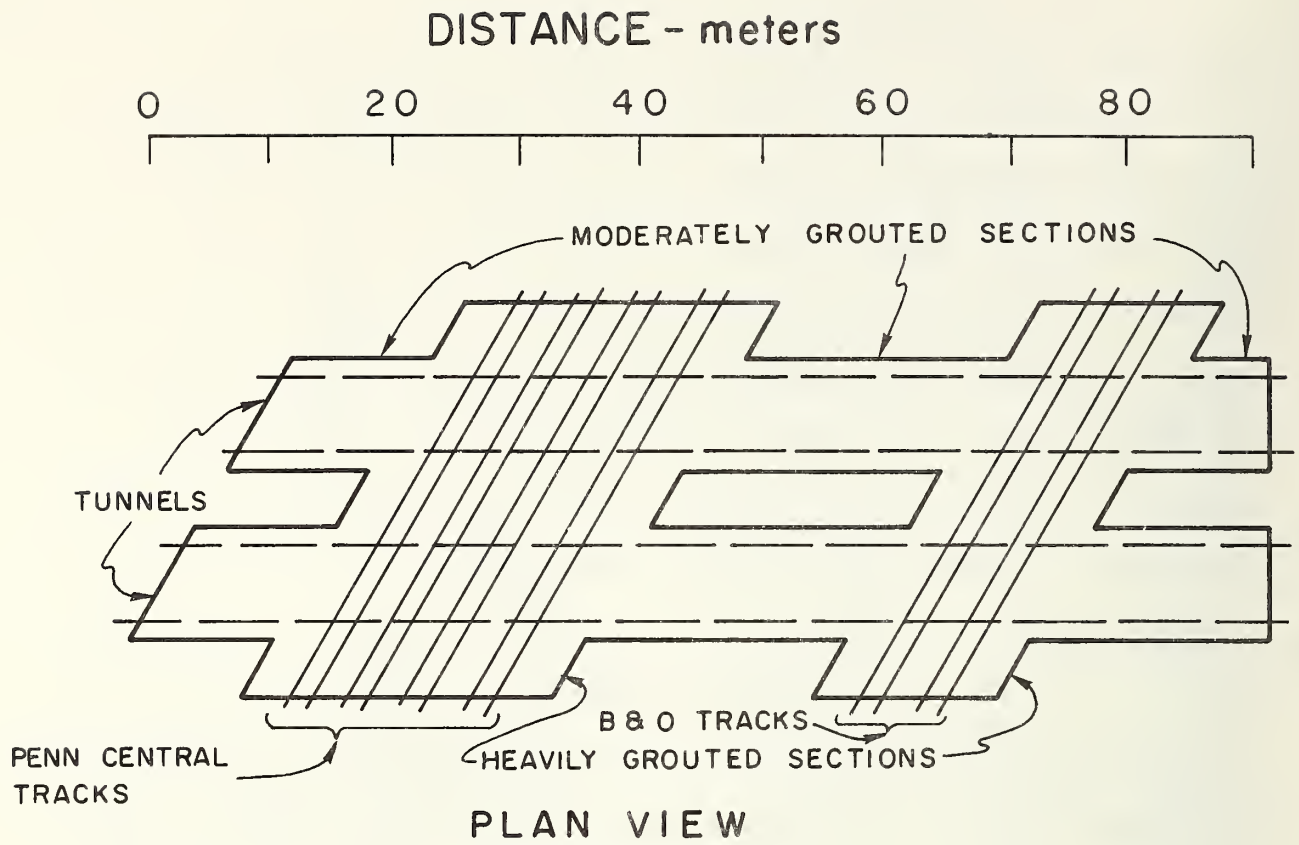


FIGURE 6.4. STABILIZED ZONES FOR PROJECT I

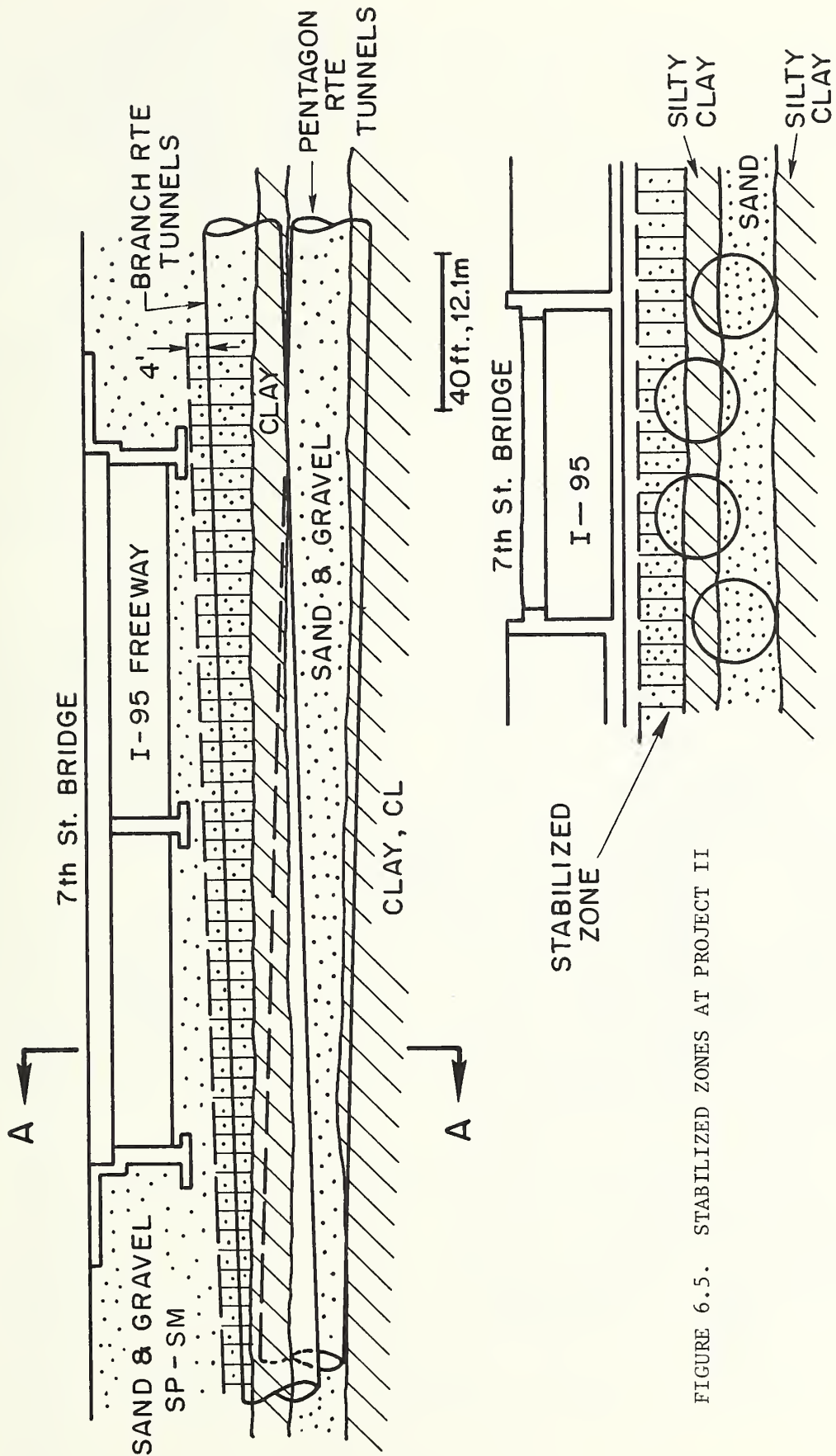
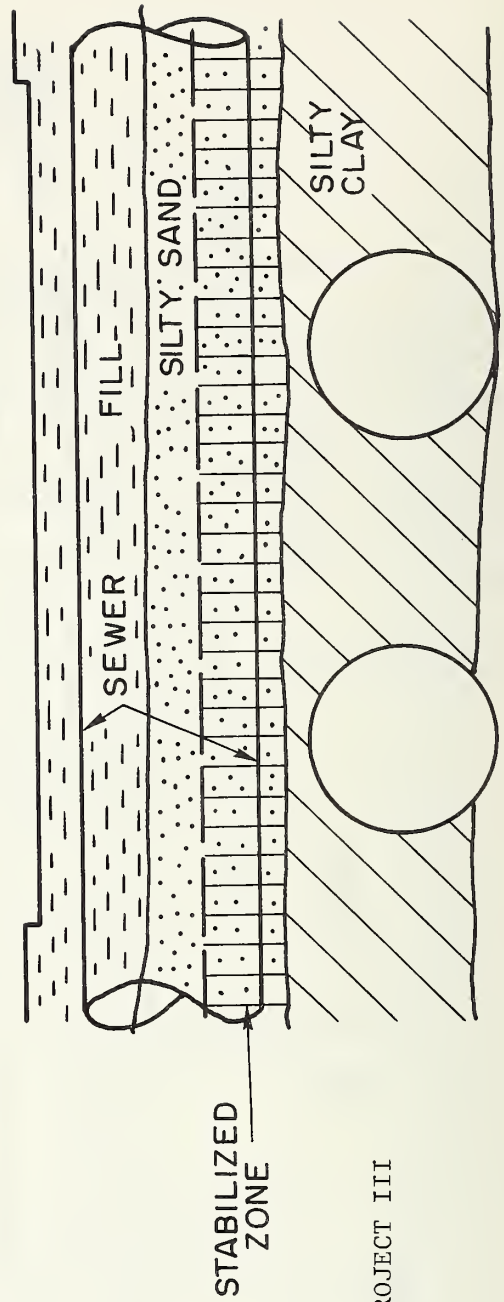
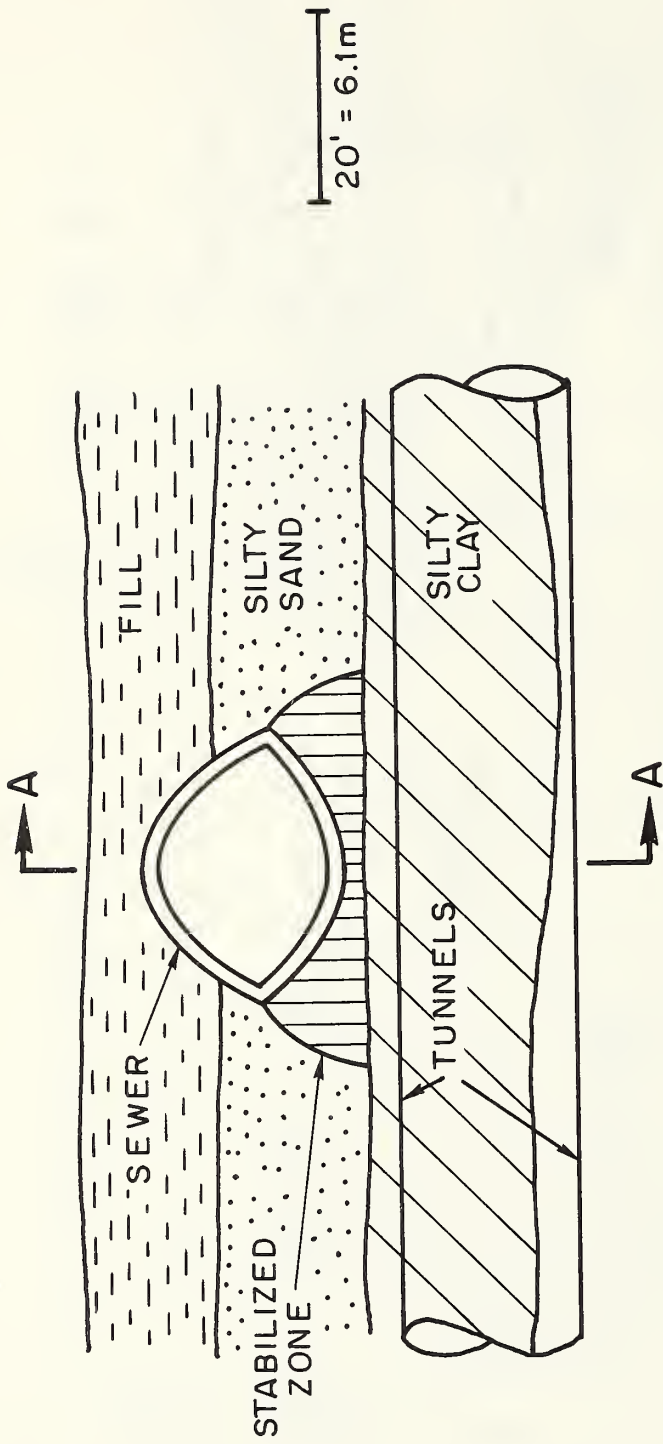


FIGURE 6.5. STABILIZED ZONES AT PROJECT II

SECTION A-A



SECTION A-A

FIGURE 6.6. STABILIZED ZONES AT PROJECT III

thick clay layer, which intersects the crown of the tunnel.

All three of the Projects were grouted from the surface using a scheme of vertical and inclined grout holes. Tube á manchette grouting techniques were employed at Project III while at I and II the grout was injected through slotted plastic pipes.

At all of the subject projects, the grout injected was primarily of a sodium silicate base type. Some pre-injection work was carried out at Project III using bentonite cement. In all cases the chemical grouts used a 50 percent sodium silicate mix. The hardener in the grouts were the same at Projects I and II, but differed at Project III. The type of hardeners are considered proprietary information and cannot be identified at this time.

At all of the sites some difficulties were experienced in grouting the sand layers because of silt seams. This was particularly true at the site of Project I. Some post grouting drilling was carried out at Projects I and II. Sandy layers were found to be stabilized essentially as specified. At Project I the upper, stabilized sand layer was found to "wander" slightly, in that its depth below the surface fluctuated. Also the thickness of the clay layers in the tunnel area varied somewhat, resulting in less stabilized sand in some areas than others.

PERFORMANCE DATA AND INSTRUMENTATION FOR PROJECT I

Monitoring of performance data is complete only at Project III since some tunneling still has to be carried out at Projects I and II. Because of the fact that the data at I and II are incomplete and still being reduced at this time and legal actions pend on Project III, details of

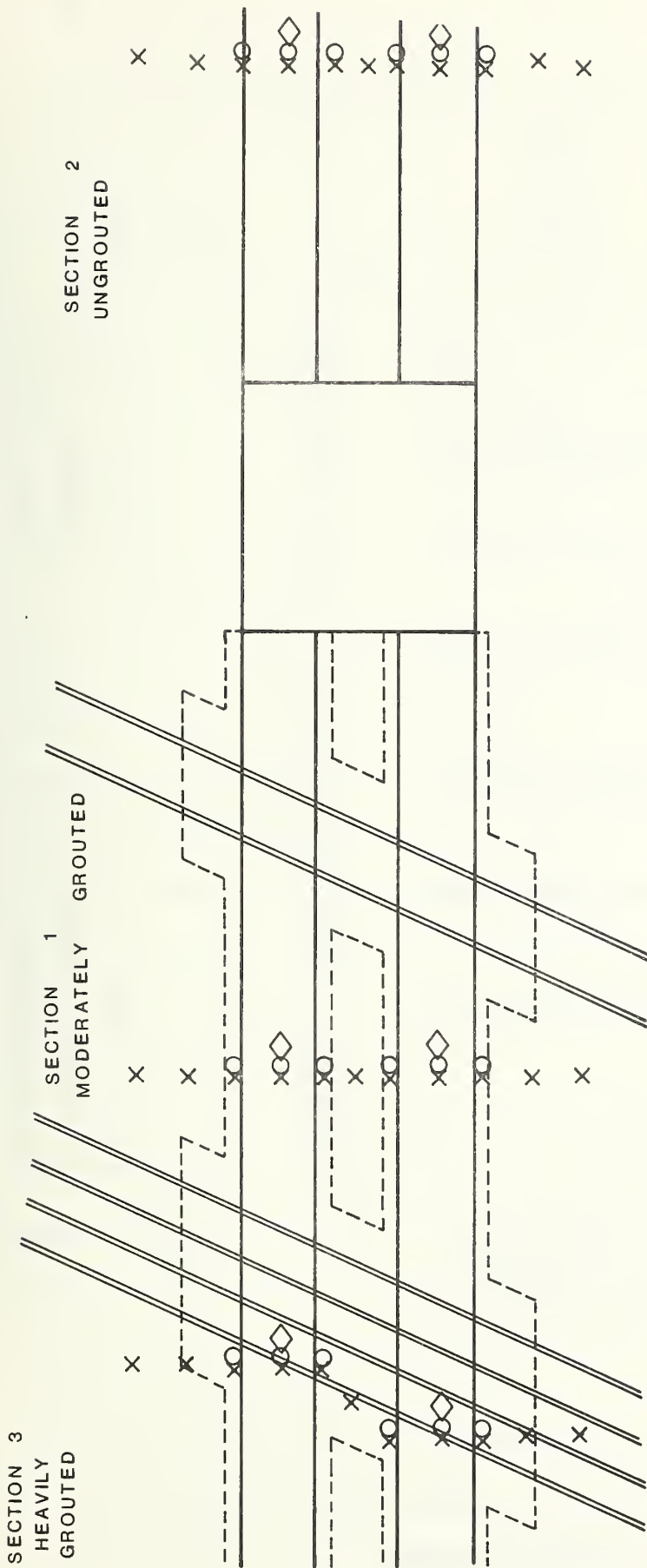
the performance will not be presented herein. By the completion of the second year of this project, it appears likely that all data will be available for publication.

Performance data at Projects II and III consist only of surface settlement measurements as monitored by survey control. However, the instrumentation network at Project I is by far the most complete that has been used to monitor the performance of a grouted tunnel project. Data for Project I are being obtained by the Hayward-Baker Company under an UMTA sponsored contract. Figs. 6.7 and 6.8 depict the layout in plan and section respectively. Three lines of instrumentation are in place, one in the heavily grouted zone, one in the moderately grouted zone and one in an area not grouted. The instruments consist of surface settlement monuments, subsurface settlement monuments, inclinometers, and piezometers. In addition, data are being kept on the behavior of the shield as to pitch or yaw.

Based on preliminary evaluations of the data from Projects I, II and III, it can be said that thus far, settlements above the tunnels have been generally limited to two inches or less. This type of performance is better than that usually observed in ungrouted soft ground tunneling sections in Washington, D.C.

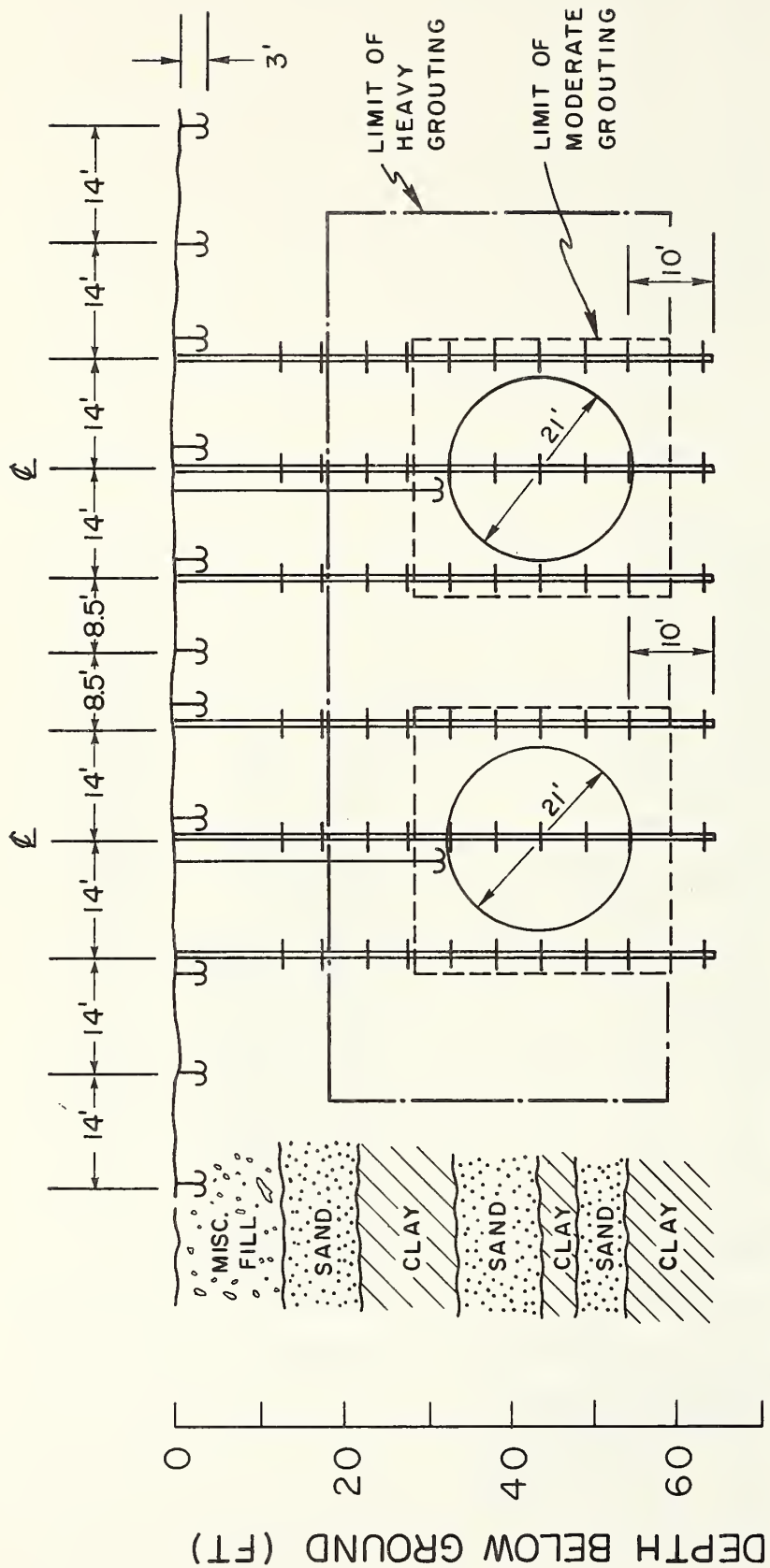
FINITE ELEMENT STUDIES OF PROJECT I

One of the purposes of documenting field performance in this investigation is to help evaluate the degree to which the finite element codes developed for analysis of grouted tunnels can model actual behavior. Because of the unusual documentation being developed for Project I, it was chosen for the first detailed finite element study. The analyses of this site were undertaken prior to any tunneling and have continued and been



- X SURFACE SETTLEMENT BORROS ANCHOR
- ◇ DEEP SETTLEMENT BORROS ANCHOR
- DEEP SETTLEMENT AND HORIZONTAL
MOVEMENT INDUCTANCE PROBE AND
INCLINOMETER CASING

FIGURE 6.7 INSTRUMENTATION LAYOUT



TYPICAL INSTRUMENTED CROSS SECTION

(SCALE: 1" = 20')

LEGEND

- ⌋ Borros Anchor
- || Incliner Casing
- ⊕ Inductance Ring

NOTE

Illustrated Borros Anchor positions are offset from true positions

FIGURE 6.8 TYPICAL INSTRUMENT DISTRIBUTION IN A SECTION

updated as more information becomes available. Further studies are anticipated.

Soil Conditions

The idealized soil profile for the site is shown in Fig. 6.1 and was described earlier in this chapter. This profile was derived from five borings in the vicinity of the grouting work which are documented in two reports by the firm Mueser, Rutledge, Wentworth and Johnston, and submitted to the Washington Metropolitan Area Transit Authority in June, 1974 and January, 1975. Locations of the borings are shown on the plan view of the site in Fig. 6.9. Logs of the borings are given in Fig. 6.10; it is important to note the fluctuations in layer sizes in the logs in order to realize that the idealized soil profile is an average condition which does not necessarily represent the actual conditions at various locations across the site.

Soil properties at the site are only available from the work reported by Mueser, Rutledge, Wentworth, and Johnston. Table 6.2 presents pertinent engineering properties of the soils as obtained from the M-R-W-J reports.

Grout Zone Locations and Properties

The theoretical boundaries of the stabilized zones at the site are shown in Fig. 6.4. However, the fluctuations in actual depths and thicknesses of groutable soils as shown on the boring logs in Fig. 6.10, indicate that the theoretical boundaries of the grout zones probably do not represent the actual boundaries, except as an average condition. Two recent post grouting borings substantiate this hypothesis; locations of the borings are given in Fig. 6.9. Logs of these borings are depicted in Fig. 6.10, and it can be seen by superposition of the theoretical

TABLE 6.2. AVERAGE PHYSICAL PROPERTIES
OF SUBSURFACE SOILS AT SITE OF PROJECT I

Soil Layer	Approx. Depth to Top Layer Ft.	Soil Classification	Blow Count Bls/Ft.	Undrained Shear Strength kN/m ²	W.C. %
Misc. Fill	0	SM-CL	6	NA*	NA
Dense Sand	12	SP-SM	28	NA	NA
Medium Clay	23	CL	NA	0.3- 1.00	17
Dense Sand	34	SM	22	NA	NA
Medium Clay	44	CL	NA	0.3- 1.00	24
Dense Sand	48	SP-SM	40	NA	NA
Stiff Clay	54	CH	NA	1.4- 2.2	25

* = not applicable

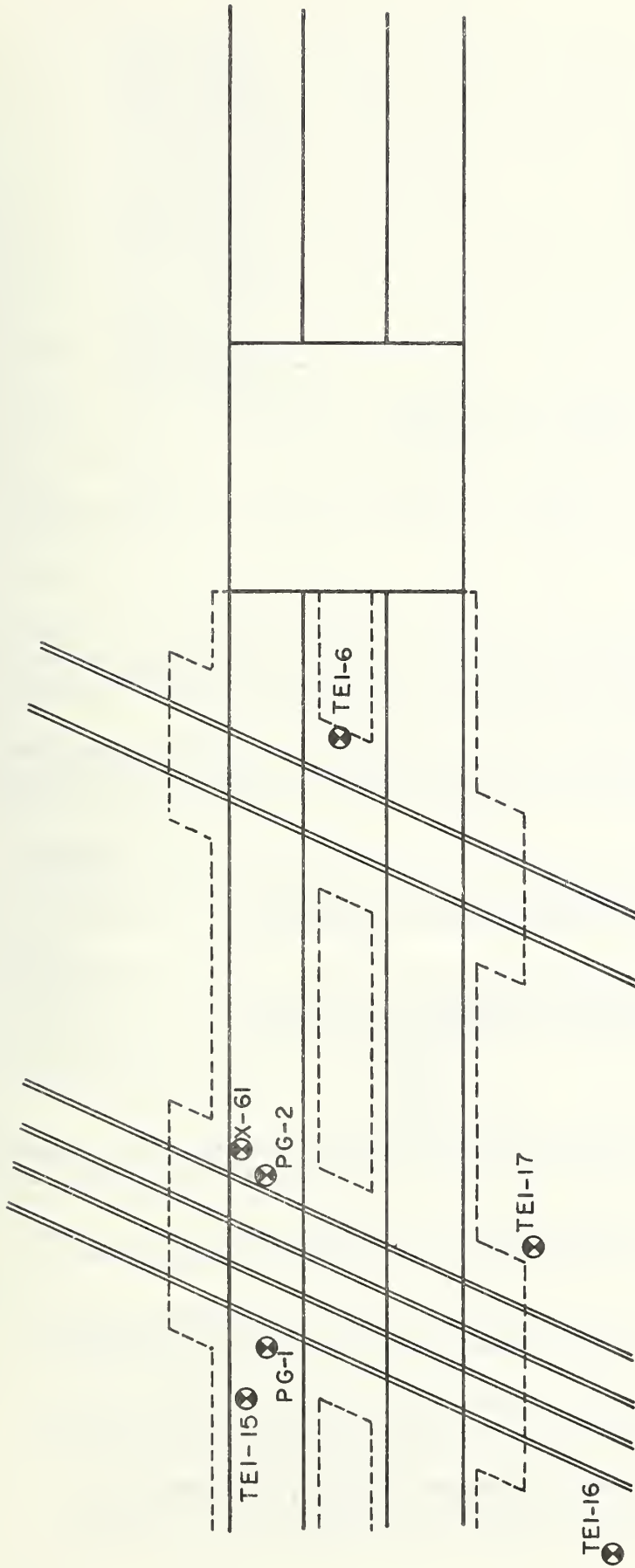
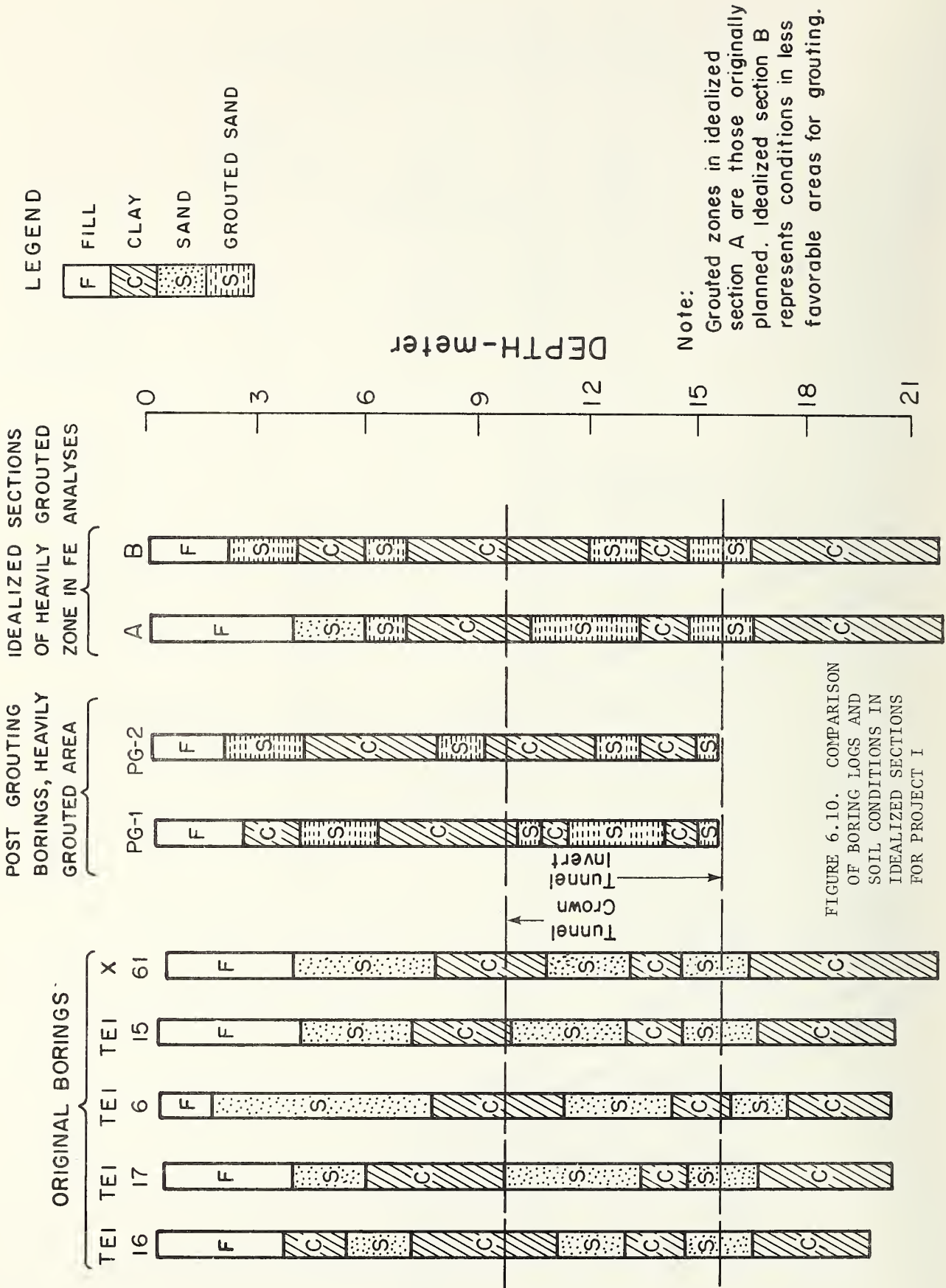


FIGURE 6.9. BORINGS AT PROJECT I



grouting boundaries onto those of the actual grouted soils, that the zones are not the same. The most important deviation occurs in Boring PG2 where the combined thicknesses of the clay layers in the vicinity of the tunnel is 2m thicker than indicated in the idealized section. Clearly, this condition will lead to more movement than for the idealized section. Thus, in analyses of the project, variations in the grouting zone boundaries need to be considered to determine the degree of their effect on performance.

As of this date, no tests have been performed on stabilized soil samples from this site. At this time, the only indication as to what parameters should be used to represent the stabilized soils comes from: (1) The fact that the unconfined compressive strength is required in the job specification to be at least 520 kN/m^2 (75 psi); and, (2) the grout being used at the site is a 50 percent sodium silicate solution, similar to those used in the test program described in Chapter III, for which data are available.

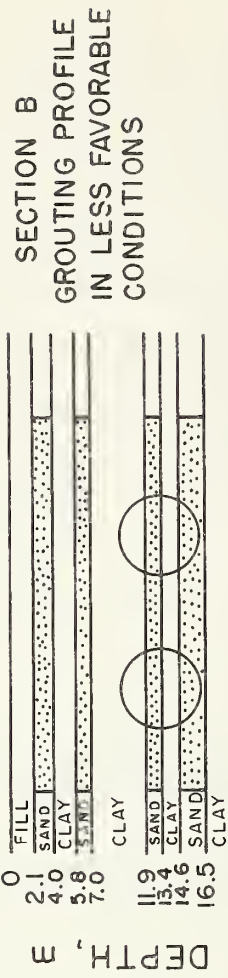
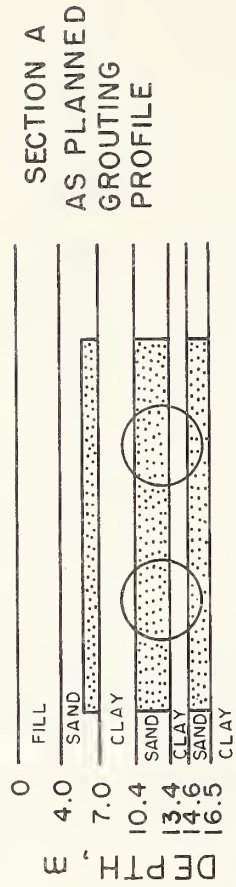
Parameters and Subsurface Profiles Used in Analyses

Because of the indicated variations in subsurface and grouting conditions due to natural and designed causes, and, because of the uncertainty concerning grouted soil properties, a series of finite element studies were performed varying the important parameters within reasonable ranges. This approach allows an assessment of the importance of fluctuations in key variables.

Four different subsurface profiles were represented as shown in Fig. 6.11 and described as follows:

1. Heavily grouted zone under railroad tracks, using idealized soil and grout locations.
2. Moderately grouted zone between the railroad tracks, using idealized soil and grout locations.

HEAVILY GROUTED



MODERATELY GROUTED

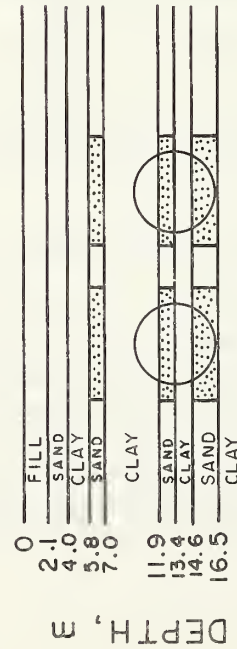
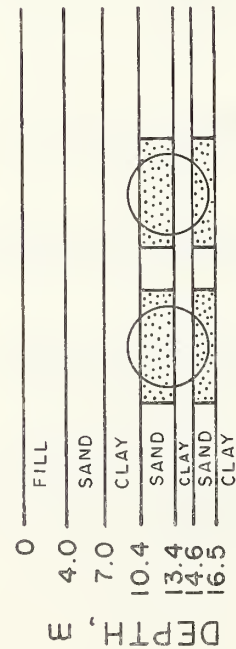


FIGURE 6.11. GROUTING PROFILES USED IN FINITE ELEMENT ANALYSES OF PROJECT I.

3. Heavily grouted zone under railroad tracks, using soil and grout locations representative of areas with large clay areas (see Fig. 6.10)
4. Moderately grouted zone between the railroad tracks, using soil and grout locations representative of areas with large clay areas (see Fig. 6.10).

In addition to the different subsurface profiles, the grouted soil was represented as either "strong" or "weak." Mohr-Coulomb parameters used to define the strength for the "strong" and "weak" cases were $\phi = 30^\circ$, $c = 115 \text{ kN/m}^2$ and $\phi = 30^\circ$, $c = 80 \text{ kN/m}^2$ respectively. The parameters employed for the "strong" case were chosen to be consistent with the known behavior of grouted soils from Chapter III and the fact that the contract specified unconfined compressive strength for the stabilized soils was 520 kN/m^2 (75 psi). The "weak" case uses a cohesion 30% less than that of the "strong" case to reflect a possible loss of strength under the loading conditions which actually occur in the field during tunneling.

The deformation model employed for both the grouted and ungrouted soil in the analyses is the nonlinear elastic approach described earlier in Chapter 4. This model utilizes modulus values consistent with the stress level and the prescribed, empirically fitted stress-strain curves. Only the strength parameters and the initial tangent modulus values are needed to define the model response. Initial tangent modulus values are assumed to vary with confining pressure as:

$$E_i = K p_a \left(\frac{\sigma_3}{p_a} \right)^n$$

This type of response was shown in Chapter 3 to reasonably fit the behavior of grouted soil and is well established for ungrouted soil. The grouted soil parameters, "K" and "n" for the present analyses were selected from

those determined in the laboratory studies on samples injected with a 50 percent silicate grout mix similar to that used at the site. These values are representative of those for relatively short-term loading and were employed for the "strong" grouted soil cases. Aging was not a major factor in these considerations since the grout was injected into the ground at the site only 30 to 60 days prior to the tunneling. For the "weak" grouted soil, the "K" value was reduced by 30 percent as was the cohesion. The "n" value was not changed since this parameter seems to be unaffected by rate of loading.

Other parameters used for the grouted soils along with those selected for the ungrouted soils are given in Table 6.3. The parameters for the ungrouted soils were selected from three test results presented by Mueser, Rutledge, Wentworth and Johnston and from other data available in the literature.

Finite Element Mesh and Boundary Conditions

The finite element mesh used in the analyses is shown in Fig. 6.12. Stabilized soil zones are indicated on the mesh for the case of the idealized soil profile and the moderately grouted zone. These locations were modified accordingly for the alternative subsurface conditions of the other analyses. The mesh is designed at present for the analysis of the effect of excavating one tunnel only since this is representative of the first step of the actual construction sequence. The second tunnel is to be opened within about six months of this date (November, 1976). The grout zones for the second tunnel are modeled in the mesh since these were in place during the excavation of the first tunnel. Left and right boundaries of the mesh were selected by trial so as to be far away enough

TABLE 6.3 SOIL PARAMETERS USED IN
FINITE ELEMENT STUDIES

Soil Layer	Depth of Top Layer Ft.	Unit Weight PCF	ν_i	ν_f	k_o	ϕ	C kN/m ²	n	K	R _f	Drained or Undrained
Fill	0	110	0.2	0.49	0.5	30	0.05	0.5	200	0.9	Drained
Dense Sand	12	130	0.3	0.49	0.4	38	0.05	0.5	1000	0.9	Drained
Medium Clay	23	110	0.48	0.49	0.8	0	0.5	0	475	0.8	Undrained
Dense Sand	34	120	0.3	0.49	0.5	35	0.05	0.5	600	0.9	Drained
Medium Clay	44	110	0.48	0.49	0.8	0	0.5	0	475	0.8	Undrained
Dense Sand	48	125	0.3	0.49	0.4	38	0.05	0.5	1000	0.9	Drained
Stiff Clay	54	125	0.48	0.49	1.0	0	1.34	0	800	0.6	Undrained
Grouted Sand 1*	Varies	135	0.48	0.49	0.5	30	2.60	0.2	2400	0.6	Undrained
Grouted Sand 2*	Varies	135	0.48	0.49	0.5	30	1.34	0.2	1700	0.6	Undrained

* Grouted Sand 1 assumes minimum specified strength obtained

Grouted Sand 2 assumes reduced cohesion and stiffness to
account for rate of loading effects.

Notes: ν = Poisson's ratio

c = cohesion

R_f = curve fitting parameter

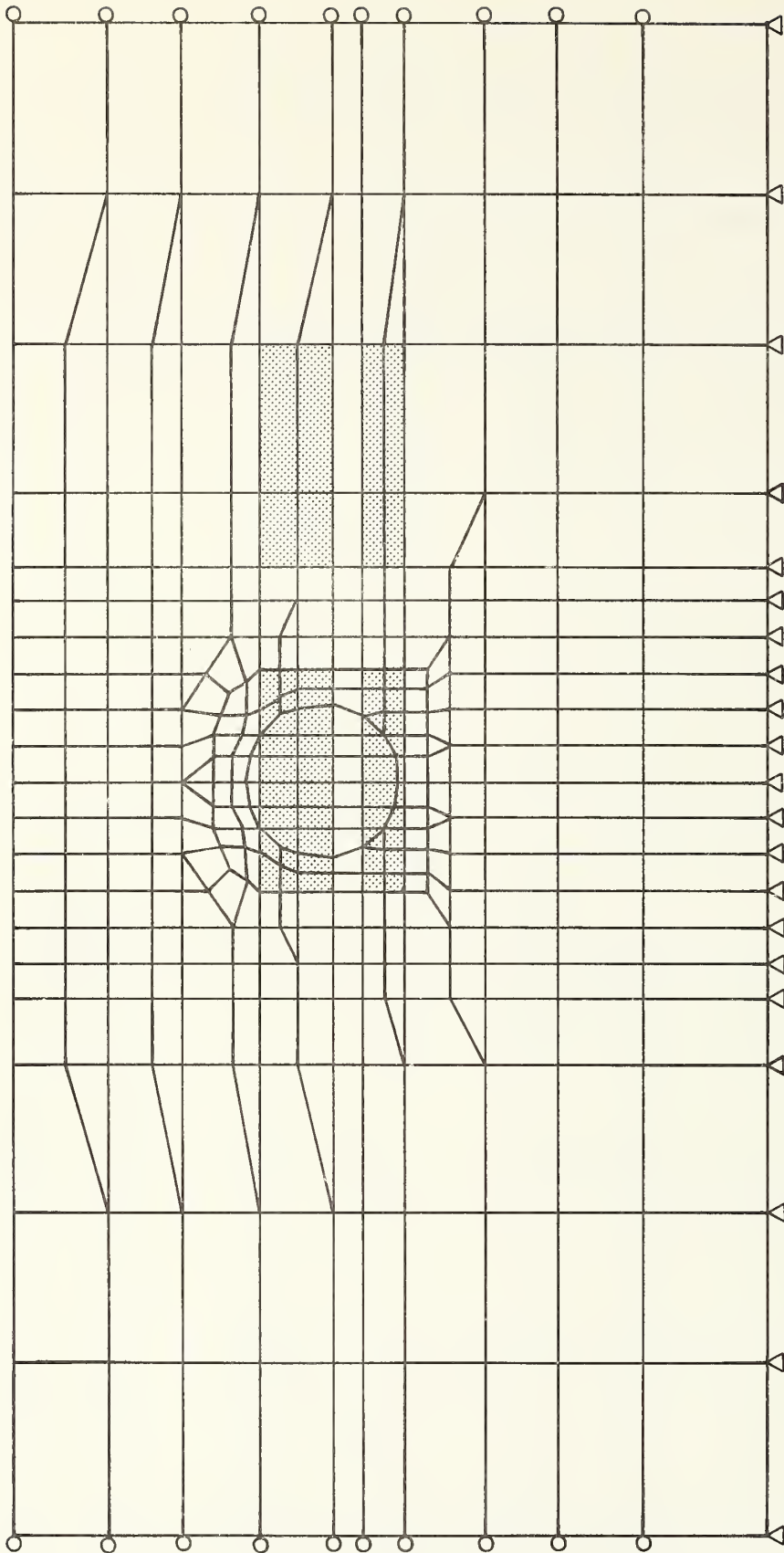


FIGURE 6.12. FINITE ELEMENT MESH USED IN ANALYSES OF PROJECT I

to exert no influence on the tunnel. The base of the mesh was at the bottom of the stiff clay layer under the tunnel. A total of 361 elements and 382 nodes were included in the mesh.

No liner spring elements were included to restrain movement around the periphery of the tunnel. In most cases, the predicted peripheral movements were not large enough to warrant concern over liner effects. However, further consideration will be given to the influence of gap closing and liner restraint as more documentation is obtained on shield orientation. These data are now on hand and are being reduced.

Initial stresses in the analyses were taken as increasing linearly with depth to be consistent with a gravity stress distribution. Horizontal stresses were assumed to follow the relationship $\sigma'_x = k_o \sigma'_z$, where σ'_x is the horizontal effective stress and σ'_z is the vertical effective stress and k_o is the coefficient of lateral earth pressure (values are given in Table 6.3).

The groundwater table was assumed to be at a depth of 4m as was measured in the field. This depth affects the stiffness of the subsurface soils since below the groundwater the soils are in a buoyant condition and the effective stresses are reduced.

Results of Finite Element Analyses

Predicted surface settlements and lateral movements along a vertical line adjacent to the tunnel are shown in Figs. 6.13 and 6.14 respectively.

The following observations may be made concerning the settlement data:

- 1. The settlements are largest for the smaller and weaker grout zones, other conditions being equal.

- I - Heavily Grouted, Idealized Section A, "Strong" Grout
- II - Moderately Grouted, Idealized Section A, "Strong" Grout
- III - Moderately Grouted, Idealized Section A, "Weak" Grout
- IV - Heavily Grouted, Section B, "Weak" Grout
- V - Moderately Grouted, Section B, "Weak" Grout

DISTANCE FROM CENTERLINE OF INBOUND TUNNEL - m.

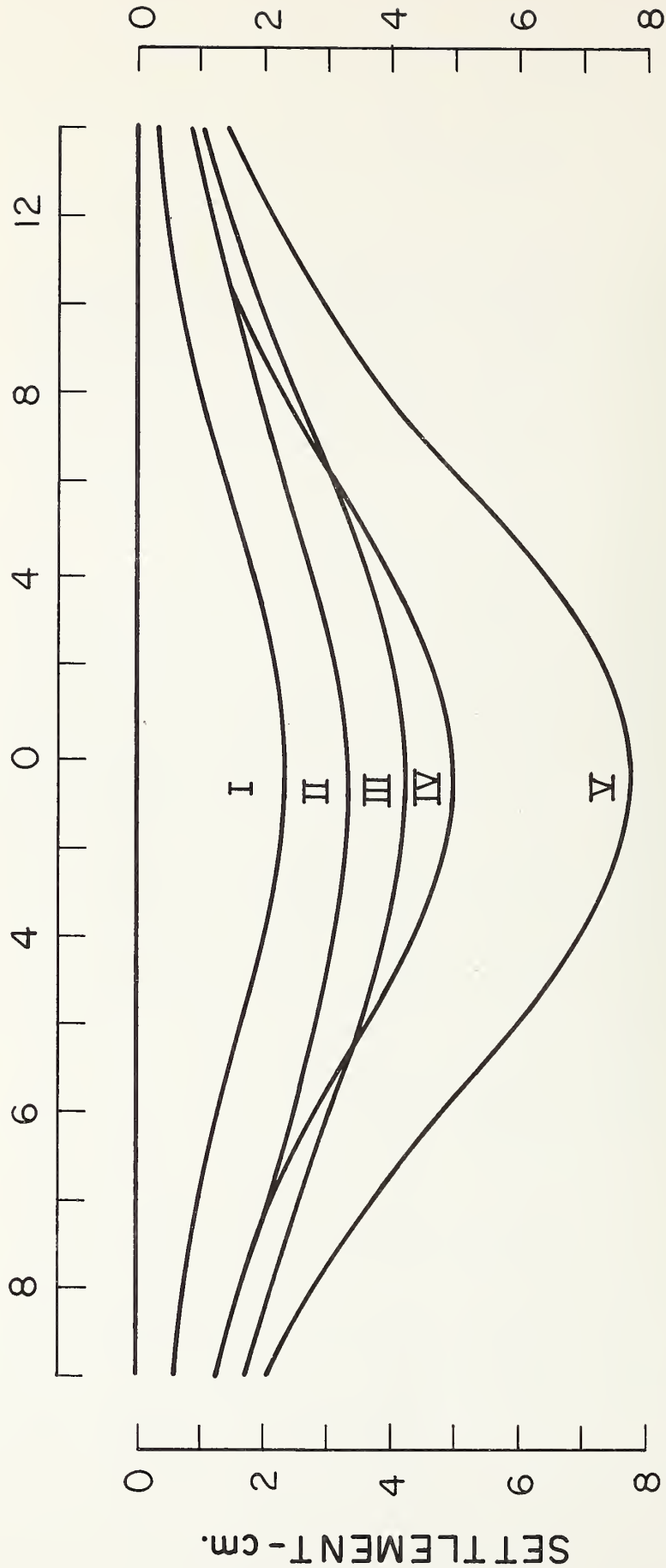


FIGURE 6.13. PREDICTED SURFACE SETTLEMENTS FOR PROJECT I

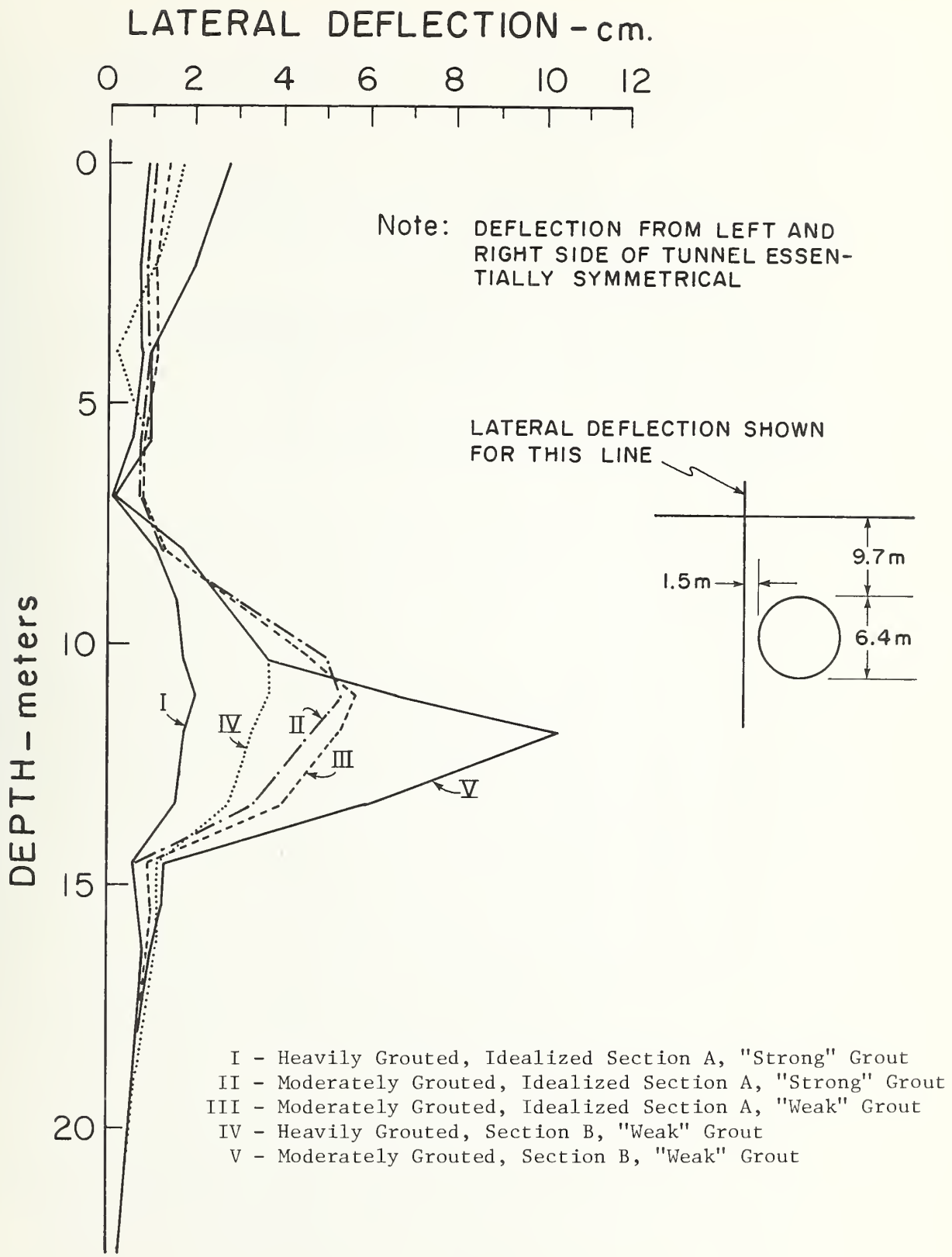


FIGURE 6.14. PREDICTED LATERAL MOVEMENTS FOR PROJECT I

2. The settlement profiles are not quite symmetrical. This is due to the presence of the grouted zone which is in place for the second tunnel advance.
3. The type of subsurface profile has a significant influence on the amount of settlement. For comparable grouted soil parameter, settlements for the original soil and grout profile (Section A) is about half of that for the less favorable soil and grout profile (Section B).
4. For the same grout and soil profile, increasing the strength of the grouted soil from "weak" to "strong" results in a reduction of settlements of 22%.
5. For the same grouted soil properties, changing from a moderately grouted to a heavily grouted profile results in a reduction in settlements of about 30%.
6. The predicted settlements are reasonably consistent with those that have been observed at the site. Observed settlements thus far have been closer to the larger predicted values; in all cases the observed behavior is bounded by the predicted behavior.

The effects of parameter changes are largely consistent with those that would be expected. The effect of the change in soil profile is particularly significant. In the case of the soil and grouting profile of Section B the effectiveness of the stabilization is reduced since the clay layer in the tunnel crown area is thicker, the grouting zones are more widely separated than in the idealized case, and the structural action of the stabilized areas is inhibited. It is readily apparent from these results that the geologic conditions in certain areas of the site diminish the favorable influences of stabilization in reducing surface settlements. On the other hand, the small predicted settlements for Section A case demonstrates that under the right conditions, stabilization can significantly reduce settlement. This was also clearly shown in the parametric studies in Chapter IV.

The lateral movements shown in Fig. 6.14 demonstrate the same trends

observed for the settlements, i.e., larger movements occur for smaller and weaker grout zones. The maximum movements are observed in the central tunnel area as expected.

SUMMARY

Case history data for performance of grouted tunnel sections are available in a number of cases for tunneling for the Washington Metro. Documentation for three of these case histories is now being obtained; others will be pursued. One of the on-going projects is heavily instrumented and will allow a detailed study of performance. Only surface survey data is available in most cases, however.

Preliminary finite element analyses of the instrumented project have provided a valuable experience in handling actual tunneling problems. The results from the analyses demonstrate that even very complicated problems can be treated. The work has also shown that precise prediction of behavior is difficult because of (1) the large number of variables required to define behavior for each of the materials in the subsurface profile; (2) variations in subsurface conditions from point to point; and (3) effects of construction procedures which are difficult to predict before tunneling. However, the results suggest that acceptable bounds may be set for expected behavior by performing analyses where key parameters are varied over reasonable limits. The analyses also obviously serve as a powerful tool in understanding the observed behavior.

CHAPTER VII

SUMMARY AND CONCLUSIONS

This report describes the results of the first year efforts of an on-going study of the use of chemical stabilization of soils around a tunnel in reducing the surface settlements caused by tunnel construction. The first year work has been devoted to:

1. Developing laboratory procedures to study load-deformation response of chemically stabilized soils.
2. Performing laboratory tests of typical stabilized soils and evaluating the observed behavior.
3. Performing load tests on soil samples grouted under field conditions.
4. Developing a finite element code which can reasonably model the effects of tunnel construction in grouted soil zones.
5. Documenting existing field case histories and applying the new finite element code to study some of the actual tunneling cases.

→ Progress in all of these areas has been made. A consistent and flexible procedure for preparation of grouted soil samples has been developed. One hundred and fourteen triaxial and unconfined load tests have been performed on treated sand samples and the results have been used to define the influence of key parameters on grouted soil behavior. Grout chemical concentrations, confining pressure, loading rate, strain level, curing time all appear to strongly influence behavior. Grain size of the sand appears to have only a small effect.

The strength and stiffness of grouted sands is shown to be a function of the dual nature of the material. At higher chemical concentrations and small strains the behavior appears to be largely influenced by the grout component while at lower chemical concentrations and higher strain levels, the sand dominates the response. As a result, the treated sand

behaves as a cemented or cohesive material with a frictional component of behavior which becomes more prominent at large strains. The behavior can be interpreted in terms of classical soil mechanics concepts.

Samples of sands treated in the field were obtained by test grouting in two locations in the Bay Area. Although tests of these samples have not been completed, it appears that the behavior of the field samples is reasonably similar to that of the laboratory grouted samples.

The finite element code for analysis of the effects of tunneling through grouted zones has been developed and fully tested. Additional work is underway on incorporating a time-dependent behavioral model into the program. Preliminary analyses have been performed which demonstrate the influence of different size and strengths of grouted zones on the surface settlements above a tunnel. It is clear that where the grouted zone completely surrounds a tunnel it acts as an efficient structural member in reducing settlement. Stronger and larger zones are shown to be more effective in this regard. The results also demonstrate that there is an optimal point beyond which increasing strength or size of the grouted zone has little influence in improving performance.

Efforts at documentation of field performance have yielded three case histories where data are available. One project, which is now underway, involves a substantive instrumentation effort. Finite element analyses of several field case histories are anticipated. As of this time (Nov., 1976), preliminary studies of the instrumented project have already been performed. The results show that the finite element code is adaptable to complex field problems. Parametric studies in which key variables are varied over reasonable ranges yield predicted results which bound preliminary observed settlements.

The finite element studies of this case history also demonstrate the difficulties involved in analysis of an actual tunneling problem. Major factors are: (1) Choice of parameters for grouted and ungrouted soils with generally limited amounts of data; (2) Variations in the subsurface profile across a site; and (3) Limited knowledge prior to construction of the actual tunneling techniques. It is doubtful that, except under unusual circumstances, all of these difficulties would be alleviated. However, it appears that acceptably accurate bounds can be established for expected behavior which can be refined based on preliminary tunneling construction work. Also, it is clear the finite element techniques offer a powerful tool in understanding observed behavior.

REFERENCES CITED

1. Association of Engineering Geologists Grouting Committee, "Grouting-- Bibliographies, Patents, Contracting Cos., Equipment Suppliers, Material Suppliers, Glossary of Terms," Grouting Symposium, Lake Tahoe, Nevada, November, 1975.
2. A.S.C.E. Committee on Grouting, "Guide Specifications for Chemical Grouting," Proceedings, Journal of the Soil Mechanics and Foundations Division, ASCE, Vol. 94, No. SM2, 1968, pp. 342-352.
3. Cambefort, P. H., "Injection des Soils," Vol. I and II, Eyrolles, Editeur, Paris, 1967.
4. Caron, C., Delisle, J.P. and Godden, W. H., "Resin Grouting with Special Reference to the Treatment of the Silty Fine Sand of the Woolwich and Reading Beds at the New Blackwall Tunnel," Proceedings, Conference on Grouts and Drilling Muds in Engineering Practice, Butterworths, London, pp. 142-145, 1963.
5. Clough, C.W., and Duncan, J. M., "Finite Element Analyses of Retaining Wall Behavior," Journal of the Soil Mechanics and Foundations Division, ASCE, Vol. 97, No. SM 12, December 1971.
6. Clough, G.W., "A Report on the Practice of Chemical Stabilization Around Soft Ground Tunnels in England and Europe," Stanford University Research Report, U.S. Department of Transportation, 1976.
7. Doherty, W.P., Wilson, E.L., and Taylor, R.L., "Stress Analysis of Axisymmetric Solids Utilizing Higher-Order Quadrilateral Finite Elements," Report No. S.E.S.M. 63-3, Structural Engineering Laboratory, University of California, Berkeley, California, Jan., 1969.

8. Duncan, J. M., and Chang, C. Y., "Nonlinear Analysis of Stress and Strain in Soils," Journal of the Soil Mechanics and Foundations Division, ASCE, Vol. 96, No. SM5, Proc. Paper 7513, September, 1970, pp. 1625-1652.
9. Dunton, C. E., Kell, J., and Morgan, H. D., "Victoria Line: Experimentation, Design, Programming and Early Progress," Proceedings, Institution of Civil Engineers, Vol. 31, pp. 1-24 and Discussions Vol. 34, 1966, pp. 447-461.
10. Gartung, E., and Kany, M., "Bericht uber Grundsatzversuche mit Silikatgelinjektion in Nuremberger Sand," Grundbarinstitut der Landes-gewerbeanstalt Bayern, Nuremberg, Germany, October, 1975, 28 pp.
11. Haffen, M., and Janin, J., "Grouting of Cohesionless Water Bearing Soils in City Tunnels," Paper presented at the 1972 North American Rapid Excavation and Tunneling Conference, Chicago, 1972.
12. Herndon, J., and Lenahan, T., "Grouting in Soils," Report No. FHWA-RD-76-26, Vol. 1, Federal Highway Administration, June, 1976.
13. Janin, J. J., and Le Sciellour, Guy F., "Chemical Grouting for Paris Rapid Transit Tunnels," Proceedings, Journal of the Construction Division, ASCE, Vol. 96, No. C01, June, 1970, pp. 61-74.
14. Karol, R. H., "Chemical Grouting Technology," Proceedings, Journal of the Soil Mechanics and Foundations Division, ASCE, Vol. 94, No. SM1, Proc. Paper 5748, Jan., 1968, pp. 175-204.
15. Koenzen, J. P., "Rheologische Eigenschaften Silikat-Injizierter Korngeruste," Ph.D. Dissertation, Universitat Karlsruhe, 1975.

16. Lenzini, P. A. and Bruss, B., "Ground Stabilization, Review of Grouting and Freezing Techniques for Underground Openings," Report No. FRA-ORD & D-75-95, University of Illinois, Urbana, Illinois, August, 1975.
17. Neelands, R. J., and James, A. N., "Formulation and Selection of Chemical Grouts with Typical Examples of Their Field Use," Proceedings, Conference on Grouts and Drilling Muds in Engineering Practice, Butterworths, London, 1963, pp. 150-155.
18. Perrott, W. E., "British Practice for Grouting Granular Soils," Journal of the Soil Mechanics and Foundations Division, ASCE, Vol. 91, No. SM6, 1965, pp. 57-79.
19. Rhone-Poulenc-Chemie-Fine, "Hardener 600 Series," January, 1975.
20. Scott, R. A., "Fundamental Considerations Governing the Penetrability of Grouts and Their Ultimate Resistance to Displacement," Proceedings, Conference on Used Grouts and Drilling Muds in Engineering Practice, Butterworths, London, 1963, pp. 10-13.
21. Raymond International, Inc., "SIROC Soil Stabilizer," New York, New York, 1972.
22. Warner, James, "Strength Properties of Chemically Solidified Soils," Proceedings, Journal of the Soil Mechanics and Foundations Division, ASCE, Vol. 98, No. SM11, Nov., 1972, pp. 1163-1186.

REQUEST FOR FEEDBACK TO The DOT Program Of University Research

DOT-TST-77-74

- | YES | NO | |
|--------------------------|--------------------------|--|
| <input type="checkbox"/> | <input type="checkbox"/> | Did you find the report useful for your particular needs?
If so, how? |
| <input type="checkbox"/> | <input type="checkbox"/> | Did you find the research to be of high quality? |
| <input type="checkbox"/> | <input type="checkbox"/> | Were the results of the research communicated effectively
by this report? |
| <input type="checkbox"/> | <input type="checkbox"/> | Do you think this report will be valuable to workers in the
field of transportation represented by the subject area of
the research? |
| <input type="checkbox"/> | <input type="checkbox"/> | Are there one or more areas of the report which need
strengthening? Which areas? |
| <input type="checkbox"/> | <input type="checkbox"/> | Would you be interested in receiving further reports in this
area of research? If so, fill out form on other side. |

Please furnish in the space below any comments you may have concerning the report. We are particularly interested in further elaboration of the above questions.

COMMENTS

**Thank you for your cooperation. No postage necessary if mailed in the U.S.A.
FOLD ON TWO LINES, STAPLE AND MAIL.**

RESEARCH FEEDBACK

Your comments, please . . .

This booklet was published by the DOT Program of University Research and is intended to serve as a reference source for transportation analysts, planners, and operators. Your comments on the other side of this form will be reviewed by the persons responsible for writing and publishing this material. Feedback is extremely important in improving the quality of research results, the transfer of research information, and the communication link between the researcher and the user.

FOLD ON TWO LINES, STAPLE AND MAIL.

Fold

Fold

DEPARTMENT OF TRANSPORTATION
OFFICE OF THE SECRETARY
Washington, D.C. 20590
Official Business

PENALTY FOR PRIVATE USE, \$300

POSTAGE AND FEES PAID
DEPARTMENT OF
TRANSPORTATION
DOT 518



Office of University Research
Office of the Secretary (TST-60)
U.S. Department of Transportation
400 Seventh Street, S.W.
Washington, D.C. 20590

Fold

Fold

IF YOU WISH TO BE ADDED TO THE MAIL LIST FOR FUTURE REPORTS, PLEASE FILL OUT THIS FORM.

Name _____ Title _____
Use Block Letters or Type

Department/Office/Room _____

Organization _____

Street Address _____

City _____ State _____ Zip _____

HE 18.5 .A39 U.
no. DOT-TST-
77-74

2
BORROWER

George Washin
George Washin
George Washin
George Washin

Form DOT F 1720.2
FORMERLY FORM DOT F 1

DOT LIBRARY



00011605

U.S. DEPARTMENT OF TRANSPORTATION
OFFICE OF THE SECRETARY
Washington, D.C. 20590

Official Business

PENALTY FOR PRIVATE USE, \$300